THESIS

EFFECTS OF CAPPING MATERIAL ON LONGEVITY OF DEGRADABLE CONTAMINANTS IN SEDIMENTS

Submitted by

Calista Emily Campbell

Department of Civil and Environmental Engineering

In partial fulfillment of the requirements

For the Degree of Master of Science

Colorado State University

Fort Collins, Colorado

Summer 2017

Master's Committee:

Advisor: Tom Sale

Jens Blotevogel
Greg Butters

ABSTRACT

EFFECTS OF CAPPING MATERIAL ON LONGEVITY OF DEGRADABLE CONTAMINANTS IN SEDIMENTS

Sediments impacted by petroleum are an emerging concern. Sediments can become contaminated with petroleum due to stormwater runoff, industrial spills, or subsurface releases. Common remediation approaches to impacted sediments include installing sorptive caps, like OrganoClay Reactive Core Mats (OC RCMs) and Activated Carbon Reactive Core Mats (AC RCMs), to protect the surface water from contamination. Sorption-based approaches are well suited for sites impacted with persistent, stable contaminants like metals or polychlorinated biphenyls (PCBs), but may not be a fit for petroleum hydrocarbons. Current sorptive remediation strategies often fail to exploit the potential for aerobic degradation of petroleum hydrocarbons. The motivation for this thesis was founded on valuing sustainable remediation, having an awareness of the diverse and complex nature of aquatic sediments, and the concern that existing sediment remedies were not leveraging the potential for aerobic degradation at groundwater-surface water interfaces.

Herein, the Oleophilic BioBarrier (OBB) studied by Chalfant (2015) is considered as an alternative capping material and is examined alongside commonly used products in a series of laboratory studies and modeling efforts to elucidate the importance of material selection. The primary objectives were to better-characterize cap materials and determine how petroleum hydrocarbon longevity and underlying sediments are impacted by capping condition.

Relative retention capacity of capping materials was observed through a non-aqueous phase liquid (NAPL) column study using commercially available diesel fuel. A series of eight columns were loaded with porous media and capped. Diesel was injected at 5 mL/day for 15 days and time to breakthrough into the surface water was monitored. The OC RCM + sand cap was the most effective at preventing diesel breakthrough into the overlying surface water; however, each capping condition led to breakthrough within 15 days, showing that absent degradation and in the presence of a constant source, each capping condition considered will fail. Additionally, diesel transport followed preferential flow paths indicating the potential for premature cap failure as the sorptive material is loaded at discrete "hot spots," possibly leaving some regions of the cap underutilized.

A more extensive column study was conducted using tidal river sediments from an impacted field site. Sediments were homogenized, spiked with benzene, toluene, ethylbenzene, and xylenes (BTEX), loaded into eight columns, and capped. Data from monitoring benzene concentrations in porewater over four months was largely inconclusive despite a general trend of concentration decrease over time. Data collection concluded with a frozen column analysis in which "hockey pucks" were cut from caps and sediments. Total benzene concentration data from hockey puck sampling indicated caps had the largest influence within the first 10 cm of sediment. Total benzene concentrations deeper within sediments did not appear to be impacted by capping conditions. Additionally, hockey puck analysis showed methane was generated in all columns, suggesting methanogenic processes dominated due to oxygen delivery through diffusion being insufficient for maintaining aerobic conditions.

Sorption studies were conducted to generate isotherms and advance characterization of cap materials. Sorption studies were performed in triplicate over 10 initial aqueous phase benzene concentrations ranging from 9 mg/L to 720 mg/L. Langmuir isotherms for aqueous phase benzene sorption were determined for the OBB, the OC RCM, and the AC RCM. As expected, the AC RCM was found to have the greatest sorptive capacity. The maximum achievable sorbed concentration $C_{s,max}$ and the equilibrium constant K_L were calculated for each of the cap materials and used as inputs for modeling efforts.

A one-dimensional, numerical cap and sediment model (CapSim 3.2a, Reible Research Group, Texas Tech University) was used to distinguish the impact of incorporating benzene sorption and/or biodegradation reactions into simulations. Modeling was also used to examine impacts of capping conditions at extended lengths of time. Sorption was shown to have a greater impact than degradation on benzene porewater concentrations in the short term, particularly for AC RCM capped sediments. Conversely, biodegradation reactions are more influential in the long term. Modeling results demonstrate the relevance of oxygen delivery for managing petroleum-impacted sediments. Modeling also indicated that aerobic benzene degradation is a diffusion-limited reaction, highlighting the relevance of oxygen delivery in sediment remediation of petroleum hydrocarbons.

Overall, the laboratory studies and modeling efforts were initiated with the hope of distinguishing cap materials based on their capacities for preventing surface water contamination and for promoting natural attenuation of petroleum hydrocarbons. Although some differences were observed between cap materials, results herein are largely inconclusive regarding the impact individual capping materials have on underlying sediments. Rather, more generalized

observations of sediment capping surfaced. For instance, due to the limitation of oxygen diffusion observed under no-flow conditions, tidal oscillations likely have a larger role in oxygen delivery and contaminant longevity than previously acknowledged. Additionally, in general, sorption is impactful in the short term, but degradation reactions generally drive benzene concentrations much lower in the long term.

ACKNOWLEDGEMENTS

The following people supported this work:

Dr. Tom Sale provided guidance and enthusiasm throughout this project. It has been a pleasure, and an honor, to work with him.

Dr. Jens Blotevogel and Dr. Greg Butters kindly served on my committee. Mark Lyverse, with Chevron, provided invaluable insight and encouragement throughout these studies. Xiaolong Shen and Danny Reible, at Texas Tech University generously provided access to CapSim 3.2a as well as incredible support and feedback throughout the modeling efforts herein. Maria Irianni Renno offered technical support, conducted microbial analyses, and provided a great deal of guidance. Helen Dungan supported this effort in many ways, ranging from the messy tasks of ordering equipment to cutting frozen core. Wes Thomas, with Arcadis, arranged sampling and shipping of field sediments, as well as detailed information on cap design. Christina Ankrom worked tirelessly to support porewater sampling and frozen column analyses, her contributions were remarkable. The entire Center for Contaminant Hydrology cohort, past and present, shared knowledge, inspiration, and solace throughout this experience; it was rewarding to work with such worthwhile humans. I leave thankful and with many great memories.

My friends and family kept me biking, climbing, snowboarding, placing puzzle pieces, drinking good beer, playing cribbage, and writing poetry – their perspectives and influence continue to be a precious resource.

Funding was provided by Chevron Energy Technology Company.

TABLE OF CONTENTS

LIST OF TABLES

LIST OF FIGURES

1. INTRODUCTION

Managing sediments impacted by petroleum is an emerging area of concern. As an example, in 2015, the State of New Jersey settled a lawsuit with a major oil company for $225 million for environmental impacts near the Bayonne refinery. In 2015, 7.1 billion barrels, or 298 billion gallons, of petroleum products were consumed in the United States (U.S. EIA, 2016). Meeting this demand necessitates extraction, refinement, transportation, and storage of petroleum hydrocarbons, which can result in accidental releases to the environment. Releases near groundwater-surface water interfaces may impact sediments and compromise surface water quality. Further, management strategies for impacted sediments are complicated by tidal fluctuations, erosion, deposition, bioturbation, hyporheic exchange, and ebullition processes at groundwater-surface water interfaces.

Common remediation approaches for impacted sediments include installing sorptive caps to protect the surface water from contamination. Sorptive-based approaches are well suited for sites impacted with persistent, stable contaminants like metals or polychlorinated biphenyls (PCBs). However, groundwater-surface water interfaces are often comprised of biologically diverse, aerobic environments, which can aid in natural attenuation of petroleum hydrocarbons (Glud, 2008; Neill et al, 2014).

Unfortunately, current remediation strategies often fail to exploit the option for aerobic degradation by relying on dredging and capping of impacted sediment with sorptive materials. These practices are costly and prone to failure, motivating the pursuit for cost-effective, sustainable solutions for managing risks to human health and the environment. Laboratory and

modeling efforts focus primarily on benzene due to its relatively high solubility and toxicity. Herein, the Oleophilic BioBarrier (OBB) studied by Chalfant (2015) is considered as an alternative capping material and is examined alongside commonly used products in a series of laboratory studies and modeling efforts to elucidate the importance of material selection. The primary objectives were to better-characterize cap materials and determine if petroleum hydrocarbon longevity is dependent on cap materials.

The Literature Review (Chapter 2) covers these topics in more detail.

1.1. **Hypothesis and Objectives**

Previous studies have suggested that the OBB is capable of maintaining conditions suitable for aerobic hydrocarbon degradation (Chalfant, 2015). And, conceptually, sorptive caps have a finite loading capacity (Hawkins, 2013), highlighting the value degradation could have on sediment management. From these observations, it was hypothesized that sorptive caps may be less sustainable than the OBB by resulting in higher concentrations of petroleum hydrocarbons in the underlying sediment in the long-term.

The primary objective of this thesis is to better-characterize cap materials and determine if petroleum hydrocarbon longevity is dependent on capping approaches. Knowledge of the relative impacts of cap materials on longevity of hydrocarbons will help site managers select the most sustainable and effective remedies.

1.2. **Organization and Content**

Chapter 2 presents fundamental background information on groundwater-surface water interfaces, sediments, remediation strategies for impacted sediments, and biodegradation of petroleum hydrocarbons. Chapter 3 details laboratory and modeling methods. Chapter 4 presents and discusses the results from laboratory experiments and modeling efforts. Chapter 5 summarizes the main ideas and conclusions resulting from this work, as well as suggestions for future work. Appendices present supplementary work and reference materials.

2. LITERATURE REVIEW

This chapter introduces key concepts behind this thesis. First, biodegradation of petroleum hydrocarbons is discussed. Second, background information on groundwater-surface water interfaces is provided. Lastly, common remedies for contaminated sediments are explored.

2.1. Sediments and Groundwater-Surface Water Interfaces

Sediments are generally defined as naturally occurring material that has been broken down and transported via wind, water, or ice. Herein, sediments are materials found below surface water (rivers, lakes, estuaries, oceans) that include solid minerals, natural organic carbon, benthic organisms, and microbial communities. Sediments can become contaminated through wastewater discharge, non-point sources, groundwater plumes, and deposition of contaminated sediments.

Contaminants associated with sediments can be transported by erosion, deposition, diffusion, advection, bioturbation, and hyporheic exchange. Bioturbation is sediment and porewater mixing near the surface layer of sediments as a result benthic organism activity (Reible, 2014). Hyporheic exchange is a term used to describe the mixing of groundwater and surface water within the subsurface (Winter et al, 2014).

Redox conditions are particularly relevant to sediments, especially when considering the potential for biodegradation. Sediments have been shown to have three main redox zones: the oxic zone at shallower depths, the suboxic zone at intermediate depths, and the reduced zone at further depths (Glud, 2008). These zones may be impacted by hydrologic processes like groundwater upwelling and tidal oscillations.

2.2. Common Remediation Strategies for Contaminated Sediments

Typically, contaminated sediments are addressed ex situ, via dredging, or in situ, via capping and monitored natural recovering (MNR). These remedies can be used individually and in combination, depending on the site. The following section briefly covers common contaminated sediment remedies.

2.2.1. *Dredging*

Dredging, or underwater excavation, involves contaminated sediment removal and off-site treatment or disposal. Sediment dredging risks resuspension of contaminants and release of contaminants into the surface water column (Bridges et al., 2008). Additionally, dredging generates wastewater that must be treated before reintroducing it to surface water (US EPA, 2005). Dredging is typically used at high-risk sites.

The National Research Council (NRC) studied 26 superfund "megasites" to determine the effectiveness of sediment dredging. Ultimately, dredging was found to be likely ineffective when used alone and should be used, for example, with capping or monitored natural recovery (NRC, 2007; Palermo and Hays, 2014).

2.2.2. *Capping*

Capping entails covering contaminated sediments with a clean layer of material to prevent contaminant resuspension and migration (Reible and Lampert, 2014). Sand has traditionally been used for sediment capping, but more modern approaches incorporate synthetic, sorptive materials (Perelo, 2010). Sorptive caps sequester contaminants and protect surface water from both

dissolved phase and non-aqueous phase constituents. Dissolved phase contaminants are typically targeted with activated carbon while non-aqueous phase contaminants are typically targeted with oleophilic clays (Reible and Lampert, 2014). ORGANOCLAY ® manufactured by CETCO Minerals Technologies (Hoffman Estates, IL, USA), is an example of oleophilic clay. Sorptive material can be applied in bulk or interwoven between geotextile and rolled into place, as with CETCO's REACTIVE CORE MATS™ ORGANOCLAY ®.

Groundwater upwelling is an advective process that can transport contaminants through the sediments and into the surface water. To mitigate the effects of upwelling low permeability clays, like AquaBlok™, are implemented. However, gas accumulation beneath these caps can lead to uplift (Reible, 2007). Additionally, flow through porous media commonly follows preferential flow paths rather than plug flow, and flow barriers may simply shift the point of contaminated discharge to a new location. Further, fingering through the sediment and cap material could result in breakthrough long before the bulk sorptive capacity is met.

2.2.3. *Monitored Natural Recovery*

Monitored natural recovery (MNR) utilizes existing biotic and abiotic processes within the sediments to degrade, stabilize, or deplete contaminants (Sylvia et al., 2005). For example, biodegradation relies on microbial communities to transform or degrade contaminants to reduce human health and ecological risks. Abiotic processes in sediment environments include sorption and deposition of new sediments; deposition of new material buries contaminants and reduces bioavailability through decreased surface sediment concentrations (Perelo, 2010). Although this is the least invasive remedy, exposure to humans and the environment due to resuspension from erosion, bioturbation, or ebullition are potential risks. Thorough site characterization is needed to

ensure natural recovery processes will occur within an acceptable amount of time and that risks associated with capping or dredging are greater than leaving sediments in place (Magar and Wenning, 2006).

2.3. **Biodegradation of Petroleum Hydrocarbons**

Microbial degradation of petroleum hydrocarbons is known to occur under aerobic and anaerobic conditions (Sylvia et al. 2005). This section describes aerobic and anaerobic conditions within sediment environments.

2.3.1. ***Aerobic conditions***

Generally, the most effective degradation of petroleum hydrocarbons in terms of rates and complete mineralization occurs under aerobic conditions (Das and Chandran, 2011). It is through aerobic oxidation, which requires molecular oxygen, that petroleum hydrocarbons can be fully degraded to carbon dioxide and water (Leahy and Colwell, 1990). Biodegradation of petroleum hydrocarbons in soil and groundwater has been found to be limited by molecular oxygen concentration (Jamison et al., 1975; von Wedel et al., 1988).

Oxygen porewater concentrations as high as 10.4 mg/L and 9.8 mg/L at 5 cm and 10 cm in river sediments, respectively, have been measured directly with a modified YSI Professional ODO handheld meter (Neill et al., 2014). Considerably lower oxygen concentrations in river sediment porewater were reported by Strayer et al. (1997). Oxygen concentrations typically decline rapidly as one moves deeper within sediments (Glud, 2008). From these examples, it can be said that oxygen concentration and penetration vary substantially depending on the site and type of

sediments (i.e. river, lake, marine). Additional factors like nutrient loading, upwelling, porosity, temperature, and bioturbation also impact oxygen concentration in sediment porewater (Boulton et al., 1998; Strayer et al., 1997; Fry, J. C., 1982). Tidal fluctuations are another prevailing influence on maintaining aerobic conditions in sediments as demonstrated through oxidation-reduction potential (ORP) monitoring in sediment porewater on a tidal river (Chalfant, 2015).

2.3.2. *Anaerobic conditions*

Although aerobic conditions lead to faster and more complete degradation, petroleum hydrocarbons concentrations can also be depleted under anaerobic conditions. Anaerobic degradation of petroleum hydrocarbons occurs through methanogenesis or anaerobic oxidation with nitrate, Fe(III), or sulfate as the electron acceptors (Chakraborty and Coates, 2004). Such conditions have been shown to exist in sediments (Fenchel and Jorgensen, 1977; Glud, 2008; Himmelheber et al., 2007).

Certain site-specific factors are more conducive for anaerobic conditions. For example, high nutrient concentrations lead to oxygen depletion and minimal benthic activity limits oxygen delivery to the underlying sediments (Boulton et al., 1998; Reible, 2014). Additionally, some petroleum hydrocarbon-degrading microorganisms are obligate anaerobes; exposure to oxygen, through diffusion or bioturbation for instance, can be inhibitory to degradation processes (Chakraborty and Coates, 2004; Sylvia et al., 2005).

3. METHODS

This chapter details the approach to column experiments, sorption studies, and sediment cap modeling efforts. The first section describes a column study which utilized non-aqueous phase liquid (NAPL) to demonstrate the longevity of capping materials. The second section explains sorption studies used to characterize capping materials. Next, the design and analytical approach for a column study using impacted field sediments are discussed. Lastly, modeling methods and inputs are presented.

3.1. NAPL Columns

Longevity of capping materials was observed through a non-aqueous phase liquid (NAPL) column study using commercially available diesel fuel. Glass columns with a fritted filter base (41 mm inner diameter x 61 cm length, Ace Glass, Inc., Vineland, NJ, US) were filled with water and loaded to 46 cm with 8-12 mesh Colorado Silica Sand (Rice Engineering, Inc., Edmonton, AB, CA) and then capped as detailed in Table 1. An image of the columns prior to adding diesel is provided in Figure 1.

Table 1. Capping scheme for NAPL Columns

Column #	Cap Material
1	Uncapped
2	Sand[1] (8 cm)
3	Oleophilic BioBarrier[2] (2 layers[+]) + Sand[1] (6 cm)
4	OrganoClay Reactive Core Mat[3] (2 layers[+]) + Sand[1] (6 cm)
5	Activated Carbon Reactive Core Mat[3] (2 layers[+]) + Sand[1] (6 cm)
6	Activated Carbon Reactive Core Mat[3] (2 layers[+]) + Sand[1] (6 cm)
7	Activated Carbon Reactive Core Mat[3] (2 layers[+]) + Sand[1] (6 cm)

[1]10-20 Mesh Colorado Silica Sand, Rice Engineering, Edmonton, AB, CA, [2] Tendrain II with 10 oz geotextile, SynTec LLC, Baltimore, MD, USA, [3]Cetco, Hoffman Estates, IL, USA, [+]Each layer has a thickness of roughly 1 cm.

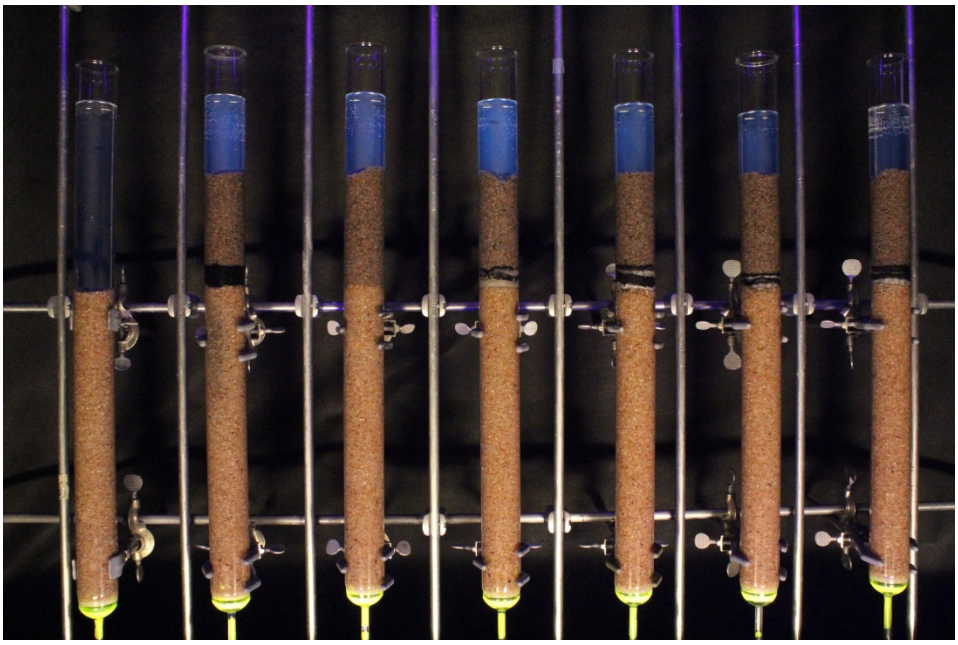

Figure 1. NAPL column study set up. From left to right, the caps are: uncapped, Oleophilic BioBarrier (OBB) + sand, Sand, OrganoClay Reactive Core Mat (OC RCM) + sand, and the last three columns are a triplicate of Activated Carbon Reactive Core Mat (AC RCM) + sand.

Over two weeks, 5 mL of diesel were injected daily into the bottom of each column. Pictures of the columns were captured with a Canon EOS Rebel T3i SLR camera (Ōta, TY, JP) every two hours under black light (120 V AC, 60 Hz, 40 W, GE Home Electric Products, Inc., Fairfield, CT, USA) using the Canon EOS Utility remote capture program for Windows. The pictures were used to monitor relative time to diesel breakthrough into surface water for the cap materials and ultimately compiled using Camtasia Studio (TechSmith, Okemos, MI, USA) to create a video of NAPL transport.

3.2. **Sorption Study**

Sorption studies were conducted for the Oleophilic BioBarrier (OBB; Tendrain II, Syntec, Baltimore, MD, USA), the OrganoClay Reactive Core Mat (OC RCM; CETCO, Hoffman Estates, IL, USA), and the Activated Carbon Reactive Core Mat (AC RCM; CETCO, Hoffman Estates,

IL, USA) to supplement the Sediment Column experiment and support modeling efforts. Specifically, the objectives were to determine sorption isotherms for each of the cap materials.

Sorption onto one square-inch of each cap material (~2.6 g/in^2 OBB, ~1.8 g/in^2 OC RCM and AC RCM; exact weight determined using analytical balance Denver Instrument, Bohemia, NY, USA) was measured in triplicate through batch experiments. A batch experiment for each material was carried out in 125 mL wide mouth septa jars (Certified 300 Series, Thermo Scientific, Waltham, MA, USA) filled with 100 mL of BTEX-spiked deionized water. A stock solution of roughly 800 mg/L BTEX (ACS grade benzene, EMD Chemicals, Gibbs Town, NJ, USA; ACS grade toluene and xylenes, Fisher Scientific, Fair Lawn, NJ, USA; GR grade ethylbenzene, Tokyo Chemical Company, Kita-Ku, TY, JP) in deionized water was prepared and diluted into four 100 mL volumes at 10 unique concentrations. Concentrations ranged from 10 mg/L to 800 mg/L BTEX. Prior to inserting sorbent materials, 2 mL water samples were collected from each jar to quantify initial concentrations. To capture losses through the lid during the course of the experiment, controls were included at each concentration. Samples from each sorption study are pictured in Figure 2, Figure 3, and Figure 4. Note: BTEX mixture was approximately 90% benzene, 8% toluene, 1% ethylbenzene, 1% xylenes to reproduce the composition found in initial porewater concentrations in the Sediment Column experiment.

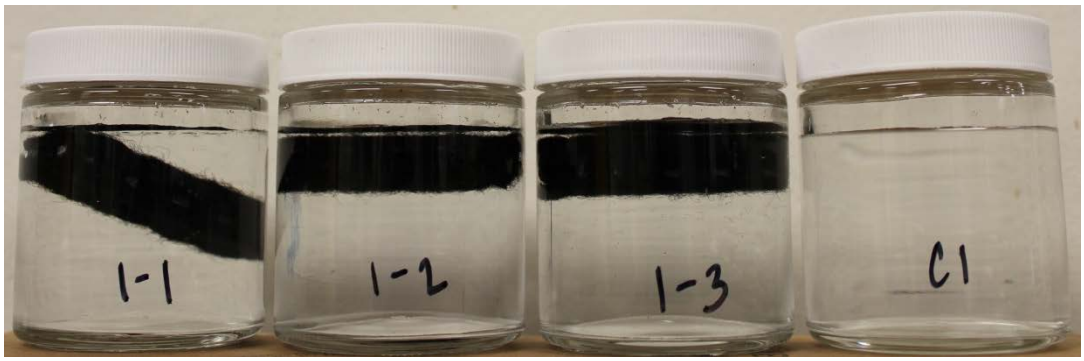

Figure 2. Triplicate of Oleophilic BioBarrier (*1-1, 1-2, 1-3*) + Control (*C1*) at concentration 1 of 10.

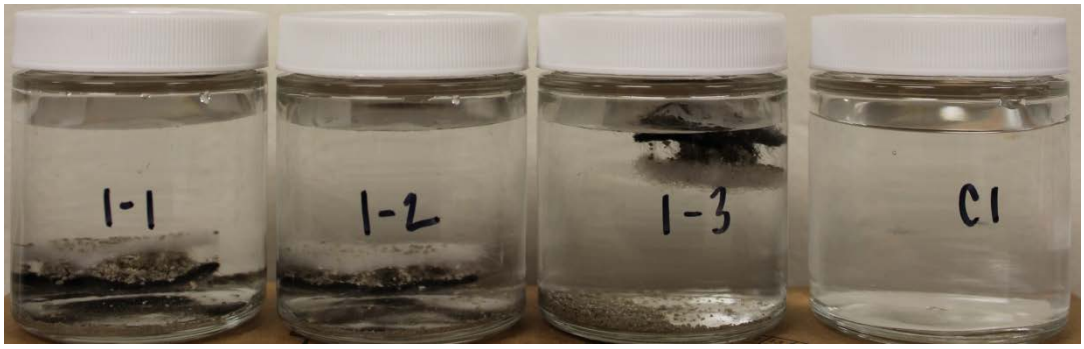

Figure 3. Triplicate of OrganoClay Reactive Core Mat (*1-1, 1-2, 1-3*) + Control (*C1*) at concentration 1 of 10.

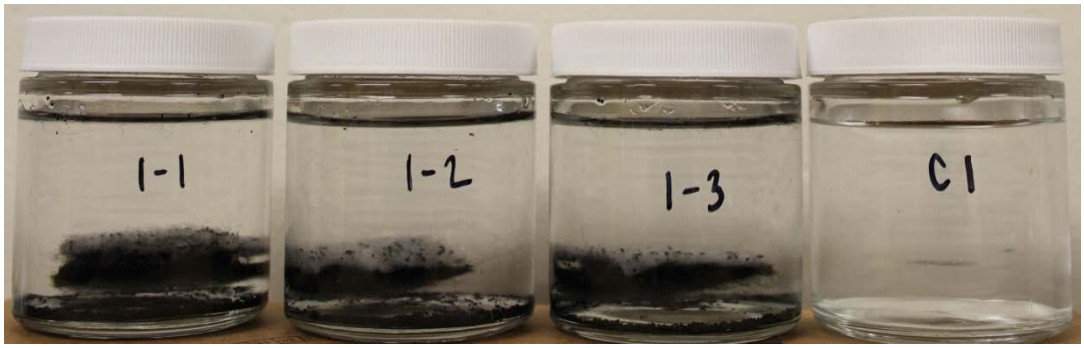

Figure 4. Triplicate of Activated Carbon Reactive Core Mat (*1-1, 1-2, 1-3*) + Control (*C1*) at concentration 1 of 10.

Each experiment was conducted for 48 hours at 18° C under gentle oscillation in an incubated shaker (MaxQ 6000, Thermo Scientific, Marietta, OH, USA). Liquid-liquid extractions with high purity (ACS/HPLC grade) n-hexane (Fisher Scientific, Fair Lawn, NJ, USA) were used to determine initial and equilibrium aqueous concentrations. Water samples and n-hexane mixtures (2 mL:2 mL) in 4 mL glass vials (VWR International, Radnor, PA, USA) were wrapped with

PTFE tape (LA-CO Industries, Inc., Elk Grove Village, IL, USA) placed on a multi-tube vortexer (Model 2600, Scientific Manufacturing Industries, Midland, ON, Canada) for 2 hours. The n-hexane phase was analyzed on an Agilent Technologies 6890N Gas Chromatograph equipped with a Flame Ionization Detector (GC/FID) and a Restek Rtx-5™ column (30 m length x 0.32 mm inner diameter x 0.25 µm film thickness). The temperature program was: 45° C for 3 min, ramp to 120° C at 10° C/min, and then ramp to 300° C at 20° C/min. A series of 6- and 8-point calibration curves were generated using a gasoline range organics (GRO) standard (Gasoline Range Organics Std 1000ug/mL, P&T Methanol, 1 mL/ampule, Restek, Bellefonte, PA, USA). Concentrations on the calibration curve ranged from 5 mg/L to 1000 mg/L for benzene, toluene, ethylbenzene, and xylenes.

The difference between initial and final (i.e. equilibrium) aqueous concentrations, minus loses, was applied to the weight of the material to yield sorbed concentrations C_s (mass of sorbate per weight of sorbent). Sorbed concentrations and equilibrium aqueous concentrations C_w (mg/L) were then applied to the Langmuir isotherm model. This model is used when the sorbents have a limited number of sorption sites and sorbed concentrations cannot increase indefinitely (Schwarzenbach et al., 2003). The Langmuir isotherm model is represented by the following equation: The solid-water distribution coefficient is defined as:

$$\boldsymbol{C_s = \frac{\Gamma_{max} \cdot K_L \cdot C_w}{1 + K_L \cdot C_w}} \quad (1)$$

where Γ_{max} is the total number of sorption sites, which can be taken as the maximum achievable sorbed concentration $C_{s,max}$ (mg/kg), and K_L (L/mg) is the equilibrium constant of the sorption reaction.

Plotting $1/C_w$ vs. $1/C_s$ for each material generates a line defined by the following equation:

$$\frac{1}{C_s} = \left(\frac{1}{C_{s,\max} \cdot K_L}\right)\left(\frac{1}{C_w} + \frac{1}{C_{s,max}}\right) \quad (2)$$

The y-intercept gives the value of $C_{s,max}^{-1}$. The slope is given as $(C_{s,max} \cdot K_L)^{-1}$, rearranging yields

$$\boldsymbol{K_L = \frac{C_{s,max}}{slope}} \quad (3)$$

These constants, $C_{s,max}$ and K_L, are inputs for the modeling program CapSim 3.2a developed by The Reible Group at the University of Texas.

3.3. **Sediment Columns**

3.3.1. ***Column Construction and Loading***

A set of eight 1-m tall columns were built from 10-cm (4-in) clear polyvinyl chloride (CPVC) pipe. Column bases were constructed using socket flanges (Spears Manufacturing, Sylmar, CA, USA) and acrylic plates. Water sampling ports were installed at four depths within the columns) using compression fittings (¼" x ¼", Cole-Parmer, Vernon Hills, IL, USA) and thick-walled glass tubing wrapped with nitex bolting cloth (153 µm aperture, Science First/Wildco, Yulee, FL, USA). During the experiment, the columns were kept in a water bath at 18° C (40" wide x 80" long x 40" tall); polytetrafluoroethylene (PTFE) tubing (0.125" O.D. x 0.602" I.D., Saint-Gobain Performance Plastics, Mickleton, NJ, USA) was used to collect samples from submerged ports.

Petroleum-impacted field sediments from a former fuel terminal in Rhode Island, USA were mixed into a slurry with water spiked with benzene, toluene, ethylbenzene, and xylenes (ACS

grade benzene, EMD Chemicals, Gibbs Town, NJ, USA; ACS grade toluene and xylenes, Fisher Scientific, Fair Lawn, NJ, USA; GR grade ethylbenzene, Tokyo Chemical Company, Kita-Ku, TY, JP). The sediment-water slurry was loaded into the columns to a height of 50 cm. The sediments were capped as described in Table 2 then topped off with 15 cm of water; water was continuously sparged with air to maintain an aerobic surface water boundary condition. A picture of the capped sediment columns is provided in Figure 5.

Table 2. Capping scheme for Sediment Columns.

Column #	Cap Material
1	Uncapped
2	Sand[1] (10 cm)
3	Glass Plate[2] + Sand[1] (10 cm)
4	Oleophilic BioBarrier[3] (2 layers[+]) + Sand[1] (8 cm)
5	OrganoClay Reactive Core Mat[4] (2 layers[+]) + Sand[1] (8 cm)
6	Activated Carbon Reactive Core Mat[4] (2 layers[+]) + Sand[1] (8 cm)
7	Activated Carbon Reactive Core Mat[4] (2 layers[+]) + Sand[1] (8 cm)
8	Activated Carbon Reactive Core Mat[4] (2 layers[+]) + Sand[1] (8 cm)

[1]8-12 Mesh Colorado Silica Sand, Rice Engineering, Edmonton, AB, CA, [2]100 mm x 10 mm PYREX™ petri dish culture cover, Corning Incorporated, Corning, NY, USA, [3] Tendrain II with 10oz geotextile, SynTec LLC, Baltimore, MD, USA, [4]Cetco, Hoffman Estates, IL, USA, [+]Each layer is roughly 1 cm thick.

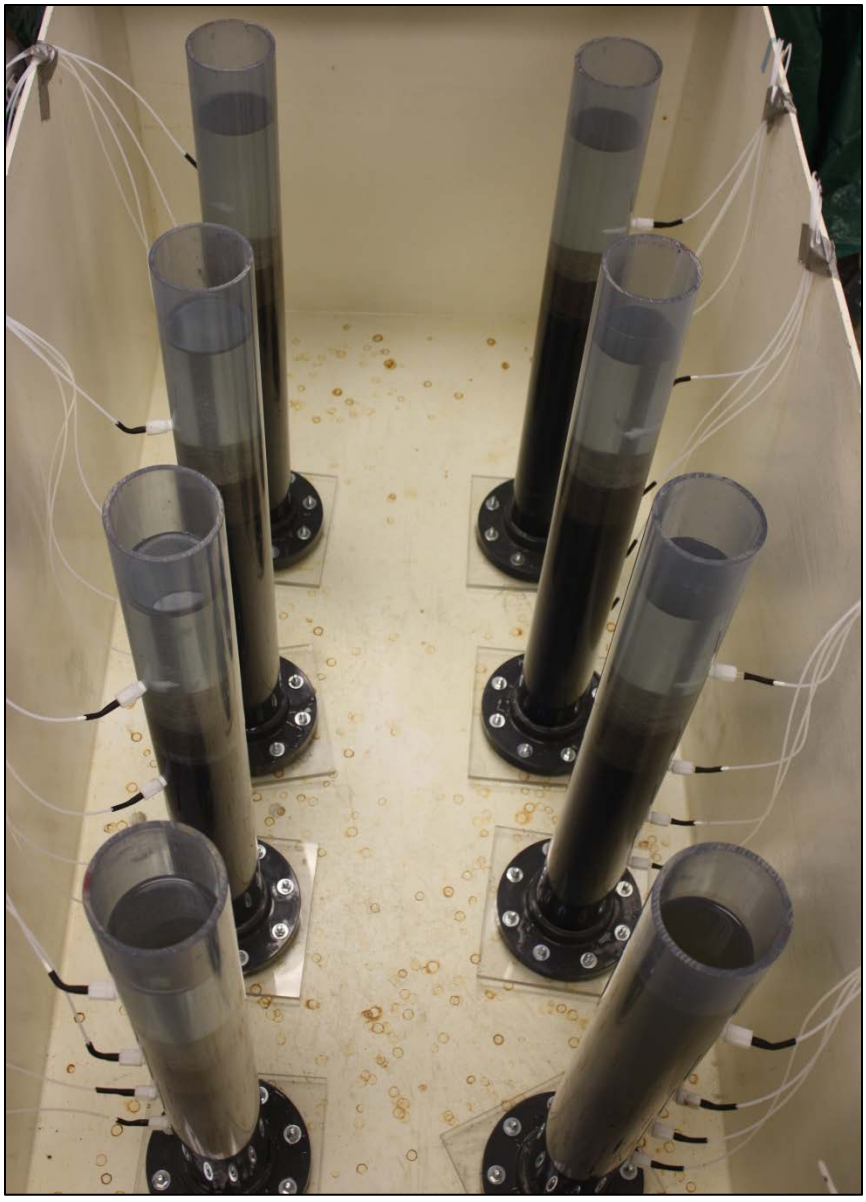

Figure 5. Sediment columns in holding tank.

3.3.2. *Water Sampling and Analysis*

Relative to the top of the column, surface water ports were located at 26 cm and three pore-water ports were located within the sediment region at 50 cm, 65 cm, and 80 cm (Figure 6). Every two weeks for 4 months, 2 mL surface water and pore water samples were collected. Water samples were analyzed on a Tekmar 7000 Headspace Autosampler Gas Chromatograph equipped with a

Flame Ionization Detector (GC/FID) and a Restek Rtx-5™ column (30 m length x 0.32 mm inner diameter x 0.25 µm film thickness). The temperature program was: 40° C for 5 min, ramp to 100° C at 10° C/min, ramp to 180° C at 30° C/min and hold for 1 min. A series of 5- and 6-point calibration curves were generated for concentration ranges of 0.25-50 mg/L for benzene, 0.75-150.5 mg/L for toluene, 0.25-50 mg/L for ethylbenzene, and 1-200 mg/L for xylenes (*m*- and *o*-) using a GRO standard (Restek, Bellefonte, PA, USA).

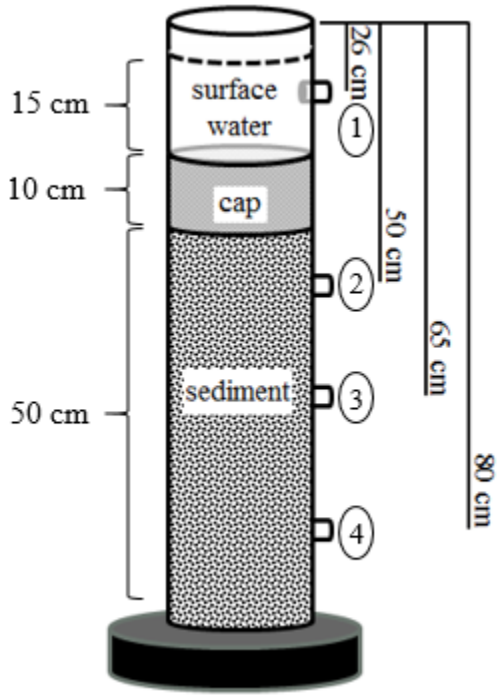

Figure 6. Water sampling port locations within the columns. “Port 1” is at 26 cm, “Port 2” is at 50 cm, “Port 3” is at 65 cm, and “Port 4” is at 80 cm.

Additionally, 4 mL samples from each the beginning, middle, and end of the four month period were extracted into 400 µL high purity (ACS/HPLC grade) n-hexane (Fisher Scientific, Fair Lawn, NJ, USA). Water samples and n-hexane mixtures (4 mL:400 µL) in Teflon tape wrapped 4 mL glass vials (VWR International, Radnor, PA, USA) were placed on a multi-tube vortexer (Model 2600, Scientific Manufacturing Industries, Midland, ON, Canada) for 30 min, then 300 µL of the n-hexane phase were preserved at -20° C for supplemental analysis. The preserved

samples were later analyzed on an Agilent Technologies 6890N Gas Chromatograph equipped with a Flame Ionization Detector (GC/FID) and a Restek Rtx-5™ column (30 m length x 0.32 mm inner diameter x 0.25 µm film thickness). The temperature program was: 45° C for 3 min, ramp to 120° C at 10° C/min, and then ramp to 300° C at 20° C/min. An 8-point calibration curve was generated using a gasoline range organics (GRO) standard (Gasoline Range Organics Std 1000ug/mL, P&T Methanol, 1 mL/ampule, Restek, Bellefonte, PA, USA). Concentrations on the calibration curve ranged from 5 mg/L to 1000 mg/L for benzene, toluene, ethylbenzene, and xylenes.

3.3.3. *Frozen Column Sampling and Analysis*

Frozen column sampling and analytical methods were modeled after methods developed by Kiaalhosseini et al. (2016) for cryogenic sampling of soils.

After 4 months of water sampling, the columns were moved to a -20° C walk-in freezer. Frozen columns were cut into 2.54 cm sub-sections, referred to as “hockey pucks”, at eight different locations: one at the top of the cap, one at the bottom of the cap, three in the sediment directly below the cap, one in the middle of the sediment, and two at the bottom of the sediment. Cuts were made using a circular saw equipped with a masonry blade (Diablo Tools, High Point, NC, USA). Each hockey puck was subsequently quartered and preserved. Figure 7 shows relative positions from which hockey pucks were recovered.

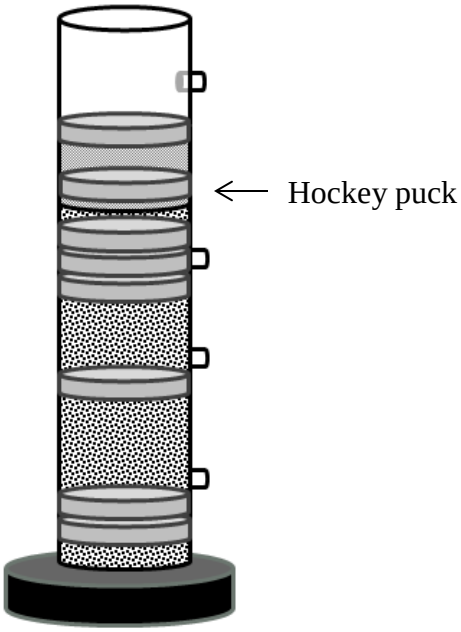

Figure 7. Schematic of the eight hockey puck sampling positions: two in the cap, three in the sediment directly below the cap, one in the middle of the sediment, and two at the bottom of the sediment.

One quarter of each hockey puck was placed in a 125 mL wide mouth septa jar (Certified 300 Series, Thermo Scientific, Waltham, MA, USA) filled with de-aired water. Displaced water m_w (M) was weighed on an analytical balance (Denver Instrument, Bohemia, NY, USA) to estimate the sample volume V_T (L^3). In addition to determining sample volume, this quarter was also used to determine methane concentrations. After shaking samples for 30 min on a multi-tube vortexer (Model 2600, Scientific Manufacturing Industries, Midland, ON, Canada), 5 mL water samples were collected. Water samples were analyzed for methane concentrations on a Tekmar 7000 Headspace Autosampler Gas Chromatograph (Teledyne Tekmar, Mason, OH, USA) equipped with a Flame Ionization Detector (GC/FID) and a column (30 m length x 0.32 mm inner diameter x 0.25 µm film thickness). The temperature program was: 45°C for 2 min, ramp to 180°C at 20°C/min, ramp to 250°C at 8°C/min, then ramp to 300°C at 30°C/min and hold for 1 min. A 5-point calibration curve was generated using a 4% methane gas standard mixture (Scotty Specialized Gases, Air Liquide America Specialty Gases, Plumsteadville, PA, USA). Methane concentration

on the calibration curve ranged from 0.05 mg/L to 2.7 mg/L. Data from water analyses yields percent methane saturation in each sample.

Following methane analysis, dry weight of sediment samples in water $M_{D(w)}$ (M) was determined by removing excess liquid per microwave oven heating methods described in ASTM D4643. Then, porosity Φ (dimensionless), pore volume V_p (L^3), and bulk density ρ_b (M/L^3) were calculated using equations (4) through (7):

$$V_T = m_w/\rho_w \tag{4}$$

$$\rho_b = M_{D(w)}/V_T \tag{5}$$

$$\Phi = 1 - \frac{\rho_b}{\rho_p} \tag{6}$$

$$V_p = V_T \cdot \Phi \tag{7}$$

where water density ρ_w is taken as 1 gm/cm^3 and particle density ρ_p is taken as the value for quartz, 2.65 gm/cm^3 (Jury and Horton).

A second quarter of each hockey puck was placed in 125 mL straight-sided jars (Kimble Chase, Vineland, NJ, USA) filled with 100 mL high purity (HPLC grade) methanol (Sigma-Aldrich, St. Louis, MO, USA). Dry weight of the sample $M_{D(MeOH)}$ (M) was determined by removing excess liquid per the microwave oven heating methods described in ASTM D4643. After 30 min on a multi-tube vortexer (Model 2600, Scientific Manufacturing Industries, Midland, ON, Canada) methanol was analyzed for benzene concentration C_{MeOH} (M/L^3) on an Agilent Technologies

6890N Gas Chromatograph (Santa Clara, CA, USA) equipped with a Flame Ionization Detector (GC/FID) and a Restek Rtx-5™ column (30 m length x 0.32 mm inner diameter x 0.25 µm film thickness; Bellefonte, PA, USA). The temperature program was: 45°C for 3 min, ramp to 120°C at 10°C/min, and then ramp to 300°C at 20°C/min. A 5-point calibration curve was generated using a gasoline range organics (GRO) standard (Gasoline Range Organics Std 1000 ug/mL, P&T Methanol, 1 mL/ampule, Restek, Bellefonte, PA, USA). Concentrations on the calibration curve ranged from 5 mg/L to 100 mg/L for benzene, toluene, ethylbenzene, and xylenes. Again, dry weight of the sample $M_{D(MeOH)}$ (M) was determined by removing excess liquid per the microwave oven heating methods described in ASTM D4643. Data from methanol extractions yield total benzene concentrations C_T (M/L^3) for each hockey puck using equations (8) and (9).

$$\mathrm{m_T} = \mathrm{C_{MeOH}} \cdot 100\ \mathrm{mL\ MeOH} \tag{8}$$

$$\mathrm{C_T} = \mathrm{m_T}/\mathrm{M}_{D(\mathrm{MeOH})} \tag{9}$$

Further, sediment concentration data can be coupled with aqueous benzene concentrations C_{aq} (M/L^3) from porewater sampling to yield sorbed benzene concentrations C_s (M/L^3) for each hockey puck. First, aqueous concentrations from the final water sampling event (from n-hexane extraction and analysis) were multiplied by the pore volume to determine the mass of benzene in the pore space m_p (M).

$$\mathrm{m_p} = \mathrm{C_{aq}} \cdot \mathrm{V_p} \tag{10}$$

The sorbed benzene mass m_s was then taken to be the difference between the total mass and the mass in the pore space (mg/L).

$$m_s = m_T - m_p \quad (11)$$

Finally, the sorbed mass was applied to the dry weight of the methanol-extracted sample to yield the sorbed concentration (mg/kg).

$$C_s = m_s / M_{D(MeOH)} \quad (12)$$

Note, porewater samples are not rigorously co-located exactly with the hockey puck samples, but still yield reasonable approximations of sorbed concentrations. For clarification, Figure 7 shows the position of the hockey puck samples relative to the pore-water ports. Also, aqueous concentrations used in (10) were determined from the n-hexane extraction and analysis described in the *Water Sampling and Analysis* section.

A third quarter from each hockey puck was wrapped in aluminum foil and stored at -30℃ for microbial DNA analysis. Microbial analysis closely followed the methods of Irianni-Renno et al. (2016). Samples were sent to Research and Testing Laboratory (Lubbock, TX, USA) for sequencing.

3.4. **Modeling**

Numerical modeling was used to (1) explore the relevance of sorption and degradation within capped sediment systems, (2) resolve the importance of sorption and degradation, and (3) evaluate processes over long periods of time. Ultimately, modeling efforts were aimed at gaining insight on implications cap materials may have for precluding contaminant degradation within sediments. To advance this objective, oxygen diffusion, benzene transport, and biodegradation were

simulated under a variety of capping conditions using CapSim 3.2a, a one-dimensional cap and sediment model developed by the Reible Research Group at Texas Tech University (publication pending). This model was specifically selected because it contains a comprehensive suite of features within a friendly user-interface. Notable features include the ability to incorporate reactions, simulate bioturbation, impose tidal oscillations on the sediment system, and choose from a variety of boundary conditions. At each layer interface, continuity of mass is applied while upper and lower boundary conditions can be manipulated. For the upper boundary (the surface water layer) a fixed concentration or mass transfer boundary condition can be selected. For the lower boundary (underlying sediments) a fixed concentration, gradient, or flux boundary condition can be applied. Results from each simulation were examined to determine the contaminant mass remaining after a given amount of time under each capping condition.

CapSim 3.2a allows users to create chemical and material databases. Items from both databases are later selected to design and perform individual simulations. The user can also input chemical reactions, specifying reaction rates as well as initial concentrations in each layer of the cap design. After defining grid size, time step, and other solver options, CapSim 3.2a conducts the simulation and graphically displays the results. The results window allows the user to select parameters to plot spatially and temporally. Additionally, data can be exported as data files for further analysis.

Modeling efforts in this thesis began with building intuition regarding modeled processes and exploring the capabilities of CapSim 3.2a by running relatively simple scenarios and monitoring the results. Components were added into each scenario interactively to observe the response of the model at each step. A schematic illustrating layers used within the model is shown in Figure 8. Ultimately, capping conditions corresponding to the Sediment Column Study, presented in

Table 3, were modeled under five scenarios (A-E) defined in Table 4. Note the glass cap condition was not simulated because CapSim 3.2a cannot execute impermeable layers.

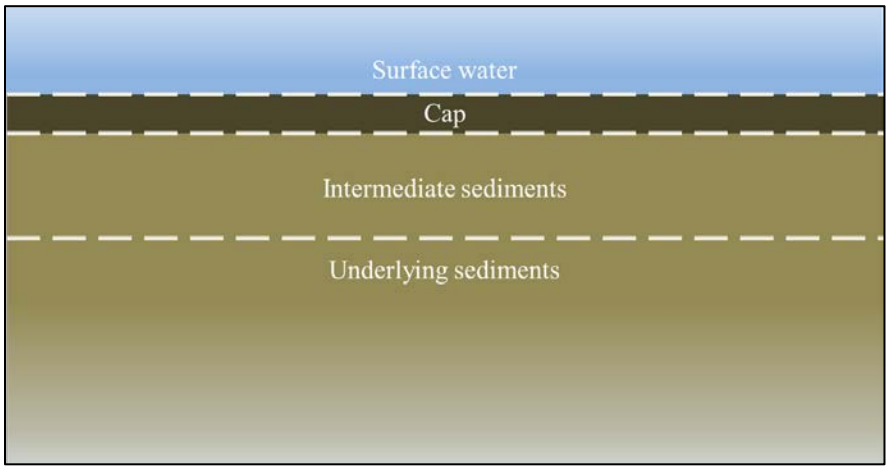

Figure 8. Schematic of modeling layers. The cap layer represents a place-holder for a variety of cap scenarios.

Table 3. List of caps modeled with CapSim 3.2a.

Capping Conditions
No cap
10 cm Sand
2 cm Oleophilic BioBarrier + 10 cm Sand
2 cm OrganoClay Reactive Core Mat + 10 cm Sand
2 cm Activated Carbon Reactive Core Mat + 10 cm Sand

Table 4. Components of each scenario modeled over the capping conditions in Table 3.

Scenario	Oxygen Concentration	Benzene Concentration	Reaction*	Sorption**
A	X			
B	X	X		
C	X	X		X
D	X	X	X	
E	X	X	X	X

*Referring to benzene degradation: $2C_6H_6 + 15O_2 \rightarrow 12CO_2 + 6H_2O, CO_2 + H_2O \rightarrow H_2CO_3$. A second order reaction coefficient of 1 L/mmol-yr was assumed for benzene degradation.
**Sorption of benzene onto sediment and capping materials.

Additionally the boundary and initial conditions are summarized in Table 5. Both the intermediate sediments and the underlying sediments began with a benzene concentration of 30 mg/L for porewater, which is consistent with initial concentrations from the Sediment Column Study. Surface water was assumed to have 8 mg/L dissolved oxygen, while Henry's Law was used to determine a carbon dioxide (CO_2) concentration of 0.6 mg/L. The molar concentration of CO_2 in the surface water can be calculated using the following equation:

$$[CO_2]_{SW} = \frac{P_{CO_2}}{k_{H_{CO_2}}} = 1.36x10^{-5}\ M \quad (13)$$

where the partial pressure of CO_2, P_{CO_2}, is 400 x 10^{-6} atm (NOAA) and the Henry constant for CO_2, $k_{H_{CO_2}}$, is 29.41 atm/M (Moran). The molecular weight of CO_2 is 44 g/mol (CRC Handbook), which is used to generate the CO_2 surface water concentration$C_{CO_2,SW}$:

$$C_{CO_2,SW} = [CO_2]_{SW}\ x\ MW_{CO_2} = 0.6\ mg/L \quad (14)$$

Further, at ~7 pH, CO2 forms H2CO3 with H2O and the H2CO3 immediately dissociates into HCO3- (Gutknecht, Moran). However, speciation reactions extended model runtime and did not

impact results. Therefore, at neutral pH values CO2 speciation reactions were ignored. More information is provided in Appendix A.

Table 5. Boundary and initial conditions used for modeling with CapSim 3.2a.

Layer	**Condition**	**Oxygen Concentration**	**Benzene Concentration**	**Carbon Dioxide Concentration**
Surface water	Fixed concentration	8 mg/L	0 mg/L	0.6 mg/L
Cap	Initial uniform concentration	0 mg/L	0 mg/L	0 mg/L
Intermediate Sediments	Initial uniform concentration	0 mg/L	30 mg/L	0 mg/L
Underlying Sediments	Fixed concentration	0 mg/L	30 mg/L	0 mg/L

Inputs for the chemical database, presented in Table 6, were generated using literature values and equations (Schwarzenbach et al., CRC Handbook of Chemistry and Physics, Hayduk and Laudie, USGS, Silberberg, Wilke and Chang). Values for the material database, shown in Table 7, were predominantly measured directly. For example, porosity and bulk density of sand and sediment were determined from frozen column analyses as described in the previous section. Volumes and weights of AC RCM, OC RCM, and OBB samples were measured using a ruler and an analytical balance (Denver Instrument, Bohemia, NY, USA) to calculate bulk densities. Porosity of OBB, OC RCM, and AC RCM was estimated from bulk sorbent porosities. Then, after basic model validation and assessment, the following solver options were selected: 1 cm grid size, 0.00273 yr time steps, and 25 yr simulation period.

Table 6. Inputs for Chemical Database in CapSim 3.2a

Property	Benzene	Oxygen	Carbon Dioxide
Density (kg/L)	0.88[1]	0.001429[5]	0.00196[5]
Molecular Weight (mol/L)	78[2]	32[2]	44[2]
Aqueous Phase Diffusion Coefficient (cm^2/s)	8.79e-6[3]	1.98e-5[6]	1.67e-5[6]
Octanol-Water Partition Coefficient (L/kg)	147.91[2]	-	-
Organic Carbon Partition Coefficient (L/kg)	59[4]	-	-

Sources: [1]Schwarzenbach et al, [2]CRC Handbook of Chemistry and Physics, [3]Estimated using Hayduk and Laudie model built into CapSim 3.2a, [4]USGS (2006), [5]Calcuated for standard temperature and pressure using the relationship Density = Molecular Weight/Standard Molar Volume, where Standard Molar Volume = 22.4 L (Silberberg), [6]Calculated with the molecular diffusion equation from Wilke and Chang (details in APPENDIX B.

Table 7. Inputs for Material Database in CapSim 3.2a

Property	**Intermediate Sediment**	**Sand**	**Oleophilic BioBarrier**	**OrganoClay Reactive Core Mat**	**Activated Carbon Reactive Core Mat**
Porosity	0.32[1]	0.25[1]	0.81[2]	0.78[2]	0.41[2]
Bulk density (g/cm^3)	1.84[1]	1.95[1]	0.22[3]	0.28[3]	0.45[3]
Fraction organic carbon, f_{oc}	0.01[4]	0	0	0.14[5]	0.7[5]
Sorption isotherms	Linear ($K_{oc}f_{oc}$)	-	Langmuir	Langmuir	Langmuir

[1]As discussed, porosity and bulk density of sediment and sand were determined from frozen column analysis data; calculations are shown in Appendix C. [2]Porosity of cap materials was measured volumetrically through water displacement, details in Appendix C. [3]As discussed, bulk density was calculated from laboratory measurements of cap material dimensions and weights; calculations are shown in Appendix C. [4]Default value for sediment in CapSim 3.2a. [5]Fraction organic carbon values for Reactive Core Mats were assumed 70% of the bulk materials. In CapSim 3.2a, the f_{oc} values for bulk OrganoClay and bulk Activated Carbon are 0.2 and 1, respectively.

4. RESULTS

This section presents results from the laboratory and modeling studies. First, results from the NAPL column study are presented. Second, sorption study results are shown. Then, the sediment column study results from surface water and porewater sampling are given, followed by the results from the frozen column analyses. Lastly, modeling results are provided.

4.1. NAPL Columns

For 16 days, 5 mL diesel were injected into the bottom of the columns on a daily basis. Pictures were taken every two hours, and the day of diesel breakthrough was recorded for each cap. Diesel is visible as a florescent yellow liquid within columns, as demonstrated in Figure 9. Times to breakthrough are shown in Figure 10. The longest time to breakthrough was observed in the OC RCM column, which is expected given it is designed to target NAPL releases. However, the take-home message is that absent degradation, breakthrough will occur under all capping conditions. Given remedies solely based on contaminant retention, breakthrough, or failure, is simply a matter of time.

Figure 9. Example of diesel (fluorescent yellow) within void space of porous media.

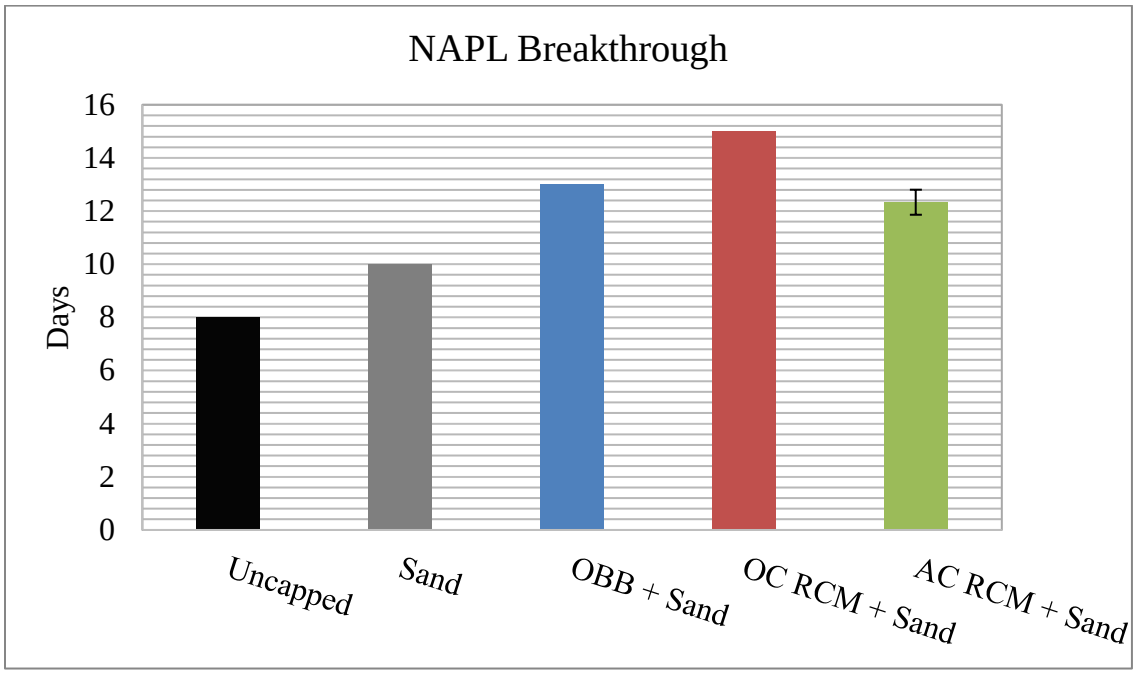

Figure 10. Time to diesel breakthrough into surface water.

Pictures compiled in Figure 11 illustrate breakthrough over time in each of the columns. These pictures indicate flow through porous media and cap materials via preferential pathways and not plug-flow. Critically, transport along sparse preferential pathways lead to a scenario where sorptive capacity of cap materials are not fully utilized. Therefore, assuming plug-flow when calculating the design life of caps may result in unrealistic expectations regarding the longevity of sorption based remedies.

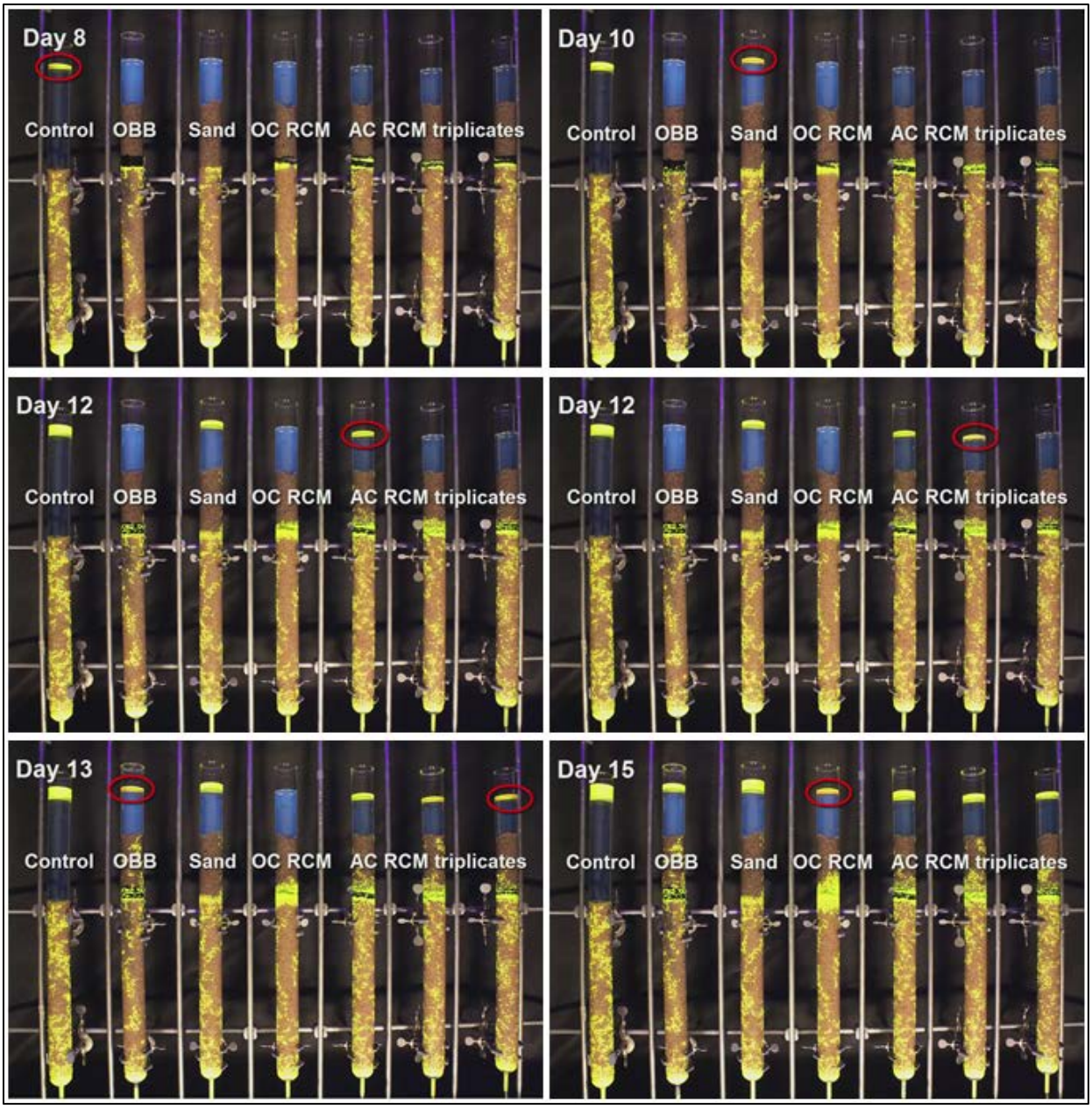

Figure 11. Visual diesel breakthrough throughout NAPL column study.

4.2. **Sorption Study**

Sorption isotherms for benzene on OBB, OC RCM, and AC RCM at 18° C were determined through a series of sorption studies. “Effective” initial benzene concentrations were calculated for each triplicate at all of the 10 concentrations by subtracting losses observed within controls to

circumvent these losses being attributed to the sorbed mass. The sorbed mass of benzene was defined as the mass difference between the final benzene concentration and "effective" initial benzene concentration. In the case that final concentrations of benzene were zero or undetected, the sample was disregarded for analyses. Sorption study data are tabulated for OBB, OC RCM, and AC RCM in Appendix D. Benzene sorption isotherms for these cap materials are shown in Figure 12. The dramatically steeper slope for AC RCM results indicates it is a much stronger sorbent for aqueous-phase benzene.

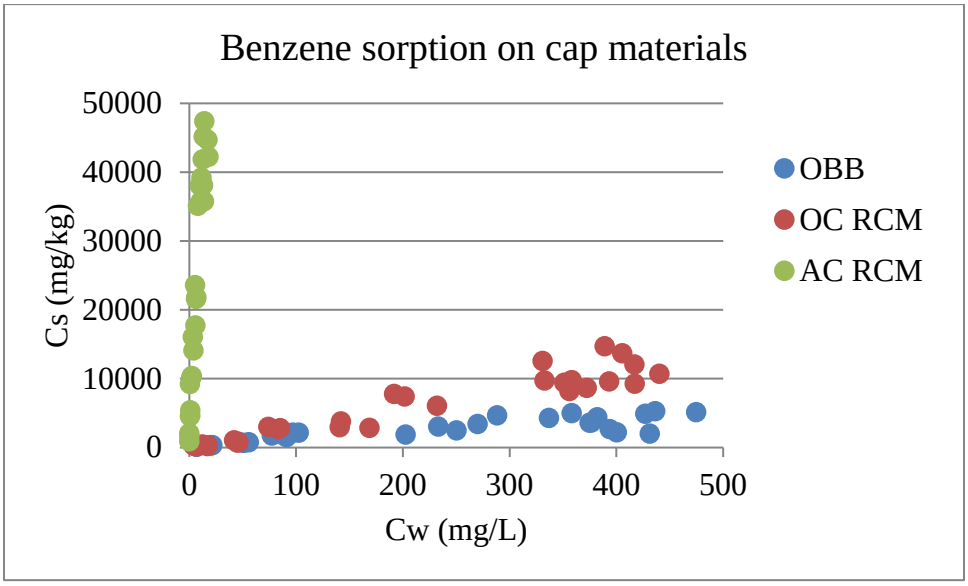

Figure 12. Benzene sorption isotherms for the Oleophilic BioBarrier (OBB), the OrganoClay Reactive Core Mat (OC RCM), and the Activated Carbon Reactive Core Mat (AC RCM).

Following the Langmuir isotherm model, inverse equilibrium aqueous concentrations were plotted against inverse sorbed concentrations for each material. The datasets were then fitted to a linear equation. The results for each cap material and the equation for the best-fit line are shown in Figure 13, Figure 14, and Figure 15 for OBB, OC RCM, and AC RCM, respectively.

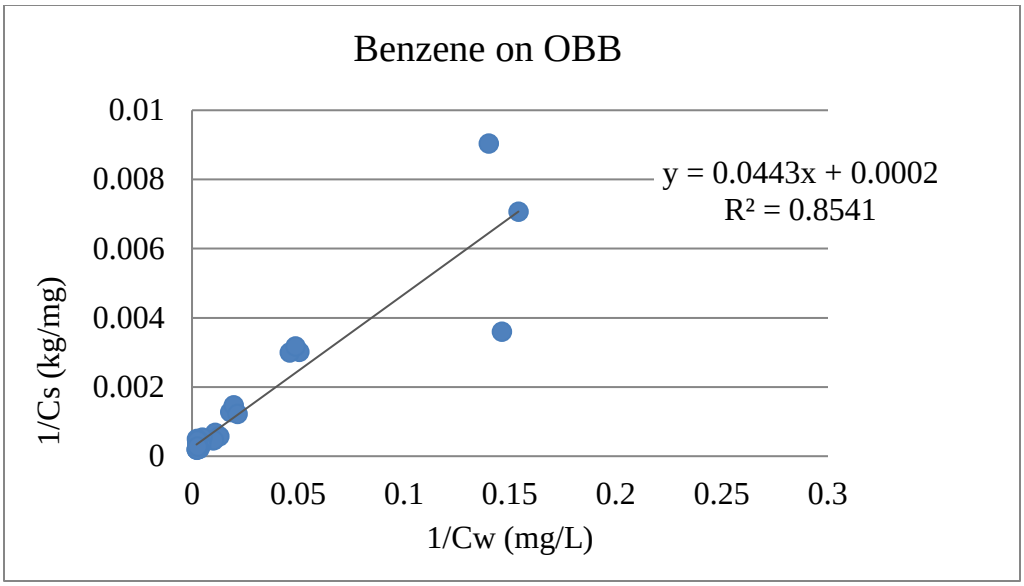

Figure 13. Benzene sorption onto the Oleophilic BioBarrier (OBB).

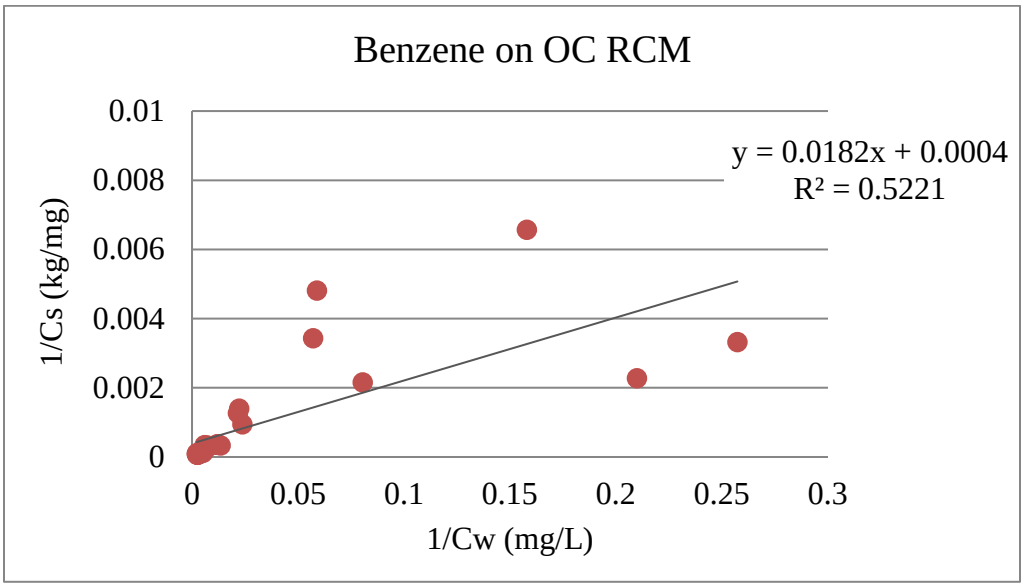

Figure 14. Benzene sorption onto the OrganoClay Reactive Core Mat (OC RCM).

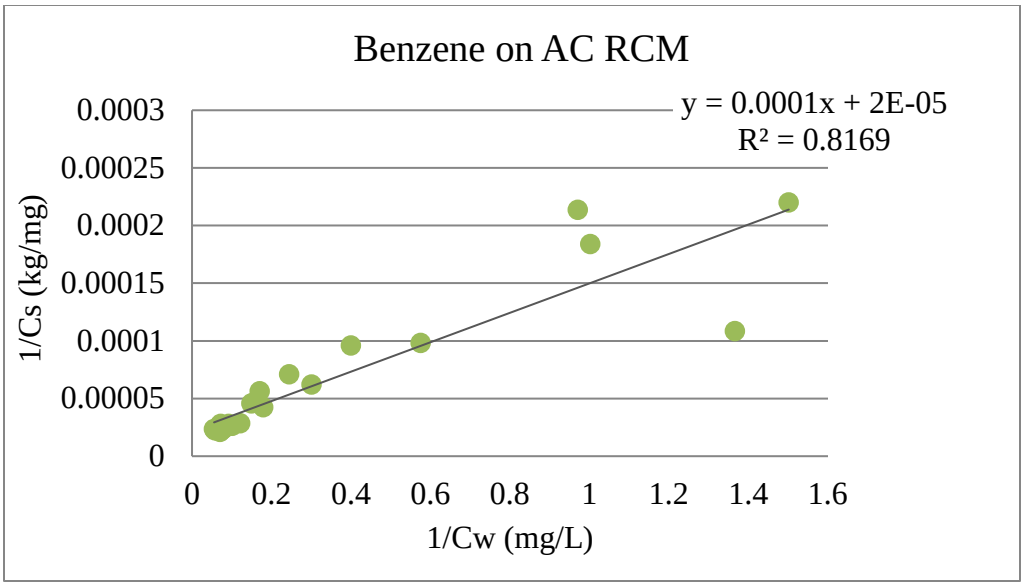

Figure 15. Benzene sorption onto the Activated Carbon Reactive Core Mat (AC RCM).

The terms for the Langmuir isotherm model are taken from the linear equations as described in *Section 3.2* and compiled in Table 8.

Table 8. Langmuir isotherm results from sorption study.

Material	**K_L** *(L/mg)*	**$C_{s,max}$** *(mg/kg)*
Oleophilic BioBarrier	4.51e-03	5000
OrganoClay Reactive Core Mat	2.2e-02	2500
Activated Carbon Reactive Core Mat	2e-01	50000

The higher value for AC RCM indicates a higher capacity for benzene sorption. The values for OBB and OC RCM indicate a comparably lower capacity for benzene sorption. Results in Table 8 were used as inputs for modeling with CapSim 3.2a.

4.3. Sediment Columns

4.3.1. *Water Sampling*

Surface water and porewater samples were collected and effectively analyzed seven times over four months. Accumulation of gas bubbles within the porespace of all columns complicated porewater sampling and may have contributed to the erratic nature of some of the data presented in the following sections. Benzene was never detected in surface water samples from Port 1, so those results are omitted. Benzene in sediment porewater samples from Ports 2, 3, and 4 through time, are shown for each capping condition in Figure 16, Figure 17, and Figure 18, respectively. For all three porewater ports in each column, there is a general trend of decreasing benzene concentration through time. Analysis of sediment sampled prior to column loading revealed that the initial porewater concentration of benzene was 30 mg/L.

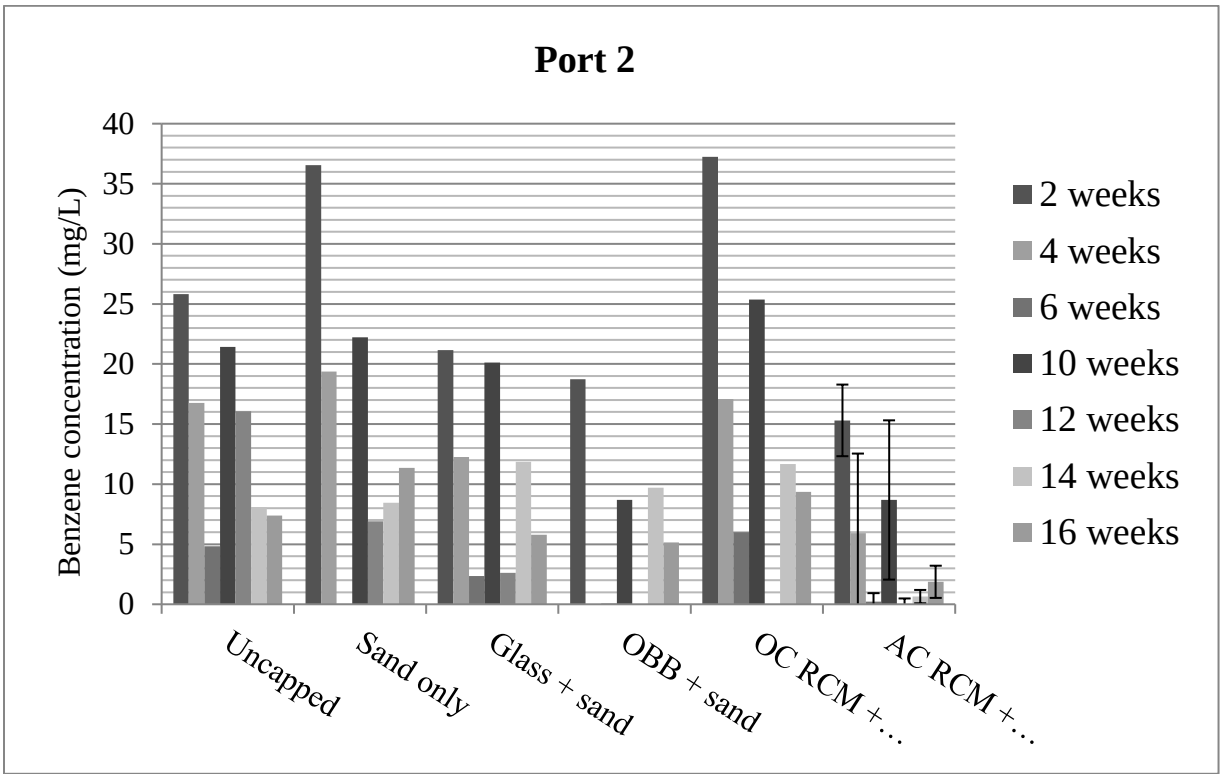

Figure 16. Benzene concentrations in Port 2 through time for all capping conditions per headspace analysis of porewater samples. AC RCM + sand is the triplicate average. Note the following abbreviations: Oleophilic BioBarrier (OBB), Organoclay Reactive Core Mat (OC RCM), Activated Carbon Reactive Core Mat (AC RCM).

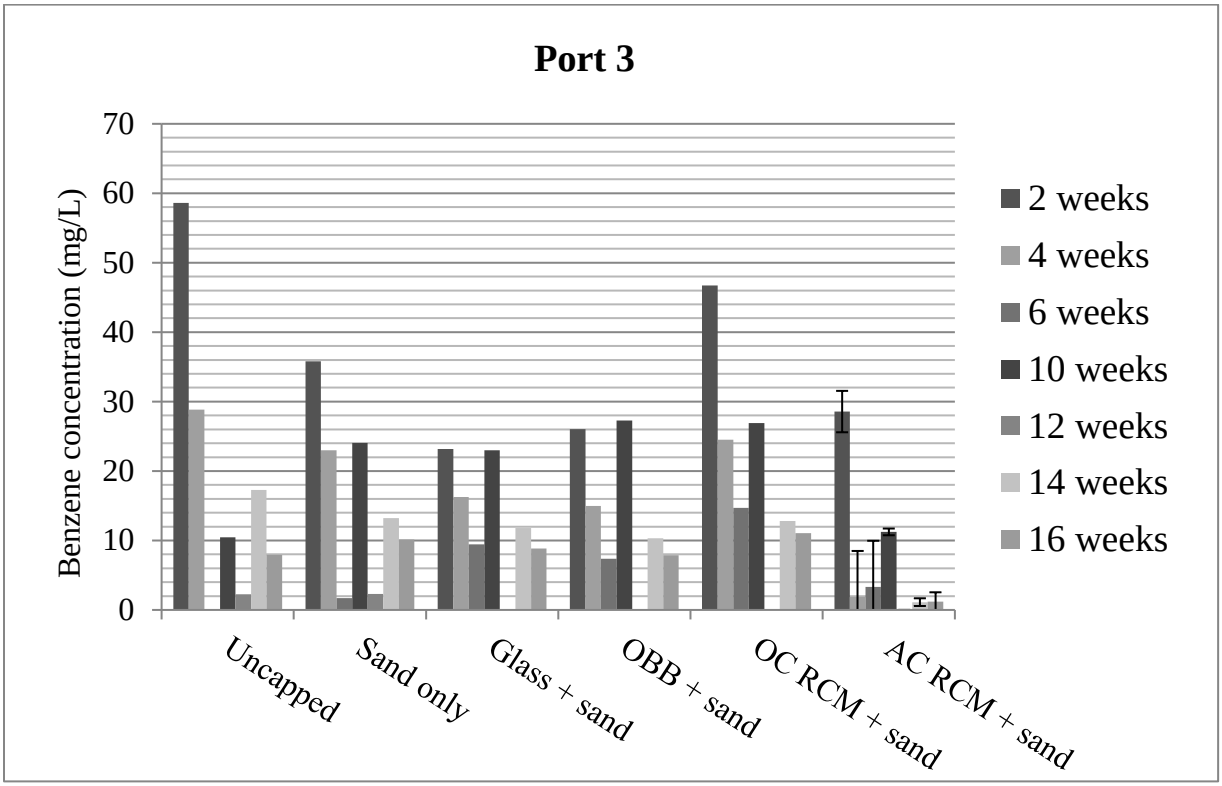

Figure 17. Benzene concentrations in Port 3 through time for all capping conditions per headspace analysis of porewater samples. AC RCM + sand is the triplicate average. Note the following abbreviations: Oleophilic BioBarrier (OBB), Organoclay Reactive Core Mat (OC RCM), Activated Carbon Reactive Core Mat (AC RCM).

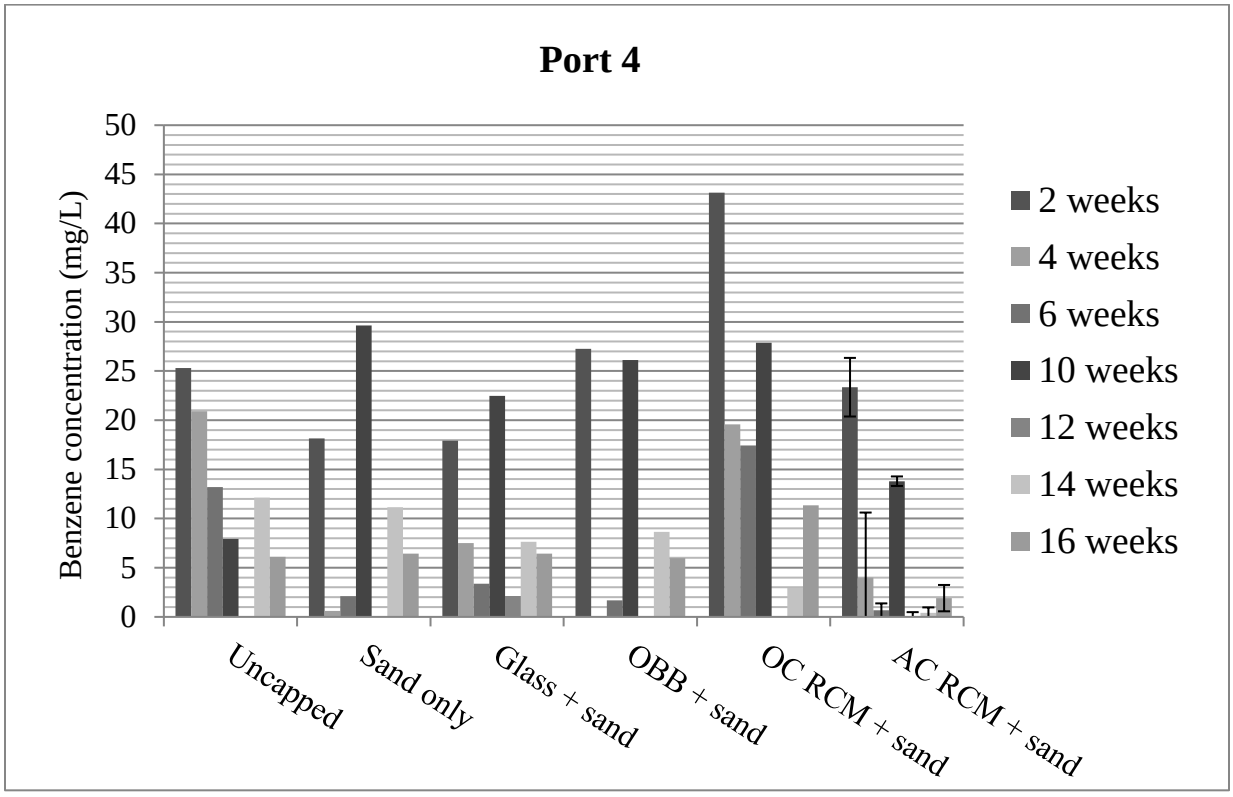

Figure 18. Benzene concentrations in Port 4 through time for all capping conditions per headspace analysis of porewater samples. AC RCM + sand is the triplicate average. Note the following abbreviations: Oleophilic BioBarrier (OBB), Organoclay Reactive Core Mat (OC RCM), Activated Carbon Reactive Core Mat (AC RCM).

The porewater sampling data was also used to generate benzene concentration profiles for each capping condition. These data are presented alongside representative columns to illustrate relative depth of sample port location. Figure 19 shows benzene concentrations (mg/L) at each depth under each capping condition over time using data from headspace analysis of porewater samples. For all sampling locations, there is still a general trend of decreasing benzene concentration through time. The most compelling results are the concentrations detected from porewater samples collected from Port 2:

- Results from Port 2, near the surface of the sediments, indicate lower concentrations in all of the columns than the results from Ports 3 and 4. One reason for this could be that oxygen

penetrates a limited distance into the cap and therefore aerobic degradation is most effective closer to the surface of the sediments. Additionally, without flow through the sediments, the sorptive capacity of the cap materials is expected to have the greatest impact on the sediments closer to the cap. With the lower concentrations near the surface of the sediment, this effect is observed.

- Porewater concentrations from Port 2 of the uncapped column could be decreasing as a result of degradation or as a result of dilution by the surface water. Surface water concentrations were not detected, however air was sparged to generate an oxygenated boundary condition and could have stripped benzene in the process.
- Relative to the uncapped column, the sand capped column has higher concentrations of benzene from Port 2. The sand layer could be limiting oxygen penetration as well as preventing dilution by the surface water.
- Benzene concentration profiles for the glass + sand capped column are consistent across the three sediment porewater ports. It is possible that the glass isolated the aerated surface water from the sediments near Ports 2, 3, and 4, generating anaerobic conditions capable of degrading benzene throughout the column.
- Benzene concentrations in sediment porewater from Port 2 of the OBB + sand capped column are lower than detected in the sand capped column. This could be due to sorption to the geotextile and/or to the material allowing oxygen to reach deeper into the sediments, aiding aerobic degradation.
- Benzene concentration profiles for the OC RCM + sand capped column are consistent across the three sediment porewater ports. As with the glass + sand cap, it is possible that the OC RCM isolated the aerated surface water from the sediments, generating anaerobic

conditions capable of degrading benzene throughout the column. Sorption could also cause degreasing benzene concentrations.

- Finally, the AC RCM + sand capping condition yielded the lowest benzene porewater concentrations. The low concentrations from Port 2 porewater samples were likely due to the sorptive capacity of the material as activated carbon targets dissolved phase constituents. Additional figures generated using headspace analysis of porewater samples are provided in Appendix E.

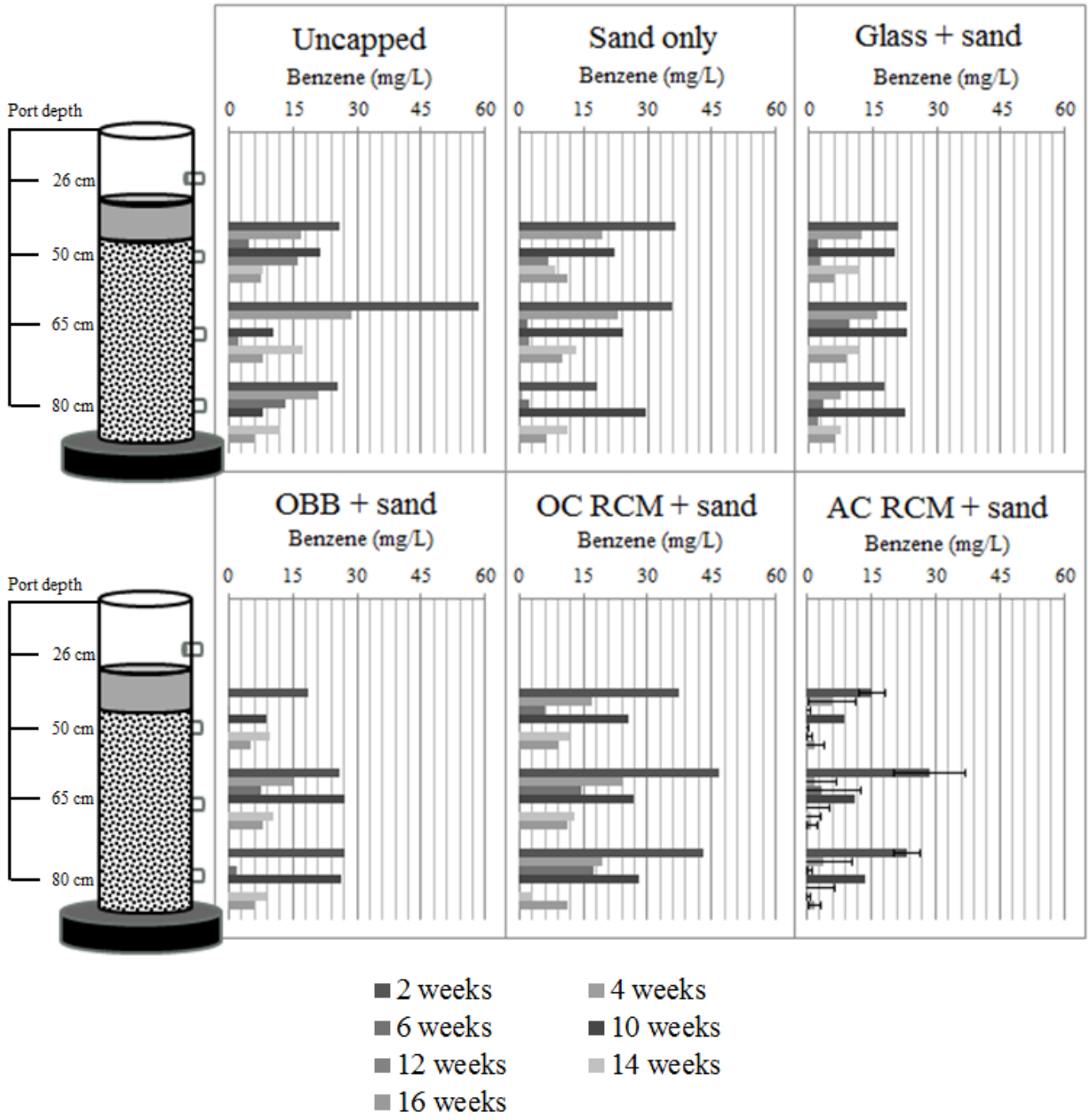

Figure 19. Benzene concentration profiles per headspace analysis over four month sampling period. AC RCM + sand is the triplicate average. Note the following abbreviations: Oleophilic BioBarrier (OBB), Organoclay Reactive Core Mat (OC RCM), Activated Carbon Reactive Core Mat (AC RCM).

In addition to headspace analysis of water samples, hexane extractions of porewater samples were conducted near the beginning, middle, and end of the sediment column study. These results are presented in Appendix F.

4.3.2. *Frozen Column Analysis*

Hockey pucks were recovered from frozen columns and used to determine volume, porosity, and methane concentrations. An overall average sediment porosity of 0.32 was calculated and Final methane saturation profiles for each capping condition are presented in Figure 20.

Analysis of initial sediment sample indicated initial methane saturation in the sample was less than 0.1%. Therefore, from Figure 20, methane was generated in all columns.

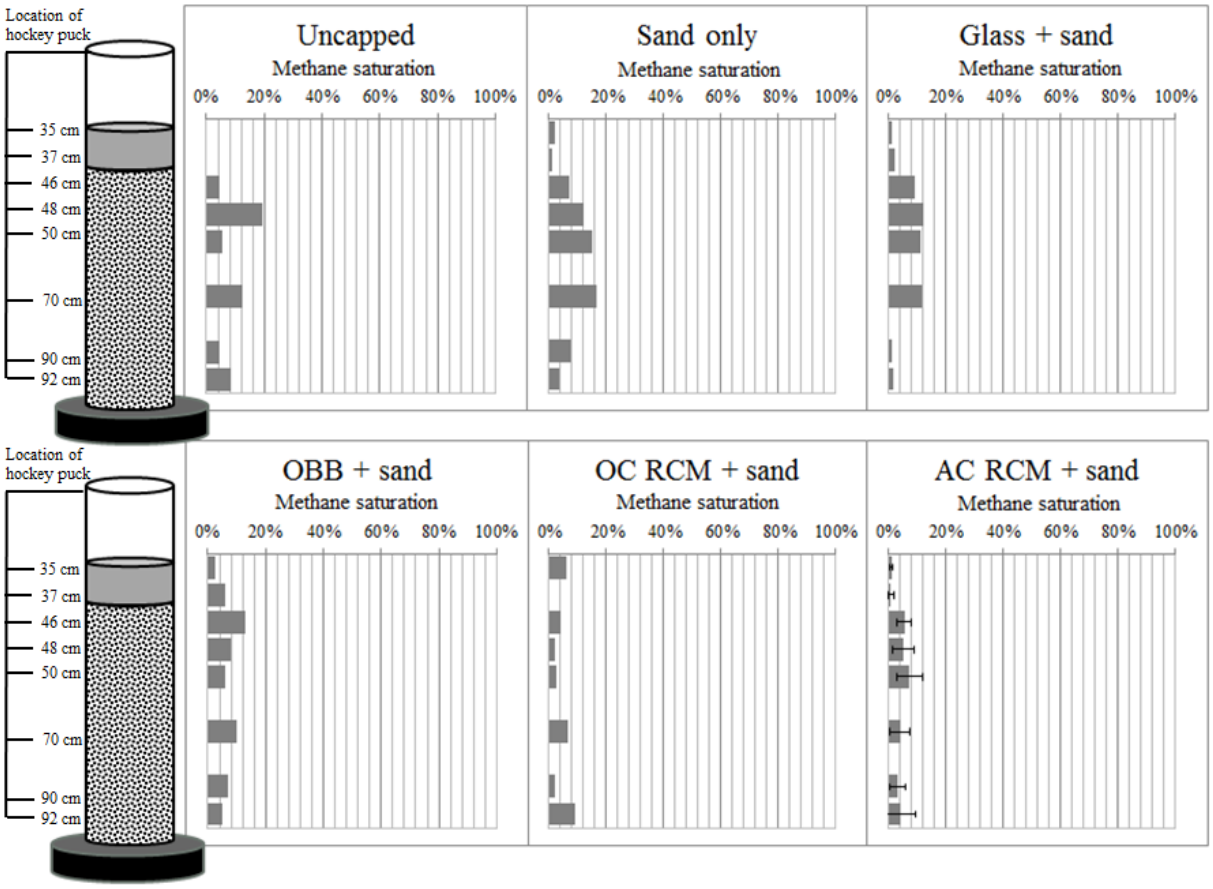

Figure 20. Profiles of final methane saturation from frozen column analysis. Activated Carbon Reactive Core Mat (AC RCM) + sand is the triplicate average. Note the following abbreviations: Oleophilic BioBarrier (OBB), Organoclay Reactive Core Mat (OC RCM), Activated Carbon Reactive Core Mat (AC RCM).

The second quarter of the hockey puck was placed in methanol to extract aqueous- and sorbed-phase benzene. Analysis of initial sediment sample indicated initial total benzene concentration was 12 mg/kg. Total benzene concentration profiles for each capping condition are presented in Figure 21. Overall, the capping conditions seem to have the greatest impact at the shallower depths within the sediment column. Potential causes for benzene concentration profiles resulting from methanol extraction analyses are discussed in the following list:

- In comparison to the uncapped column, the sediments near the surface in the sand capped column have higher concentrations of benzene. As mentioned in discussion of porewater concentration data, the sand layer could be limiting oxygen penetration as well as preventing dilution by the surface water.
- The OBB + sand cap may be helping to promote biodegradation near the sediment surface. Oxygen consumption in the upper-most layer of sediment could be limiting oxygen penetration into deeper layers.
- Benzene concentrations for the OC RCM + sand capped sediments are similar to the concentrations observed in the OBB + sand capped sediment. However, given the results from the porewater sampling, it is likely that these benzene concentrations are due to anaerobic degradation rather than aerobic degradation. Sorption could also cause lower concentrations in the upper layers of sediment.
- Benzene concentrations observed in the glass + sand capped column could be the result of anaerobic degradation. The higher concentration in the upper-most sediment layer could be due to oxygen entering through the perimeter of the glass plate and interfering with anaerobic degradation.

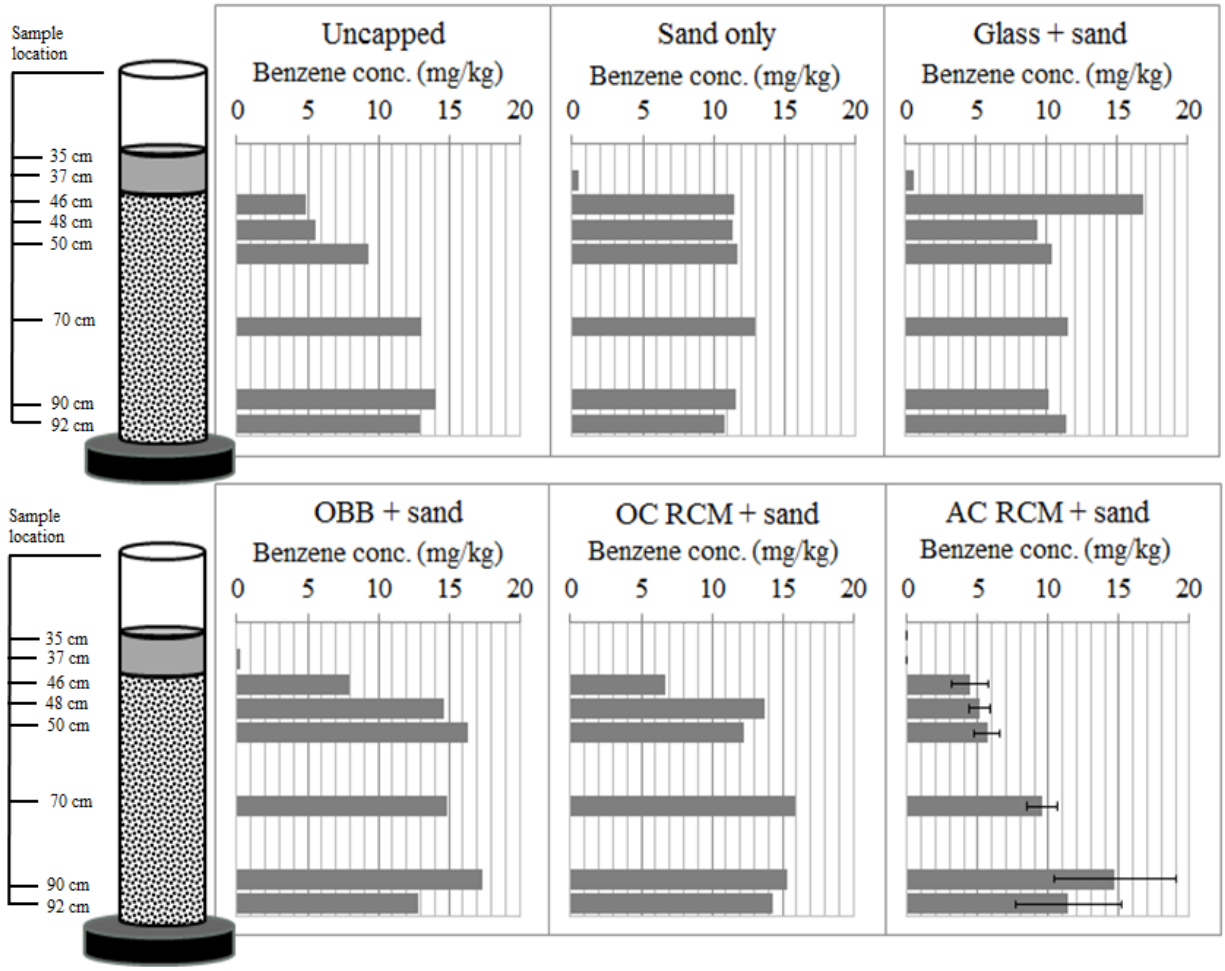

Figure 21. Final total benzene concentration profiles from methanol extraction analysis of frozen column samples. Concentrations are in mg of benzene per kg of dry sediment sample. Activated Carbon Reactive Core Mat (AC RCM) + sand is the triplicate average. Note the following abbreviations: Oleophilic BioBarrier (OBB), Organoclay Reactive Core Mat (OC RCM), Activated Carbon Reactive Core Mat (AC RCM).

Coupling benzene concentration data from methanol extractions with benzene concentration data from the final porewater sampling event, sorbed concentrations of benzene were inferred. Sorbed benzene concentration profiles, presented in Figure 22, follow the same trend as seen in the total benzene concentration profiles. Sorbed benzene concentration in initial sediment sample was 14.65 mg/kg.

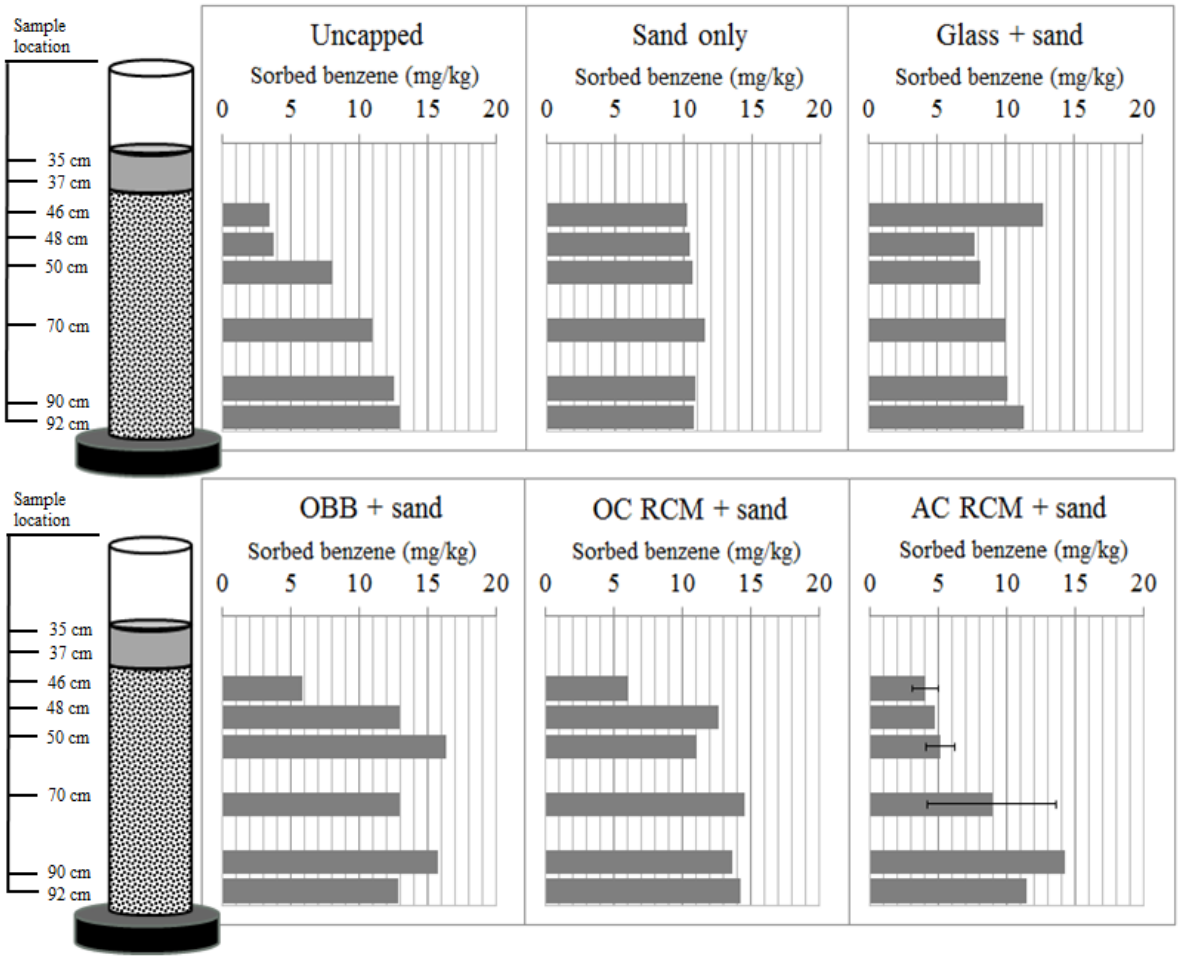

Figure 22. Final sorbed benzene concentration profiles estimated with results from frozen column analysis and porewater sampling. Concentrations are in mg of sorbed benzene per kg of dry sediment sample. Activated Carbon Reactive Core Mat (AC RCM) + sand is the triplicate average. Note the following abbreviations: Oleophilic BioBarrier (OBB), Organoclay Reactive Core Mat (OC RCM), Activated Carbon Reactive Core Mat (AC RCM).

The third quarter of the hockey puck was preserved for DNA analyses. Preliminarily, a total of five samples from the glass + sand capped sediments, uncapped sediments, initial sediment sampling were sequenced to determine if a more detailed investigation would be informative. From these samples, there were no significant differences observed between samples. Therefore, additional samples were withheld from analysis. Results from the sediment samples that were sequenced are provided in Appendix G.

4.4. **Modeling**

Scenarios C, D, and E, recalled in Table 9, are the most pertinent as they simulate benzene degradation and sorption. Profiles of benzene and oxygen porewater concentrations were generated from data for scenarios C, D, and E after four months. Unfortunately, CapSim 3.2a could not be used to generate sorbed and total benzene concentration profiles at the time this work was completed. A four-month period was selected to align with the sediment column study, which lasted four months.

Table 9. Components of scenarios C, D, and E modeled with CapSim 3.2a

Scenario	**Reaction***	**Sorption****
C		X
D	X	
E	X	X

*Referring to benzene degradation: $2C_6H_6 + 15O_2 \rightarrow 12CO_2 + 6H_2O, CO_2 + H_2O \rightarrow H_2CO_3$
**Sorption of benzene onto sediment and capping materials.

Benzene and oxygen porewater concentrations at specific depths for the three scenarios (E – reaction and sorption, D – reaction only, C – sorption only) are presented in Figure 23 and Figure 24, respectively. Using the cap surface as the datum, data was taken from the cap porewater at 1 cm and 9 cm deep, and from the intermediate sediments porewater at 11 cm, 12 cm, 13 cm, 25 cm, 55 cm, and 56 cm deep. Cross-sections of capped sediment are provided left of the plots to indicate which regions the data represent.

Comparing these three scenarios emphasizes the roles of reaction/degradation and sorption in capped sediment systems. The impact is particularly significant for the benzene concentration data as shown in Figure 23. Further, comparing these scenarios highlights which process has the

greatest impact on benzene concentrations under each capping condition. For example, the difference between the "reaction only" results and the "reaction and sorption" and "sorption only" results in AC RCM + sand capped sediment indicates that sorption plays the biggest role under this condition. Sorption plays a less significant role in OBB + sand and OC RCM + sand capped sediments. Further, capping conditions do not appear to affect sediments 25 cm deep and below.

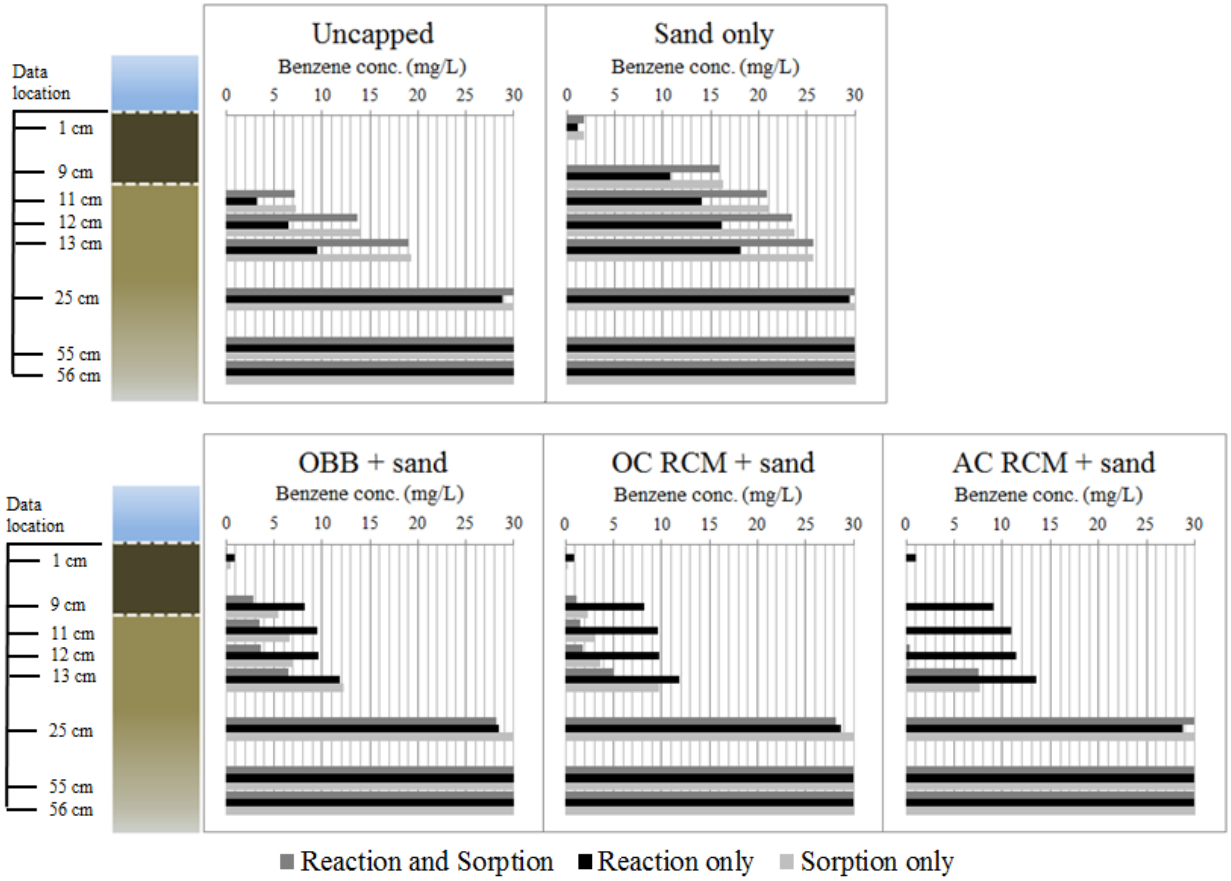

Figure 23. Benzene porewater concentrations at four months per scenarios E, D, and C. Note the following abbreviations: Oleophilic BioBarrier (OBB), Organoclay Reactive Core Mat (OC RCM), Activated Carbon Reactive Core Mat (AC RCM).

From Figure 24, oxygen concentration data indicates that degradation may be diffusion limited at 4 months with the assumed reaction rate coefficient of 1 L/mmol-yr. And again, capping conditions do not appear to affect sediments 25 cm deep and below.

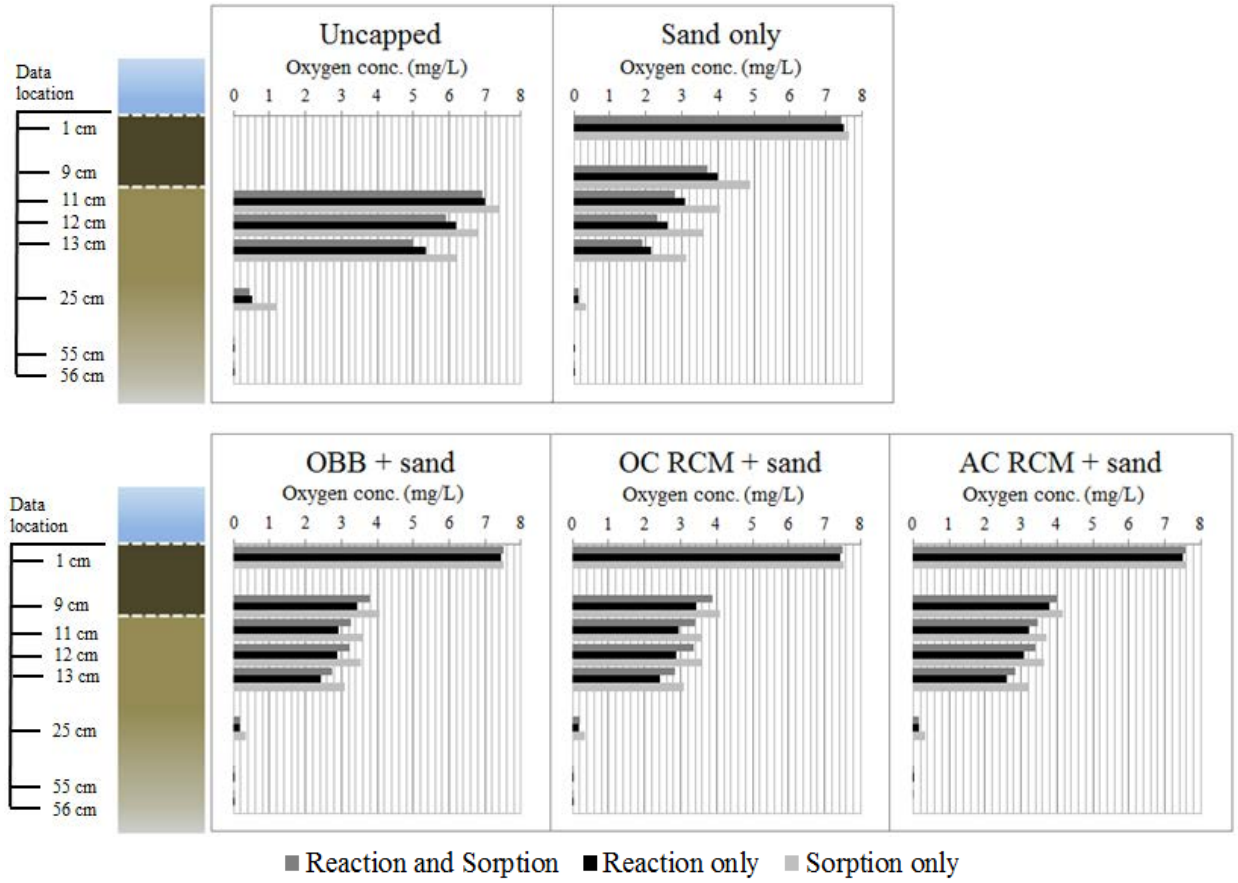

Figure 24. Oxygen porewater concentrations at four months per scenarios E, D, and C. Note the following abbreviations: Oleophilic BioBarrier (OBB), Organoclay Reactive Core Mat (OC RCM), Activated Carbon Reactive Core Mat (AC RCM).

Long-term results provide insight toward the sustainability of the capping conditions; therefore, profiles of benzene and oxygen porewater concentrations over the three scenarios (E – reaction and sorption, D – reaction only, C – sorption only) were also generated from data at the end of 25-year simulation period (Figure 25 and Figure 26, respectively). From the benzene concentration data in Figure 25, sorptive processes dominate benzene concentrations under AC RCM + sand capping conditions while degradation reactions dominate under OBB + sand and OC RCM + sand capping conditions. Comparing the data from the 25-year simulation period with the data from 4 months of simulation, benzene degradation is shown to be generally more

impactful over time. Again, capping conditions do not appear to affect sediments 25 cm deep and below.

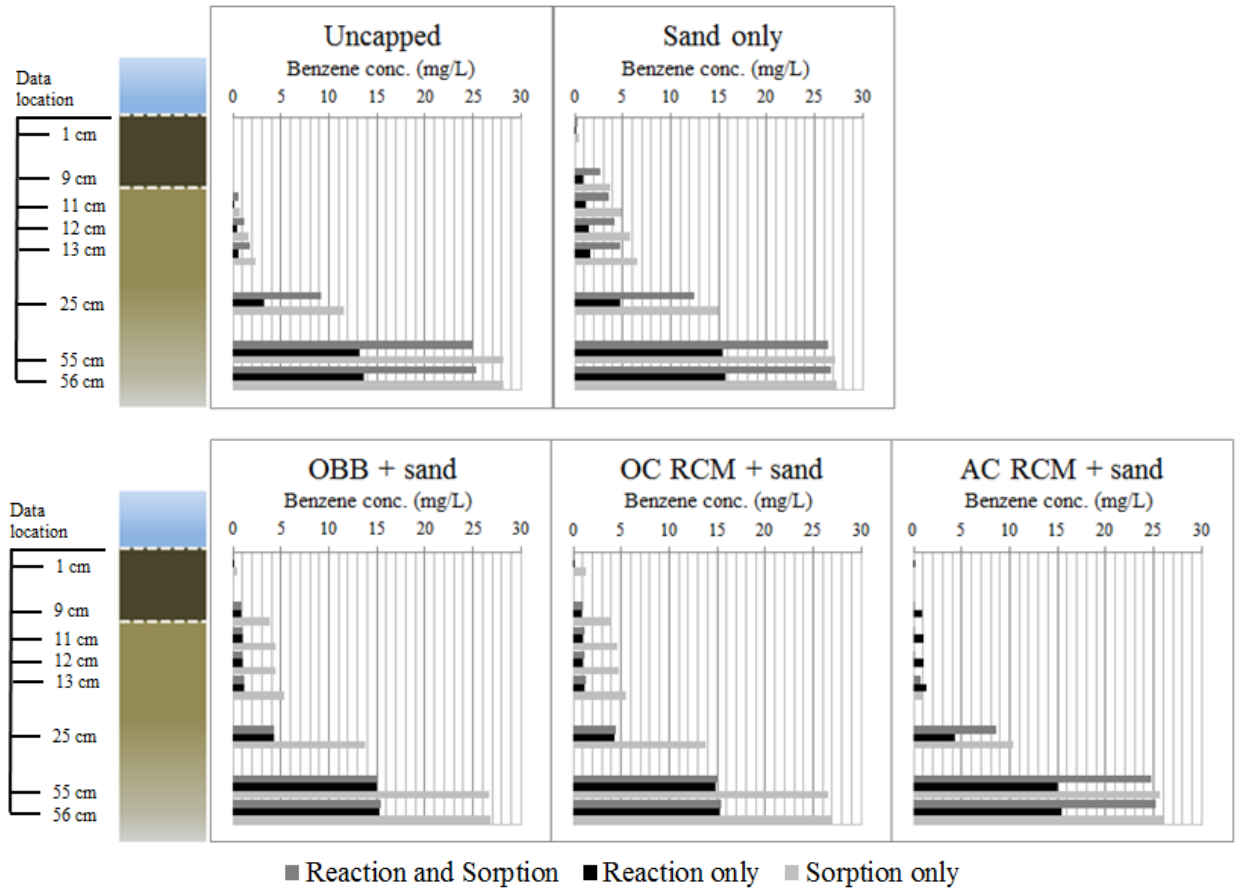

Figure 25. Benzene porewater concentrations at 25 years per scenarios E, D, and C. Note the following abbreviations: Oleophilic BioBarrier (OBB), Organoclay Reactive Core Mat (OC RCM), Activated Carbon Reactive Core Mat (AC RCM).

As with the oxygen concentration data from the four-month simulation period, the oxygen concentration data after the 25-year simulation in Figure 26 indicates that degradation may be diffusion limited over long time periods. Oxygen concentrations are higher deeper within the sediments across all capping conditions when only sorption is simulated, relative to the 4-month simulation. This indicates that over time, absent degradation, oxygen will diffuse deeper into the sediments. Consideration of reaction simulations show oxygen diffusing into the sediment will

be consumed. Over longer time periods it becomes clear that benzene degradation is limited by oxygen diffusion.

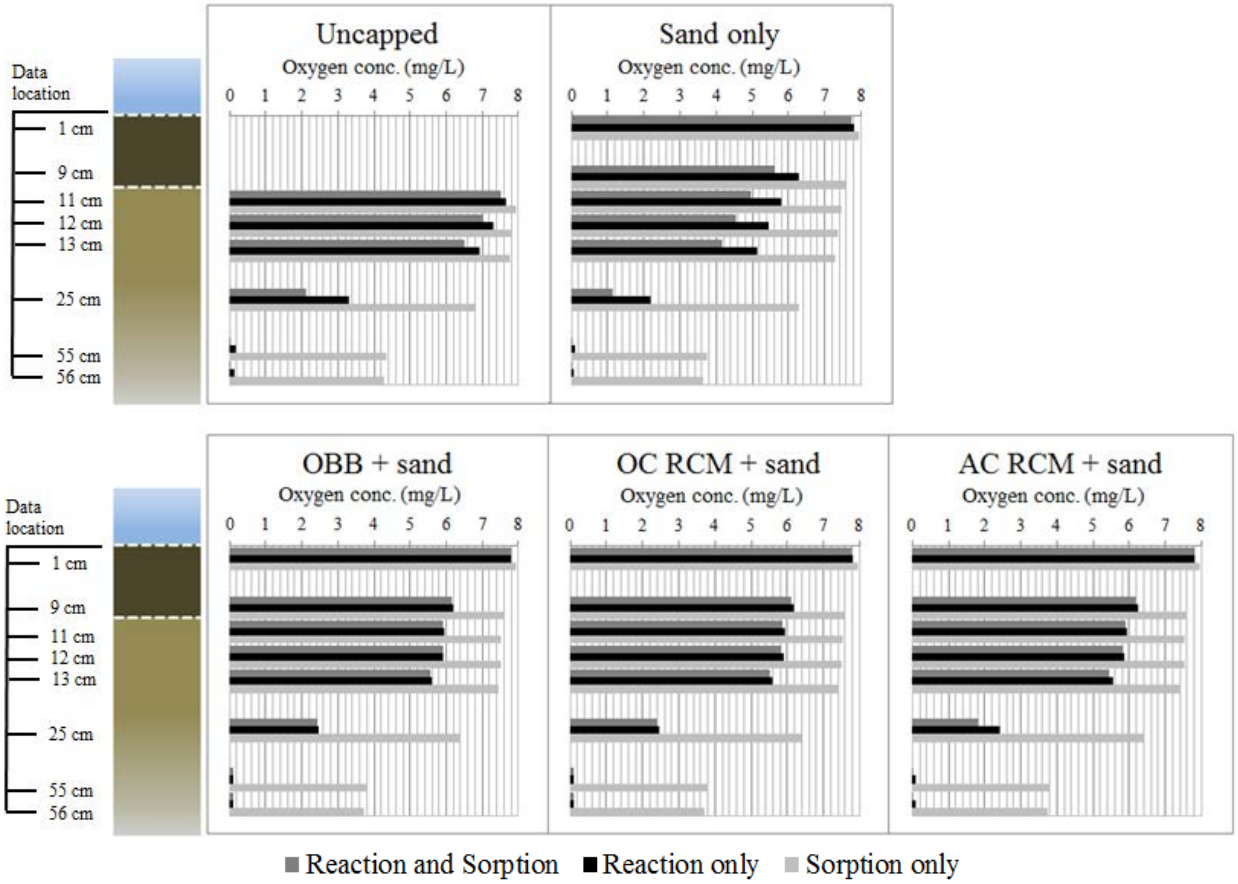

Figure 26. Oxygen porewater concentrations at 25 years per scenarios E, D, and C. Note the following abbreviations: Oleophilic BioBarrier (OBB), Organoclay Reactive Core Mat (OC RCM), Activated Carbon Reactive Core Mat (AC RCM).

Benzene concentrations through time are shown in Figure 27, Figure 28, and Figure 29 for scenarios with reaction and sorption, reaction only, and sorption only, respectively. From these profiles, higher concentrations of benzene are observed when only sorption is simulated and lower concentrations are observed with degradation reactions. Overall, relevance of degradation increases with time.

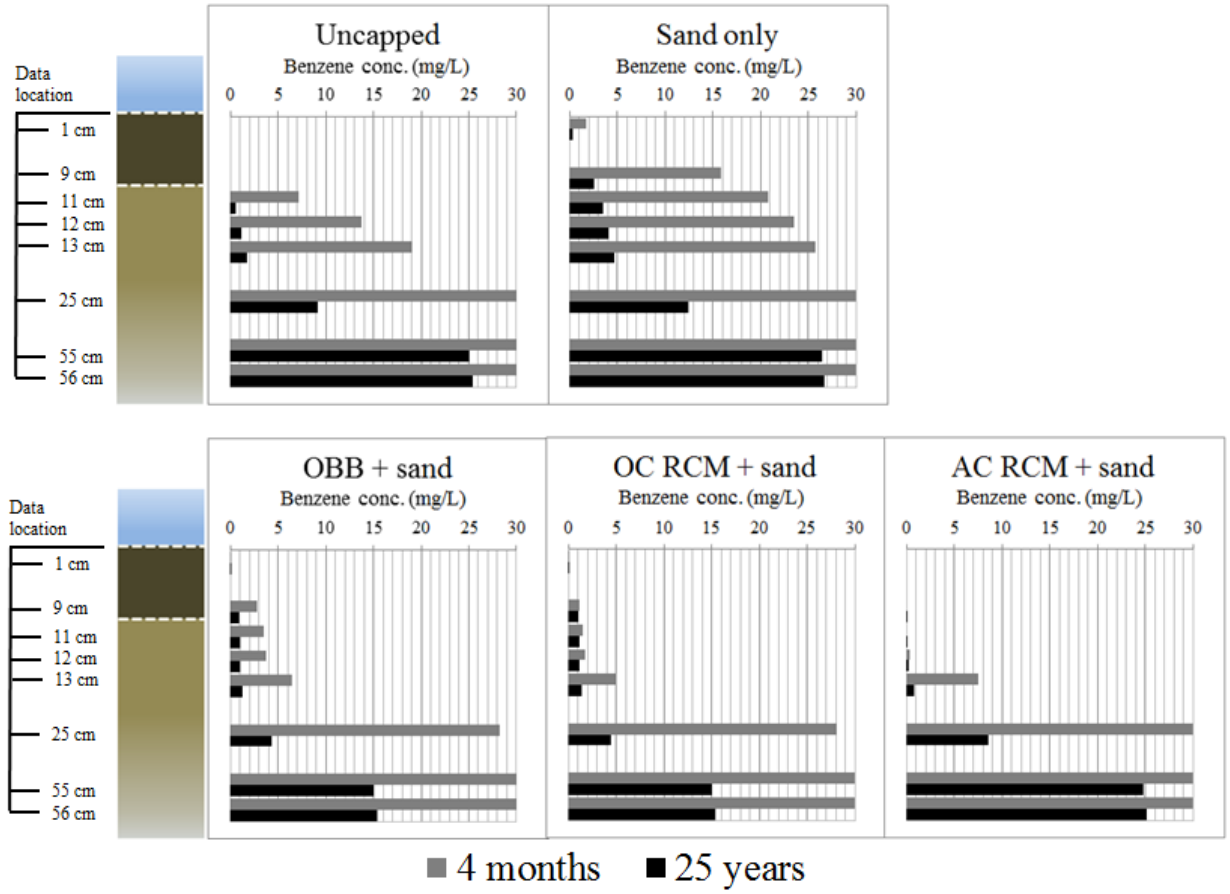

Figure 27. Benzene porewater concentration profiles from scenario E (reaction and sorption). Note the following abbreviations: Oleophilic BioBarrier (OBB), Organoclay Reactive Core Mat (OC RCM), Activated Carbon Reactive Core Mat (AC RCM).

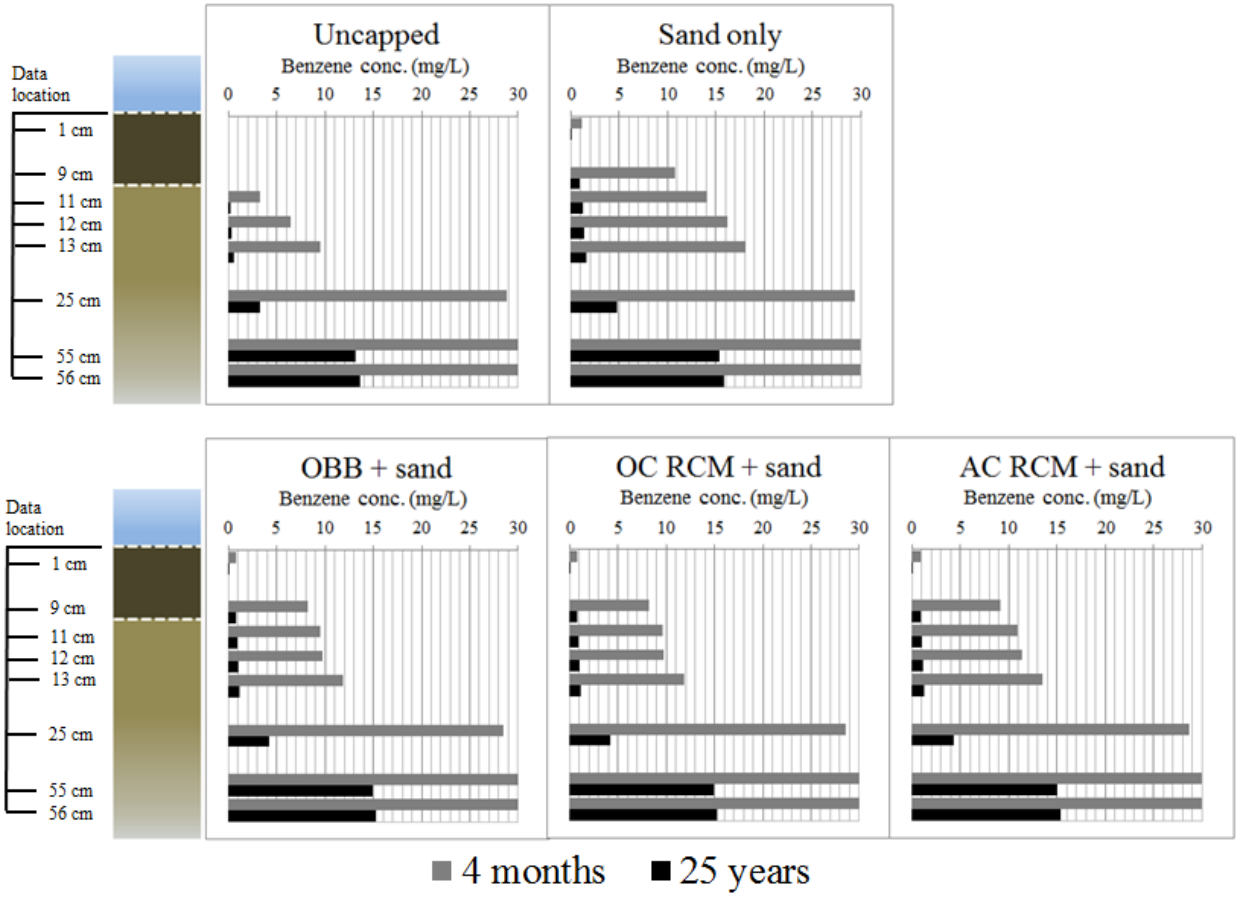

Figure 28. Benzene porewater concentration profiles from scenario D (reaction only). Note the following abbreviations: Oleophilic BioBarrier (OBB), Organoclay Reactive Core Mat (OC RCM), Activated Carbon Reactive Core Mat (AC RCM).

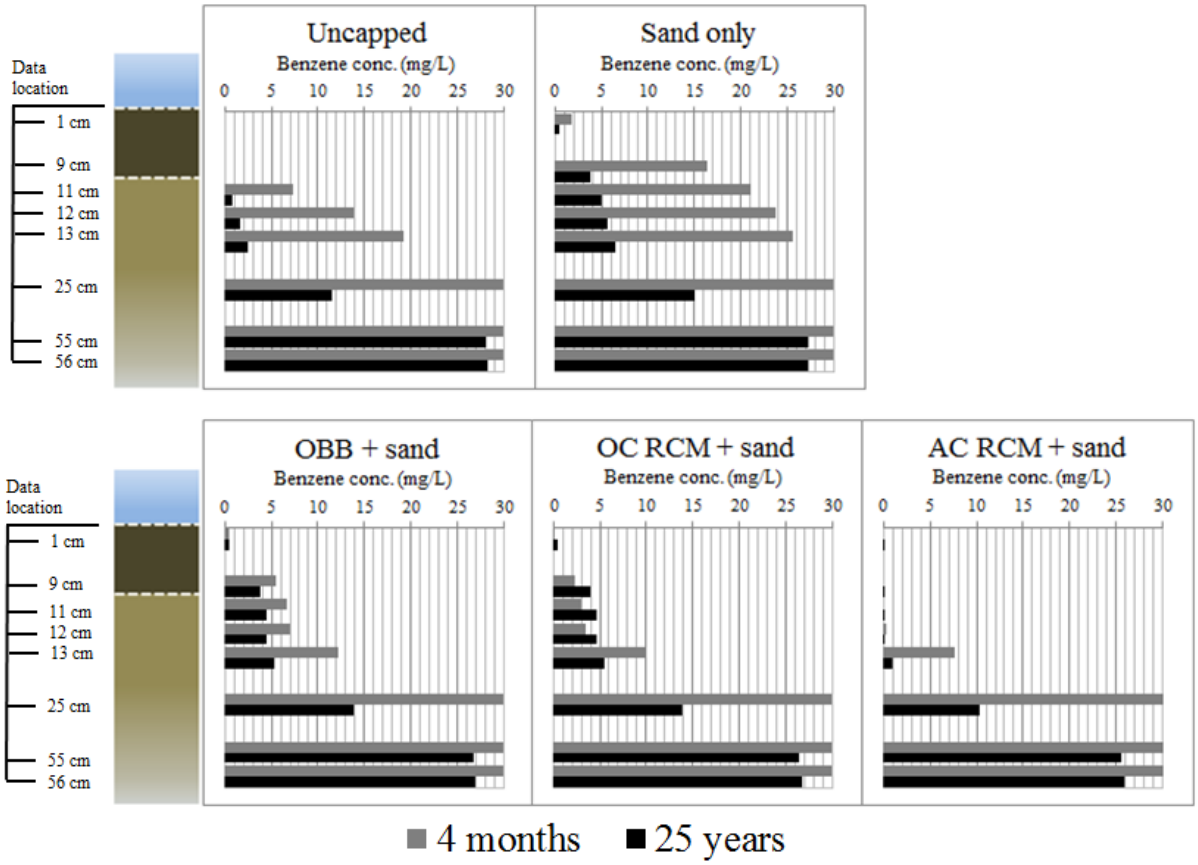

Figure 29. Benzene porewater concentration profiles from scenario C (sorption only). Note the following abbreviations: Oleophilic BioBarrier (OBB), Organoclay Reactive Core Mat (OC RCM), Activated Carbon Reactive Core Mat (AC RCM).

Similarly, oxygen concentrations through time are shown in Figure 30, Figure 31, and Figure 32 for scenarios with reaction and sorption, reaction only, and sorption only, respectively. From these profiles deeper oxygen diffusion is observed when only sorption in simulated, suggesting degradation is limited to oxygen diffusion.

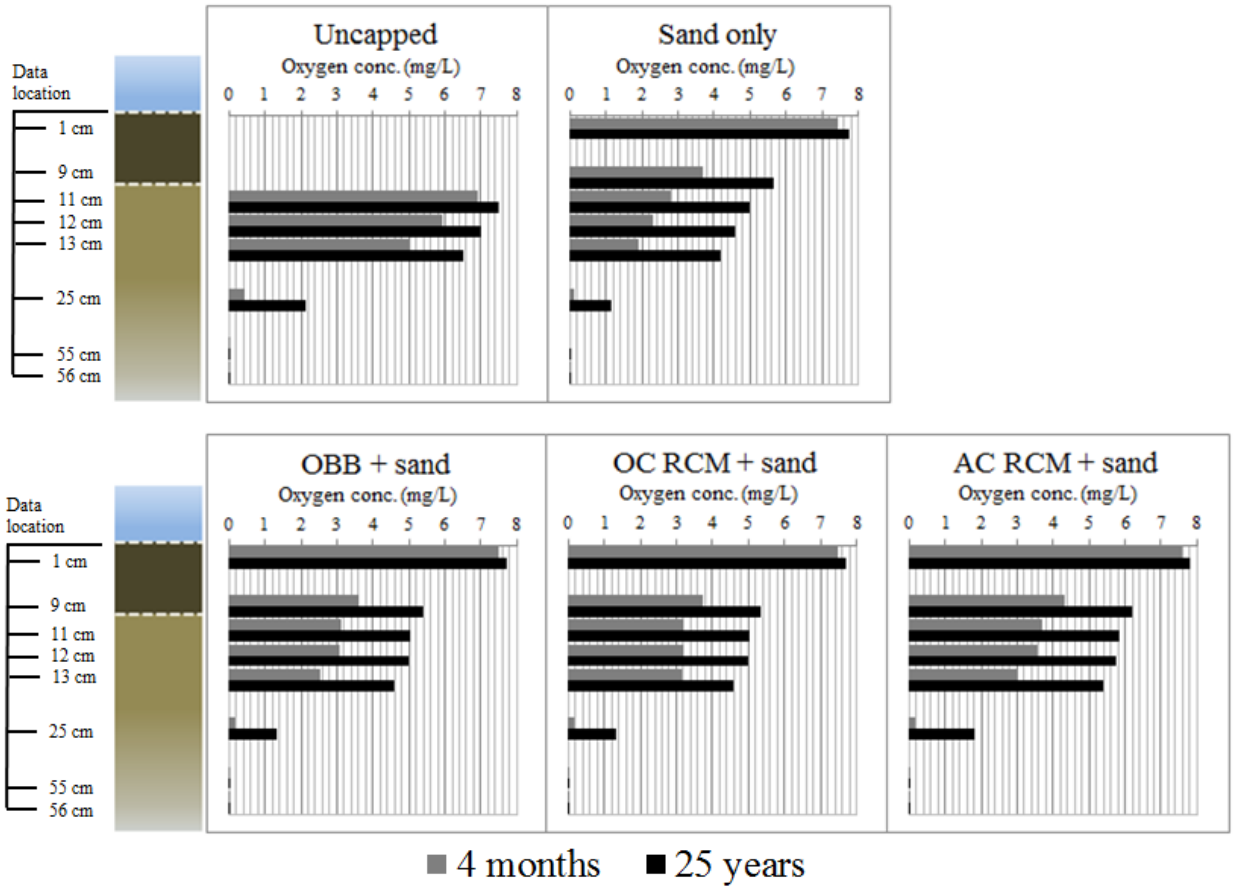

Figure 30. Oxygen porewater concentration profiles from scenario E (reaction and sorption). Note the following abbreviations: Oleophilic BioBarrier (OBB), Organoclay Reactive Core Mat (OC RCM), Activated Carbon Reactive Core Mat (AC RCM).

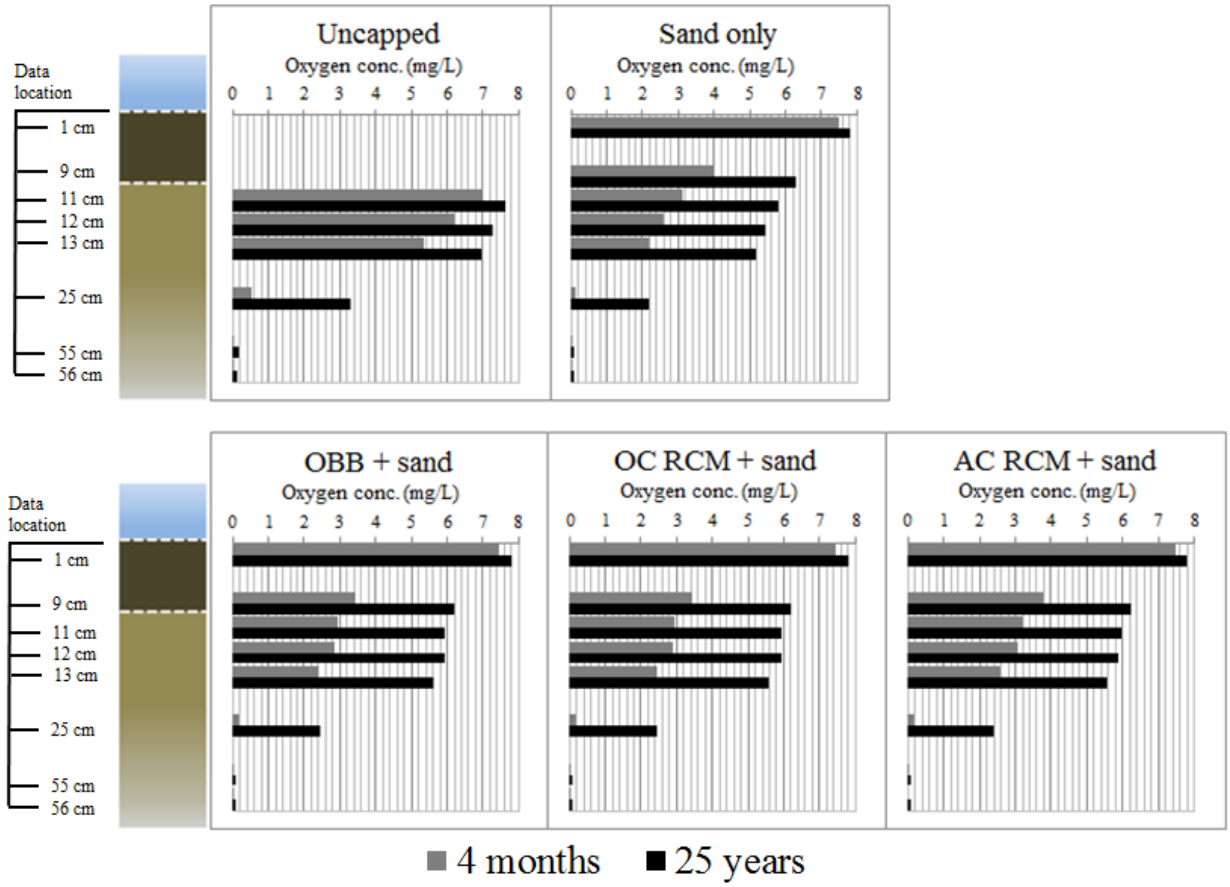

Figure 31. Oxygen porewater concentration profiles from scenario D (reaction only). Note the following abbreviations: Oleophilic BioBarrier (OBB), Organoclay Reactive Core Mat (OC RCM), Activated Carbon Reactive Core Mat (AC RCM).

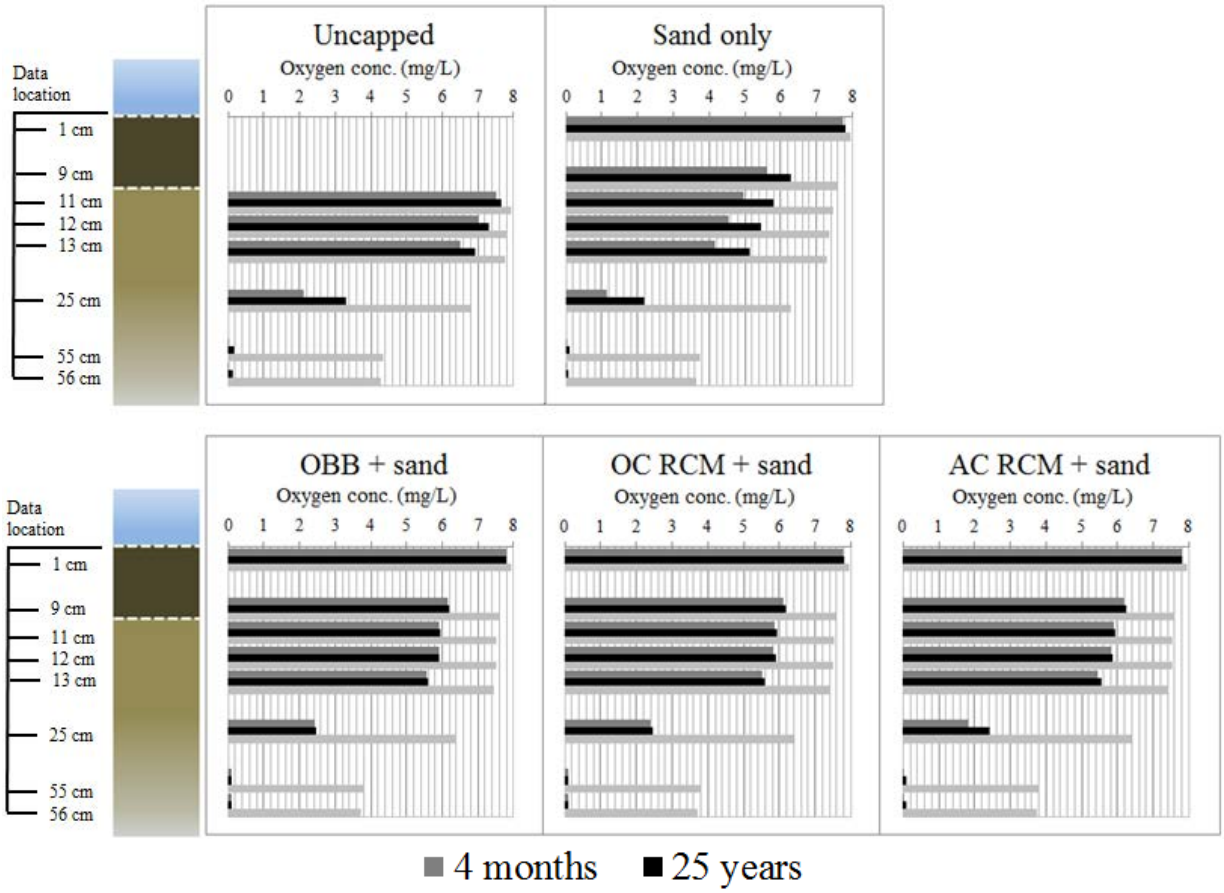

Figure 32. Oxygen porewater concentration profiles from scenario C (sorption only). Note the following abbreviations: Oleophilic BioBarrier (OBB), Organoclay Reactive Core Mat (OC RCM), Activated Carbon Reactive Core Mat (AC RCM).

5. SUMMARY AND CONCLUSIONS

This chapter summarizes the preceding chapters, beginning with the main ideas as well as an overview of the results. Second, suggestions for future work are discussed.

5.1. Main Ideas, Results, and Discussion

The motivation for this thesis was founded on valuing sustainable remediation, having an awareness of the diverse and complex nature of aquatic sediments, and the concern that existing sediment remedies were not leveraging the potential for aerobic degradation at groundwater-surface water interfaces. A sorption study was conducted to characterize cap materials. Column studies were utilized to compare capping impacts on contaminant breakthrough and longevity in underlying sediment. Lastly, modeling was conducted to explore processes at larger time frames and compare the effects of modeling sorption and reaction.

5.1.1. *Sorption Study*

The sorption study was completed in triplicate at BTEX concentrations over three orders of magnitude to determine Langmuir isotherm coefficients for benzene sorption onto AC RCM, OC RCM, and OBB. Although sand (0% organic carbon) and glass materials were considered in this thesis, their sorptive capacities were negligible. As expected, the AC RCM was the strongest sorbent for dissolved phase benzene. Isotherm coefficients resulting from this study were used as model inputs for CapSim 3.2a.

5.1.2. *NAPL Column Study*

A NAPL column study was conducted to compare the retention capacity of AC RCM + sand, OC RCM + sand, OBB + sand, and sand only caps. Diesel was injected into the bottom of capped sand columns at 5 ml per day. Water columns above the caps were monitored for diesel breakthrough. The uncapped control was the first column to release diesel to the overlying water. The sand only capped column broke through next, followed by the AC RCM + sand and OBB + sand capped columns. The OC RCM + sand capped column was the last to breakthrough. These results were expected as the OC RCM material is designed to target NAPL. However, each cap broke through showing that absent degradation and in the presence of a constant source, each capping condition considered will fail. This highlights the importance of considering degradation in remediation of petroleum-impacted sediments. Depletion through degradation, rather than retention through sorption, could increase the longevity of cap design.

Additionally, pictures were captured every two hours throughout the NAPL column study and merged to create a video of diesel transport. Instead of plug flow, fingering patterns through the columns were observed. This underscores the potential for premature cap failure, as the sorptive material is loaded primarily at these “hot spots,” possibly leaving some regions of the cap underutilized.

5.1.3. *Sediment Column Study*

In addition to the NAPL column study, a more extensive sediment column study was conducted. For this experiment, tidal river sediments from an impacted field site were homogenized, spiked with BTEX, and loaded into a series of eight columns. Sand, glass + sand, OBB + sand, OC RCM

+ sand caps were placed, as well as three AC RCM + sand caps, leaving one column uncapped. Porewater concentrations of benzene were monitored at three depths within the sediment columns over four months. At the end of the four months, the columns were frozen at -20° C, then cut into one-inch thick "hockey pucks" which were quartered and preserved for analyses of total benzene concentration, methane saturation, porosity, and microbial DNA community.

Benzene concentrations from porewater samples were largely inconclusive although there was a general trend of concentration decrease over time. Total benzene concentrations from hockey puck sampling indicated the caps had the largest influence within the first 10 cm of sediment as variations in underlying sediments were most distinct between capping conditions within the first 10 cm beneath the cap. Benzene concentrations within deeper regions of underlying sediment were indistinguishable by capping condition. Of all the columns, the upper-most layer of sediment in the glass + sand capped column had the highest concentration of benzene suggesting that the glass may have hindered oxygen diffusion. Therefore, disconnecting surface water from underlying sediment may result in increasing contaminant longevity. Results from OBB + sand and OC RCM + sand capped columns are comparable and could be due to either sorption or biodegradation; RNA data would have been ideal for substantiating causation. Sediments from the AC RCM + sand capped column showed the lowest concentrations within the first 10 cm of sediment, which can be attributed to the sorptive capacity of activated carbon.

Methane was detected in all columns. There was no flow through these columns, so diffusion was the sole mechanism for oxygen delivery. Diffusion may not have been sufficient for maintaining aerobic conditions, leading methanogenic processes to dominate within these columns.

Microbial DNA analysis was conducted on a preliminary set of samples from glass + sand capped sediments, uncapped sediments, and initial sediment sampling. However, no significant differences were observed between these samples and further investigation seemed futile and suggests that four months was not long enough to change the microbial community on the DNA level. Microbial RNA analysis is generally more effective at detecting changes in communities; unfortunately, these methods were not thoroughly developed at the time of sampling.

Overall, the sediment column study was initiated with the hope of distinguishing underlying sediment conditions based on cap materials. Although some differences were observed between columns, results herein are inconclusive regarding the impact individual capping materials have on underlying sediments. Insignificant differences in underlying sediments were likely due to no-flow conditions within the columns and insufficient oxygen delivery via diffusion. Tidal oscillations likely have a larger role in oxygen delivery than previously recognized and therefore may have a greater impact on contaminant longevity in sediments compared to oxygen delivery via diffusion alone. Further, frozen column analyses were the most informative and should be built upon for use in future studies. Longer experiment times are ideal for ensuring effects on underlying sediments are captured.

5.1.4. *Modeling*

Modeling efforts were focused on understanding the capacity of CapSim 3.2a and distinguishing the impact of incorporating sorption and/or biodegradation reactions. Modeling was also used as an attempt to examine impact of capping conditions at extended lengths of time. Simulations were carried out under capping conditions as established in column studies. Although results for all capping conditions were impacted by sorption, sorption proved most relevant in AC RCM

capped sediments. Additionally, sorption is most relevant over shorter times as sorption-only simulations resulted in lower benzene porewater concentrations than reaction-only simulations at four months. Degradation dominates in the long term as reaction-only simulations resulted in lower benzene porewater concentrations than sorption-only simulations at 25 years. Resulting profiles of benzene and oxygen concentrations suggested that degradation was diffusion-limited at a rate of 1 L/mmol-yr. Modeling results herein demonstrate the importance of prioritizing oxygen delivery in sustainably managing sediments.

In navigating CapSim 3.2a and assessing the output files, it became clear that this is a powerful tool for modeling capped sediments. Unfortunately, time prevented analysis of more complex simulations. Recommended simulations are discussed in the following section.

5.2. **Future Work**

The sediment column studies conducted for this thesis were an introductory comparison of the relative impact cap materials have on contaminant longevity and underlying sediment conditions. Additionally, preliminary modeling efforts primarily consisted of becoming familiar with the features and capacities of CapSim 3.2a. This section presents recommendations for advancing the work of this thesis.

5.2.1. ***Sediment Column Studies***

Sediment column studies were focused on determining the impact cap materials have on contaminant longevity and underlying sediment conditions. For simplicity, column studies were conducted in batch. However, it became evident that non-batch column studies would be more

constructive in illuminated the differences between cap materials as the influence of permeability and retention capacities would surface. Further, sediment environments are rarely stagnant and instead experience surface water flow, groundwater upwelling, and/or tidal oscillations. Replicating these hydraulic processes in the laboratory would provide valuable insight to processes occurring at field sites.

Data collection throughout this study included contaminant concentration monitoring through porewater sampling. During sampling events, ORP and pH measurements were attempted but gas bubbles within the porespace prevented accurate readings if any at all. Microelectrodes may have prevented this as they require smaller sample volumes for collecting measurements. Additionally, dissolved oxygen measurements with mircoelectrodes could have elucidated oxygen diffusion through cap materials. Further, monitoring microbial communities through time with aerobic count plates is recommended for future column studies. Aerobic count plates are useful for gaining insight on relative changes in microbial communities. Monitoring counts could help inform microbial activity over time and could highlight sediment regions for more extensive and costly microbial analysis.

These column studies were concluded with frozen column analyses of total contaminant concentrations, methane saturations, and microbial community. The microbial communities in a preliminary set of samples were assessed through DNA sequencing, but the results were uninformative. Microbial communities could have been better assessed through RNA analyses. Methods for RNA analyses are underdevelopment, but are a better measure of short-term activity and changes in microbial communities. Observing changes in microbial communities through DNA analyses requires longer times than allowed for this study.

5.2.2. *Modeling with CapSim 3.2a*

Time allowed for an introduction to CapSim 3.2a, but full utilization of the model was not feasible. First, reaction rates for biodegradation of contaminants deserve more attention. For this work, a relatively arbitrary value of 1 L/mmol-yr was used for benzene biodegradation. The model could be calibrated by adjusting the reaction rate given the availability of sufficient laboratory data. Then, with a reliable reaction rate, more advanced scenarios could be simulated.

Simulations with established cap materials were conducted under no-flow conditions and without bioturbation. Tidal oscillation, upwelling, and bioturbation features should be explored moving forward. Sensitivity to model inputs, like porosity and Langmuir isotherms, should also be well understood.

More extensive, steadfast modeling was partially inhibited because publications are still pending for the framework behind this model. If calibration and sensitivity analyses could be avoided, use of the model for simulated complex capping conditions for sediments impacted with multiple contaminants would be streamlined; particularly with literature to consult.

6. REFERENCES

Boulton, A. J., Findlay, S., Marmonier, P., Stanley, E. H., Valett, H. M. (1998), The functional significance of the hyporheic zone in streams and rivers. *Annual Review of Ecology, Evolution, and Systematics 29,* 59-81.

Bridges T. S., Ells S., Hayes D., Mount, D., Nadeau, S., Palermo, M., Patmont, C., Schroeder, P. (2008), The Four Rs of Environmental Dredging: Resuspension, Release, Residual, and Risk. Technical Report TR-08-4. U.S. Army Engineer Research and Development Center, Vickburg, MS.

Chakraborty, R. and Coates, J. (2004), Anaerobic degradation of monoaromatic hydrocarbons. *Applied Microbiology and Biotechnology 64(6),* 437-446

Chalfant, M. W. (2015), *Oleophilic BioBarriers for control of hydrocarbon sheens at groundwater-surface water interfaces*, CSU Thesis, Colorado State University Libraries.

Clean Water Act of 1972, 33 U.S.C. § 1251 et seq. (2002). Retrieved from http://epw.senate.gov/water.pdf

Coates, J. D., Anderson, R. T., Woodward, J. C., Phillips, E. J. P., and Lovley, D. R. (1996), Anaerobic hydrocarbon degradation in petroleum-contaminated harbor sediments under sulfate-reducing and artificially imposed iron-reducing conditions. *Environmental Science and Technology*, *30*(9), 2784–2789.

CRC Handbook of Chemistry and Physics (2014), CRC Press, West Palm Beach, FL.

Das, N., Chandran, P. (2011), Microbial degradation of petroleum hydrocarbon contaminants: an overview. *Biotechnology Research International*

Fenchel T., Jorgensen B. B. (1977). Detritus food chains of aquatic systems: the role of bacteria. *Advances in Microbial Ecology*. Plenum Press.

Fry, J. C. (1982), *Methods in aquatic bacteriology*. John Wiley & Sons.

Glud, R.N. (2008), Oxygen dynamics of marine sediments. *Marine Biology Research, 4,* 243-289.

Gutknecht, J., Bisson, M. A., and Tosteson, F.C. (1977), Diffusion of Carbon Dioxide through Lipid Bilayer Membranes: Effects of Carbonic Anhydrase, Bicarbonate, and Unstirred Layers. *The Journal of General Physiology 69(6),* 779-794.

Hawkins, A. M. (2013). *Processes controlling the behavior of LNAPLs at groundwater surface water interfaces*, CSU Thesis, Colorado State University Libraries.

Himmelheber, D., Pennel, K., and Hughes, J. (2007), Natural attenuation processes during in situ capping. *Environmental Science and Technology 41(15),* 5306-5313.

Irianni-Renno, M., Akhbari, D., Olson, M.R., Byrne, A.P., Lefèvre, E., Zimbron, J., Lyverse, M., Sale, T.C., De Long, S.K. (2016), Comparison of bacterial and archaeal communities in depth-resolved zones in an LNAPL body. *Applied Microbiology and Biotechnology, 100(7),* 3347-3360.

Jamison, V. M., Raymond, R. L., Hudson Jr., J. O. (1975), Biodegradation of high-octane gasoline in groundwater. *Developments in Industrial Microbiology 16,* 305-312.

Jury, W.A. and Horton, R. (2004), *Soil Physics* (6^{th} ed.). John Wiley & Sons.

Kiaalhosseini, S., Johnson, R. L., Rogers, J. C., Irianni Renno, M., Lyverse, M., Sale, T. C. (2016), Cryogenic Core Collection (C_3) from Unconsolidated Subsurface Media. *Groundwater Monitoring and Remediation 36(4),* 41-49.

Leahy, J. and Colwell, R. (1990), Microbial Degradation of Hydrocarbons in the Environment. *Microbiological Reviews 54(3),* 305-315.

National Oceanic and Atmospheric Administration (NOAA), U.S. Department of Commerce. https://www.esrl.noaa.gov/gmd/ccgg/trends/

National Research Council (2007), Sediment Dredging at Superfund Megasites: Assessing the Effectiveness. National AcademiesPress, Washington, DC.

Neill, M., Walsh, N., Lucey, J. (2014), Direct measurement of oxygen in river substrates, *Water and Environment Journal 28,* 566-571.

Magar, V. S., Wenning, R. J. (2007), The role of monitored natural recovery in sediment remediation. *Integrated Environmental Assessment and Management 2(1),* 66-74.

Moran, J. L. and Posner, J. D. (2014), Role of Solution Conductivity in Reaction Induced Charge Auto-Electrophoresis (Supplementary Information). *Physics of Fluids 26(4),* 1-7.

Palermo, M. and Hays, D. F. (2014), Sediment Dredging, Treatment and Disposal. *Processes, Assessment and Remediation of Contaminated Sediments*. Springer.

Perelo, L. W. (2010), Review: In Situ and Bioremediation of Organic Pollutants in Aquatic Sediments. *Journal of Hazardous Materials 177,* 81-89.

Reible, D. D. (2007), Anacostia Active Capping Demonstration Status, Slides.

Reible, D. D. (2014), Sediment and Contaminant Processes, *Processes, Assessment and Remediation of Contaminated Sediments*. Springer.

Reible, D. D. and Lampert, D. J. (2014), Capping for Remediation of Contaminated Sediments, *Processes, Assessment and Remediation of Contaminated Sediments*. Springer.

Schwarzenbach, R. P., Gschwend, P. M., and Imboden, D. M. (2003), *Environmental Organic Chemistry (2nd ed.)*. John Wiley & Sons, Inc., New Jersey.

Silberberg, M. S. (2009), *Chemistry (5th ed.).* McGraw-Hill Higher Education.

Sylvia, D. M., Fuhrmann, J. J., Hartel, P. G., and Zuberer, D. A. (2005), *Principles and Applications of Soil Microbiology (2nd ed.)*. Pearson Education Inc.

U.S. Energy Information Administration (2016), Product Supplied. Washington, DC. http://www.eia.gov/dnav/pet/pet_cons_psup_dc_nus_mbbl_a.htm

U.S. Environmental Protection Agency (2005), Contaminated Sediment Remediation Guidance for Hazardous Waste Sites. Office of Superfund Remediation and Technology Innovation.

U.S. Geological Survey. (2006), Fate and Transport of Petroleum Hydrocarbons in Soil and Ground Water at Big South Fork National River and Recreation Area

von Wedel, R. J., Mosquera, J. F., Goldsmith, C. D., Hater, G. R., Wong, A., Fox, T. A., Hunt, W. T., Paules, M. S., Quiros, J. M., and Wiegand, J. W. (1988), Bacterial biodegradation of petroleum hydrocarbons in groundwater: *in situ* augmented bioreclamation with encrichment isolates in California. *Water Science Technology 20,* 501-503.

Wilke, C. R. and Chang, P. (1955), Correlation of Diffusion Coefficients in Dilute Solutions. *AIChE Journal 1(2),* 264-270.

Winter, T. C., Harvey, J. W., Franke, O. L., and Alley, W. M. (2013), Ground Water and Surface Water A Single Resource. U.S. Geological Survey Circular 1139.

7. APPENDIX A

To ensure eliminating CO_2 speciation reactions did not alter results for benzene and oxygen concentrations, 100 cm of sediment was modeled with and without the speciation. For the case with speciation, the dissociation of carbonic acid into bicarbonate and hydrogen was assumed instantaneous (Gutknecht et al, 1977) and the formation of carbonic acid was taken as the rate-limiting step. The speciation was therefore simplified from

$$CO_2 + H_2O \rightarrow H_2CO_3 \rightarrow HCO_3^- + H^+$$

to solely

$$CO_2 + H_2O \rightarrow HCO_3^- + H^+$$

using the rate constant k = 3.7 x 10^{-3} s^{-1} for carbonic acid formation (Gutknecht et al, 1977). Further, bicarbonate concentration in the surface water was estimated using equilibrium relationships between species (Moran, 2014):

$$K_{H_2CO_3} = \frac{[H_2CO_3]}{[CO_2]} = 1.7x10^{-3} \quad (15)$$

$$K_{HCO_3^-} = \frac{[HCO_3^-][H^+]}{[H_2CO_3]} = 4.47x10^{-7} \quad (16)$$

Rearranging (15), and using [CO_2] from (13),

$$[H_2CO_3]_{SW} = 1.7x10^{-3}\,[CO_2]_{SW} = 2.31x10^{-8}M \quad (17)$$

Then, rearranging (16) and using $[H_2CO_3]$ from (17) and assuming pH = 7

$$[HCO_3^-] = \frac{4.47x10^{-7}[H_2CO_3]}{[H^+]} = 1.03x10^{-7}M \quad (18)$$

Multiplying the molecular weight of HCO_3^-, which is 61 g/mol (CRC Handbook), to (18) yields the surface water concentration of HCO_3^-, $C_{HCO_{3,SW}^-}$, in mg/L:

$$C_{HCO_{3,SW}^-} = [HCO_3^-]\, x\, MW_{HCO_3^-} = 0.0063\, mg/L \quad (19)$$

With the results from (14) and (19), the conditions for the simulations with and without CO_2 speciation are given in Table 10 and Table 11.

Table 10. Boundary and Initial Conditions for simulation without CO_2 speciation.

Layer	**Condition**	**Oxygen Concentration**	**Benzene Concentration**	**Carbon Dioxide Concentration**
Surface water	Fixed concentration	8 mg/L	0 mg/L	0.6 mg/L
Intermediate Sediments	Initial uniform concentration	0 mg/L	30 mg/L	0 mg/L
Underlying Sediments	Fixed concentration	0 mg/L	30 mg/L	0 mg/L

Table 11. Boundary and Initial Conditions for simulation with CO_2 speciation.

Layer	**Condition**	**Oxygen Concentration**	**Benzene Concentration**	**Bicarbonate Concentration**
Surface water	Fixed concentration	8 mg/L	0 mg/L	0.0063 mg/L
Intermediate Sediments	Initial uniform concentration	0 mg/L	30 mg/L	0 mg/L
Underlying Sediments	Fixed concentration	0 mg/L	30 mg/L	0 mg/L

Results for benzene concentrations from the case without CO_2 speciation did not differ from the case with CO_2 speciation, and therefore speciation was disregarded in subsequent scenarios.

8. APPENDIX B

The equation for molecular diffusion D (cm^2/s) from Wilke and Chang 1955

$$D = \frac{7.4x10^{-8}\, T\sqrt{\times MW}}{\eta V^{0.6}} \tag{20}$$

where temperature T is 291.15 K, the dimensionless association parameter × is 2.6 (Wilke and Chang, 1955), molecular weight MW of solvent is 18 g/mol, viscosity of solution η is taken as 1.063 cP, and solute molar volume V is 25.6 cm^3/g-mol for O_2 and 34 cm^3/g-mol for CO_2. Carrying out (20) for O_2 and CO_2 yields diffusion coefficients of 1.98e-05 cm^2/s and 1.67e-07 cm^2/s, respectively.

9. APPENDIX C

9.1. Bulk Density of Sand and Sediment

Frozen Column Analysis data was used to calculate bulk density ρ_b of sand and sediment using the following definition (Jury and Horton, 2004):

$$\rho_b = \frac{dry\ weight\ of\ sample\ (g)}{volume\ of\ sample\ (mL)} \tag{21}$$

9.2. Bulk Density of Cap Materials

Length, width, depth and mass were measured for samples of AC RCM, OC RCM, and OBB using a tape measure and an analytical balance (Denver Instrument, Bohemia, NY, USA). Results are provided in Table 12.

Table 12. Cap material dimensions.

Material	**Length (cm)**	**Width (cm)**	**Depth (cm)**	**Mass (g)**
Activated Carbon Reactive Core Mat	3.81	4.45	1	7.69
OrganoClay Reactive Core Mat	3.81	4.45	1	4.67
Oleophilic BioBarrier	3.81	4.45	1.2	4.41

The product of length, width, and depth of each sample was then taken to yield the volume of each sample, V_s. Results are provided in Table 13.

Table 13. Volume of cap material samples.

Material	**Volume of sample (cm^3)**
Activated Carbon Reactive Core Mat	16.95

OrganoClay Reactive Core Mat	16.95
Oleophilic BioBarrier	20.35

Then, bulk density ρ_b was calculated using the definition (21). presented in Section 9.1. Results are provided in Table 14.

Table 14. Bulk density of cap materials.

Material	**Bulk density ρ_b (g/cm^3)**
Activated Carbon Reactive Core Mat	0.454
OrganoClay Reactive Core Mat	0.275
Oleophilic BioBarrier	0.217

9.3. **Porosity of Sand and Sediment**

Porosity Φ of sand and sediment was determined by rearranging Equation 1.22 from Jury and Horton to yield:

$$\Phi = 1 - \frac{\rho_b}{\rho_s}$$

where density of solids ρ_s is assumed to be 2.65 g/cm^3.

9.4. **Porosity of Cap Materials**

Porosity of cap materials was determined volumetrically through measuring water displacement. Cap material samples of known volume V_{total} were placed into 50 mL of water. The volume of water displaced is equal to the volume of solids in the sample V_{solid}. The difference between these two volumes is equal to the volume of the voids V_{voids} (22). Results are shown in

Table **15**.

$$V_{voids} = V_{total} - V_{solids} \tag{22}$$

Then, the definition of porosity (23) can be used to determine the porosity of the cap material.

$$\Phi = \frac{V_{voids}}{V_{total}} \tag{23}$$

Table 15. Values and results from volumetric porosity calculations.

Material	**V_{total} (cm^3)**	**V_{solid} (cm^3)**	**V_{voids} ($cm^{3)}$**	**Φ**
Activated Carbon Reactive Core Mat	10	3	7	0.7
OrganoClay Reactive Core Mat	10	2	8	0.8
Oleophilic BioBarrier	12	3	9	0.75

10. APPENDIX D

Table 16. Sorption study results for benzene on the Oleophilic BioBarrier.

Concentration group	*Triplicate count*	"Effective" initial mass (mg)	Final concentration (mg/L)	Final mass (mg)	Sorbed mass (mg)	Sorbent mass (mg)	Sorbed concentration (mg/kg)
1	*1*	1.43	6.84	0.67	0.76	2.75	278
	2	0.98	7.14	0.70	0.28	2.49	111
	3	1.03	6.49	0.64	0.39	2.75	141
2	*1*	2.86	19.76	1.94	0.92	2.78	332
	2	2.97	21.69	2.13	0.85	2.54	334
	3	2.87	20.47	2.01	0.86	2.74	315
3	*1*	7.61	55.70	5.46	2.15	2.74	785
	2	6.95	50.99	5.00	1.96	2.88	679
	3	6.77	46.48	4.56	2.21	2.71	816
4	*1*	13.42	88.90	8.71	4.70	2.69	1,748
	2	12.87	91.06	8.92	3.95	2.65	1,489
	3	12.17	77.45	7.59	4.58	2.63	1,740
5	*1*	15.46	102.48	10.04	5.41	2.49	2,174
	2	15.63	96.81	9.49	6.14	2.82	2,178
	3	25.07	202.70	19.86	5.21	2.79	1,867
6	*1*	35.27	269.99	26.46	8.81	2.58	3,413
	2	31.42	250.30	24.53	6.89	2.79	2,471
	3	31.07	233.29	22.86	8.21	2.69	3,053
7	*1*	49.93	382.10	37.45	12.49	2.83	4,413
	2	46.07	393.86	38.60	7.47	2.79	2,677
	3	40.01	288.47	28.27	11.74	2.51	4,679
8	*1*	55.36	427.21	41.87	13.49	2.76	4,889
	2	49.10	358.28	35.11	13.99	2.81	4,978
	3	47.09	376.73	36.92	10.17	2.77	3,673
9	*1*	47.23	431.33	42.27	4.96	2.47	2,010
	2	44.57	400.40	39.24	5.33	2.41	2,211
	3	43.26	336.86	33.01	10.24	2.38	4,304
10	*1*	60.77	474.88	46.54	14.24	2.77	5,139
	2	56.50	436.55	42.78	13.72	2.6	5,278
	3	46.83	375.14	36.76	10.06	2.78	3,619

Table 17. Sorption study results for benzene on the OrganoClay Reactive Core Mat.

Concentration group	*Triplicate count*	"Effective" initial mass (mg)	Final concentration (mg/L)	Final mass (mg)	Sorbed mass (mg)	Sorbent mass (mg)	Sorbed concentration (mg/kg)
1	*1*	1.24	4.76	0.47	0.77	1.76	439
	2	0.89	6.33	0.62	0.27	1.77	152
	3	0.91	3.89	0.38	0.53	1.75	301
2	*1*	2.24	17.49	1.71	0.53	1.82	291
	2	2.03	16.97	1.66	0.37	1.76	208
	3	2.08	12.43	1.22	0.86	1.86	463
3	*1*	5.92	46.17	4.52	1.40	1.77	788
	2	5.69	44.90	4.40	1.29	1.81	712
	3	5.94	42.11	4.13	1.81	1.72	1,051
4	*1*	13.04	83.31	8.16	4.87	1.83	2,661
	2	13.17	85.28	8.36	4.81	1.72	2,795
	3	12.82	74.25	7.28	5.55	1.86	2,981
5	*1*	19.37	140.97	13.81	5.56	1.89	2,940
	2	21.59	168.80	16.54	5.04	1.75	2,882
	3	20.75	142.17	13.93	6.82	1.8	3,790
6	*1*	32.72	201.84	19.78	12.94	1.74	7,434
	2	33.53	191.87	18.80	14.72	1.89	7,790
	3	33.37	232.02	22.74	10.64	1.75	6,078
7	*1*	51.52	372.47	36.50	15.02	1.73	8,684
	2	49.45	356.13	34.90	14.55	1.77	8,218
	3	50.43	332.78	32.61	17.82	1.83	9,738
8	*1*	56.20	330.85	32.42	23.78	1.89	12,580
	2	53.04	358.27	35.11	17.93	1.83	9,799
	3	51.67	351.24	34.42	17.25	1.83	9,424
9	*1*	57.42	417.23	40.89	16.53	1.78	9,285
	2	63.82	416.90	40.86	22.96	1.9	12,084
	3	56.78	393.31	38.54	18.23	1.9	9,597
10	*1*	62.95	440.37	43.16	19.79	1.85	10,699
	2	64.26	405.62	39.75	24.51	1.79	13,694
	3	66.08	389.27	38.15	27.93	1.9	14,699

Table 18. Sorption study results for benzene on the Activated Carbon Reactive Core Mat.

Concentration group	*Triplicate count*	"Effective" initial mass (mg)	Final concentration (mg/L)	Final mass (mg)	Sorbed mass (mg)	Sorbent mass (mg)	Sorbed concentration (mg/kg)
1	*1*	1.56	0.08	0.01	1.55	1.72	903
	2	1.38	0.00	-	-	-	-
	3	1.27	0.00	-	-	-	-
2	*1*	3.02	0.00	-	-	-	-
	2	3.46	0.08	0.01	3.45	1.68	2,053
	3	3.13	0.05	0.01	3.13	1.83	1,708
3	*1*	9.38	1.00	0.10	9.29	1.71	5,431
	2	7.87	1.03	0.10	7.77	1.66	4,679
	3	8.57	0.67	0.07	8.50	1.87	4,546
4	*1*	18.36	2.50	0.25	18.11	1.74	10,410
	2	19.21	1.74	0.17	19.04	1.87	10,179
	3	16.40	0.73	0.07	16.33	1.77	9,227
5	*1*	26.69	3.32	0.33	26.36	1.64	16,075
	2	24.51	4.10	0.40	24.11	1.71	14,099
	3	31.24	5.88	0.58	30.67	1.73	17,728
6	*1*	41.01	6.71	0.66	40.35	1.85	21,812
	2	39.91	6.45	0.63	39.28	1.82	21,582
	3	-	-	-	-	-	-
7	*1*	40.41	5.58	0.55	39.86	1.69	23,586
	2	59.84	8.24	0.81	59.04	1.68	35,141
	3	69.49	12.58	1.23	68.26	1.63	41,876
8	*1*	77.25	14.22	1.39	75.86	1.6	47,413
	2	74.96	13.54	1.33	73.63	1.63	45,173
	3	69.87	9.87	0.97	68.90	1.81	38,068
9	*1*	66.81	13.85	1.36	65.45	1.83	35,767
	2	74.80	18.06	1.77	73.03	1.73	42,216
	3	65.63	13.03	1.28	64.35	1.69	38,079
10	*1*	71.31	11.41	1.12	70.19	1.79	39,212
	2	67.61	10.85	1.06	66.54	1.86	35,777
	3	77.24	17.30	1.70	75.55	1.69	44,702

11. APPENDIX E

Results from headspace analysis of the first and final porewater sampling events (12/11/2015 and 3/31/2016, respectively) are profiled in Figure 33. Further, changes in concentrations between these two sampling events are shown in Figure 34.

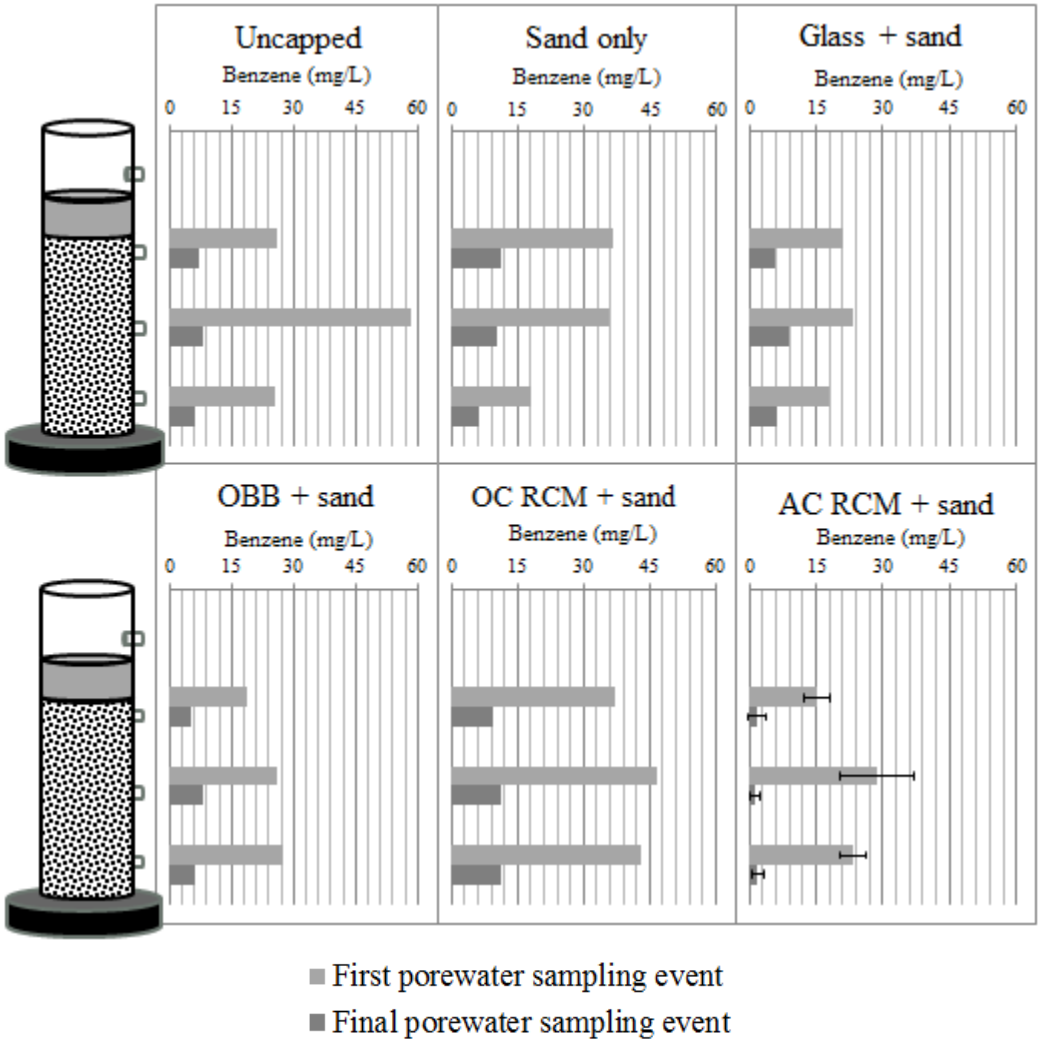

Figure 33. Benzene concentration profiles with results from the first and final porewater sampling events (12/11/2015 and 3/31/2016) per headspace analysis of samples.

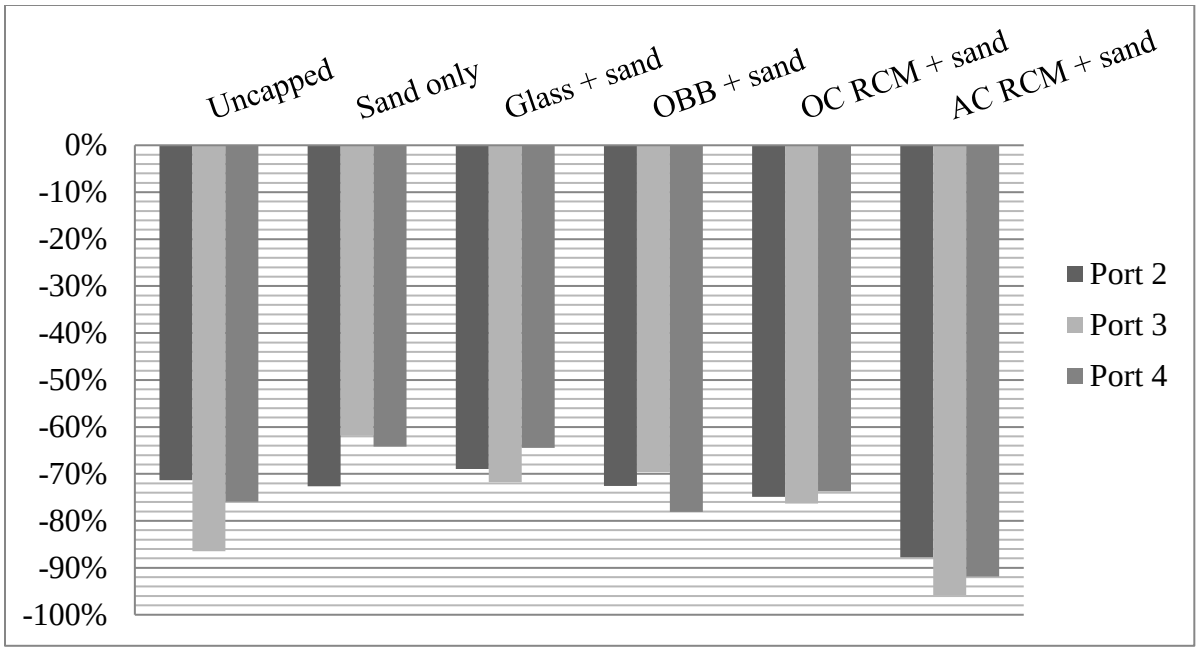

Figure 34. Benzene concentration changes at the three sediment sampling ports over four months per headspace analysis of porewater samples. Activated Carbon Reactive Core Mat (AC RCM) + sand is the triplicate average. Note the following abbreviations: Oleophilic BioBarrier (OBB), Organoclay Reactive Core Mat (OC RCM), Activated Carbon Reactive Core Mat (AC RCM).

12. APPENDIX F

Results from hexane extraction of porewater samples are provided in the following figures. Figure 35 shows benzene concentrations (mg/L) at each depth under each capping condition over time using data from hexane extractions of porewater samples. Additionally, this data is presented for Ports 2, 3, and 4 under each capping condition are presented in Figure 36, Figure 37, and Figure 38, respectively. These results are different from the headspace analysis data; however, the trends are similar.

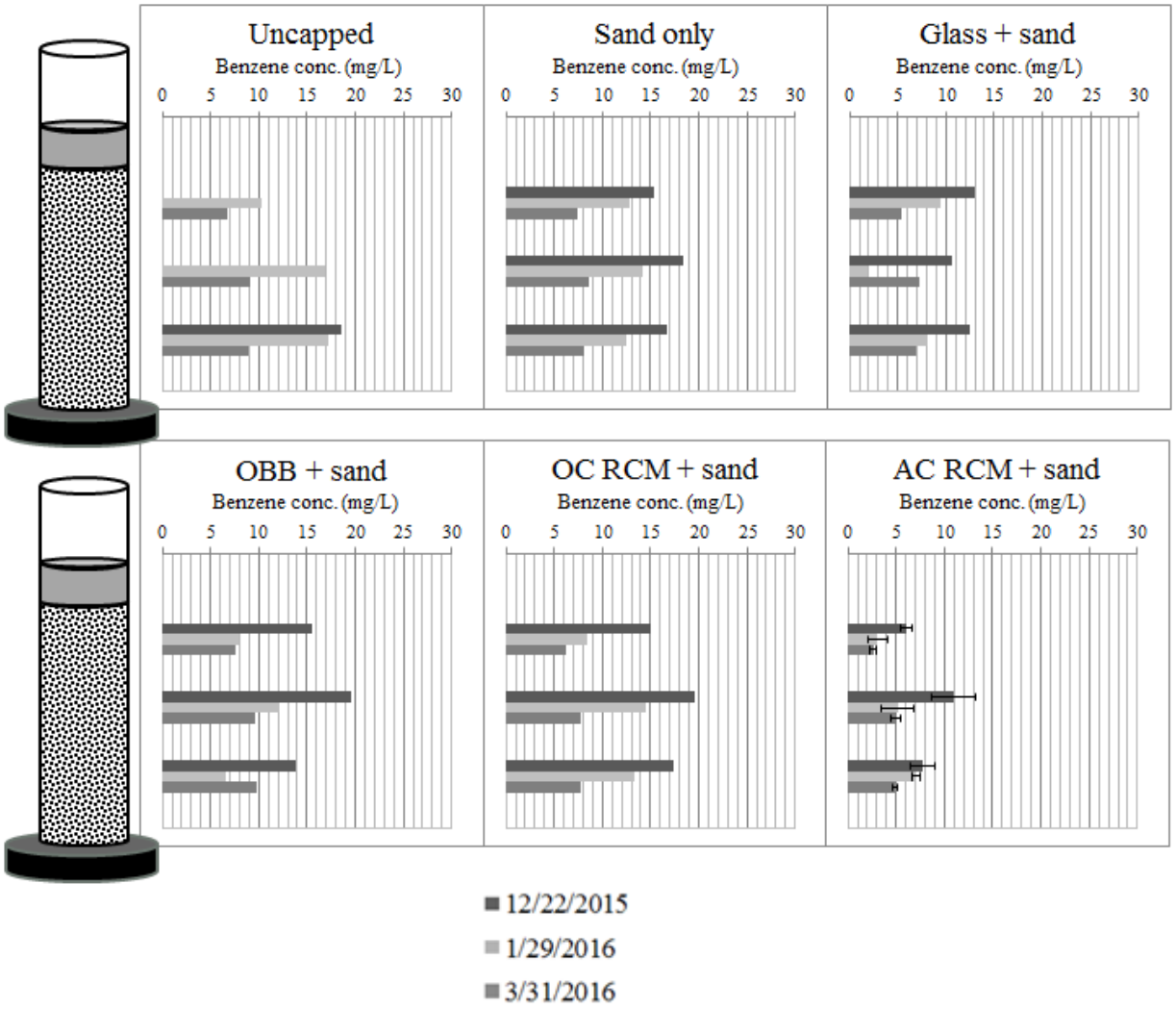

Figure 35. Benzene concentration profiles per hexane extractions over three month sampling period.

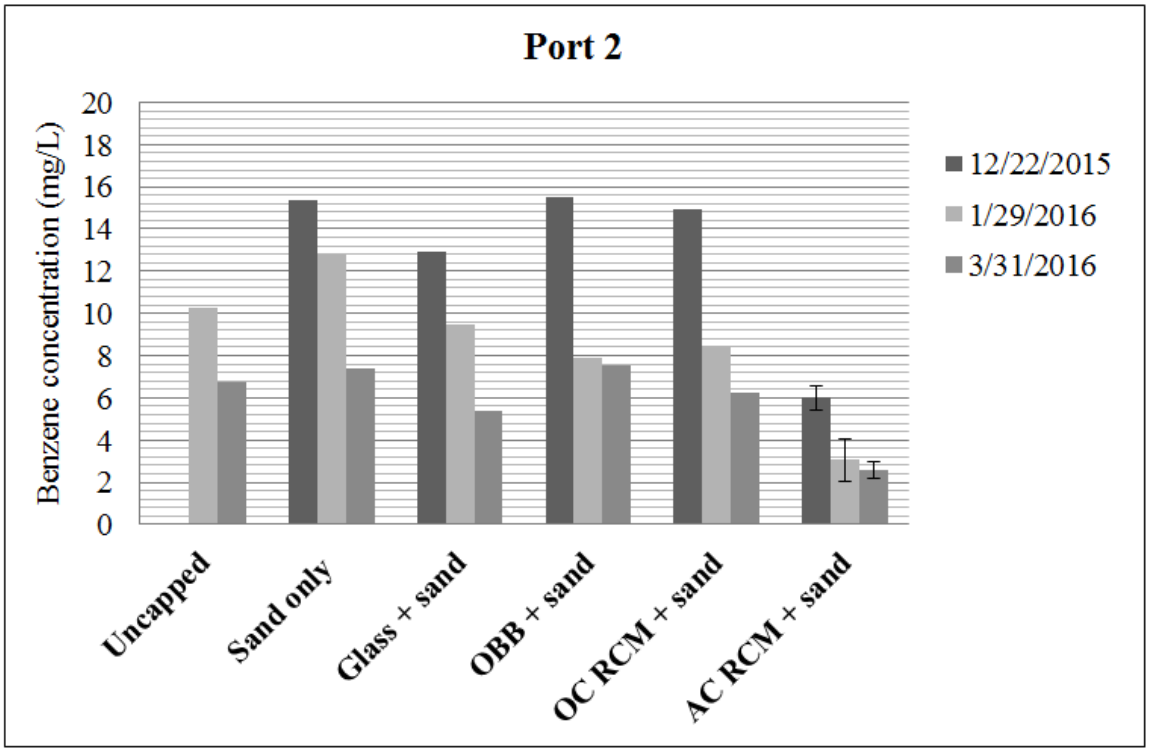

Figure 36. Benzene concentrations in Port 2 through time for all capping conditions per hexane extraction data. Activated Carbon Reactive Core Mat (AC RCM) + sand is the triplicate average. Note the following abbreviations: Oleophilic BioBarrier (OBB), Organoclay Reactive Core Mat (OC RCM), Activated Carbon Reactive Core Mat (AC RCM).

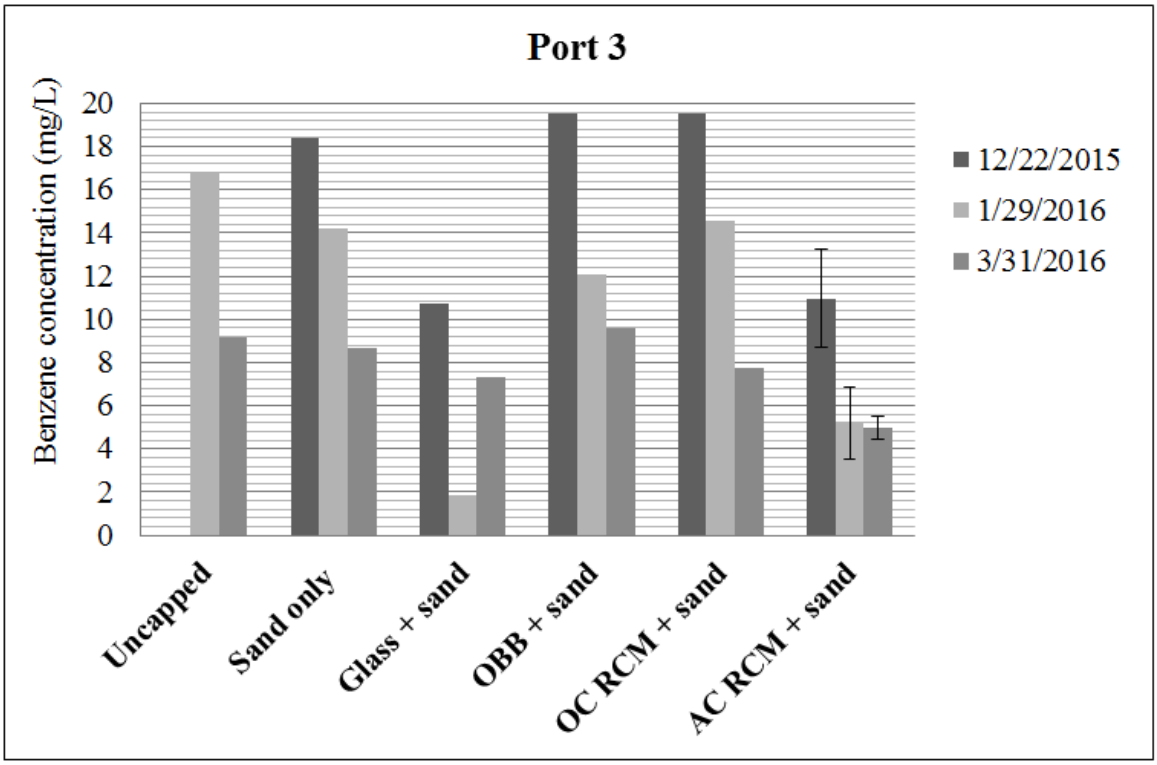

Figure 37. Benzene concentrations in Port 3 through time for all capping conditions per hexane extraction data. Activated Carbon Reactive Core Mat (AC RCM) + sand is the triplicate average. Note the following abbreviations: Oleophilic BioBarrier (OBB), Organoclay Reactive Core Mat (OC RCM), Activated Carbon Reactive Core Mat (AC RCM).

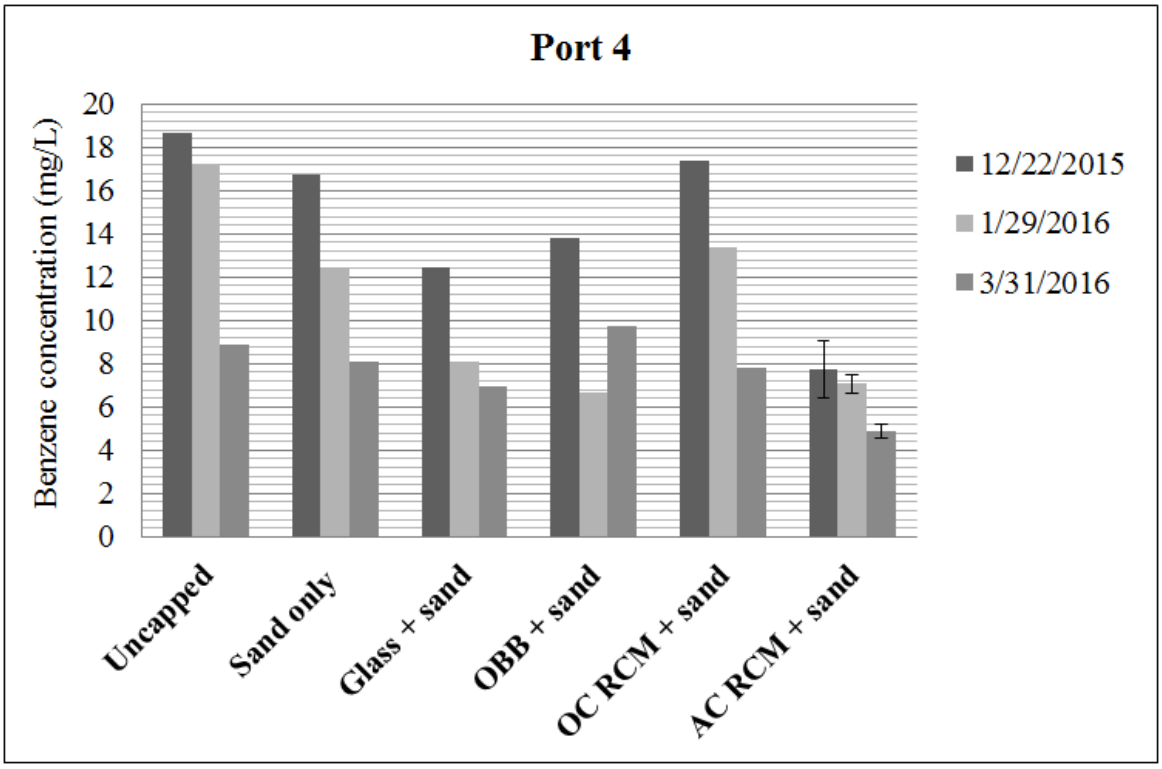

Figure 38. Benzene concentrations in Port 4 through time for all capping conditions per hexane extraction data. Activated Carbon Reactive Core Mat (AC RCM) + sand is the triplicate average. Note the following abbreviations: Oleophilic BioBarrier (OBB), Organoclay Reactive Core Mat (OC RCM), Activated Carbon Reactive Core Mat (AC RCM).

Additionally, benzene concentration changes over the three month period between the first hexane extractions to the final hexane extractions are given for each port under each capping condition in Figure 39.

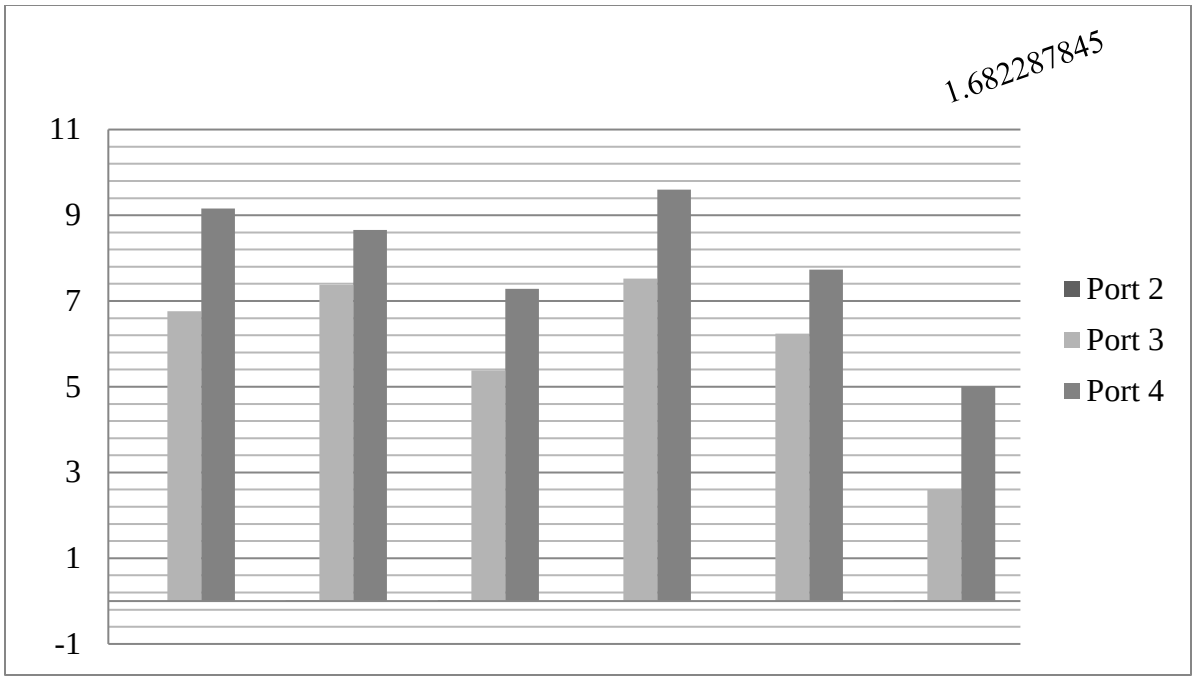

Figure 39. Benzene concentration changes at the three sediment ports over 3 months per hexane extraction data. Activated Carbon Reactive Core Mat (AC RCM) + sand is the triplicate average. Note the following abbreviations: Oleophilic BioBarrier (OBB), Organoclay Reactive Core Mat (OC RCM), Activated Carbon Reactive Core Mat (AC RCM).

13. APPENDIX G

This section contains DNA sequencing results for sediment samples from the glass + sand capped column, the uncapped column, as well as the initial sediment sampled prior to column loading.

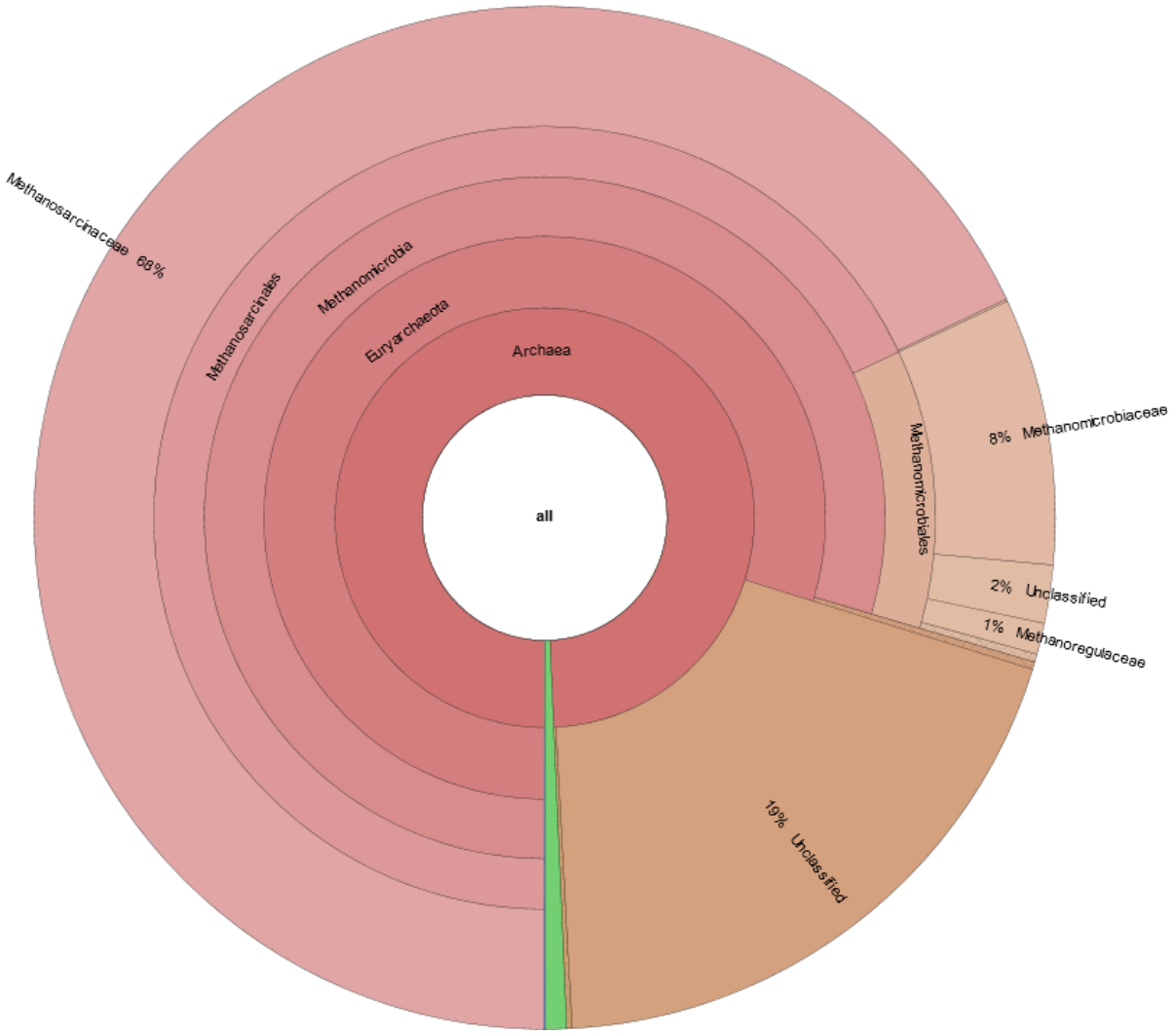

Figure 40. Archea hits in upper-most sediment sample from Glass + sand capped column.

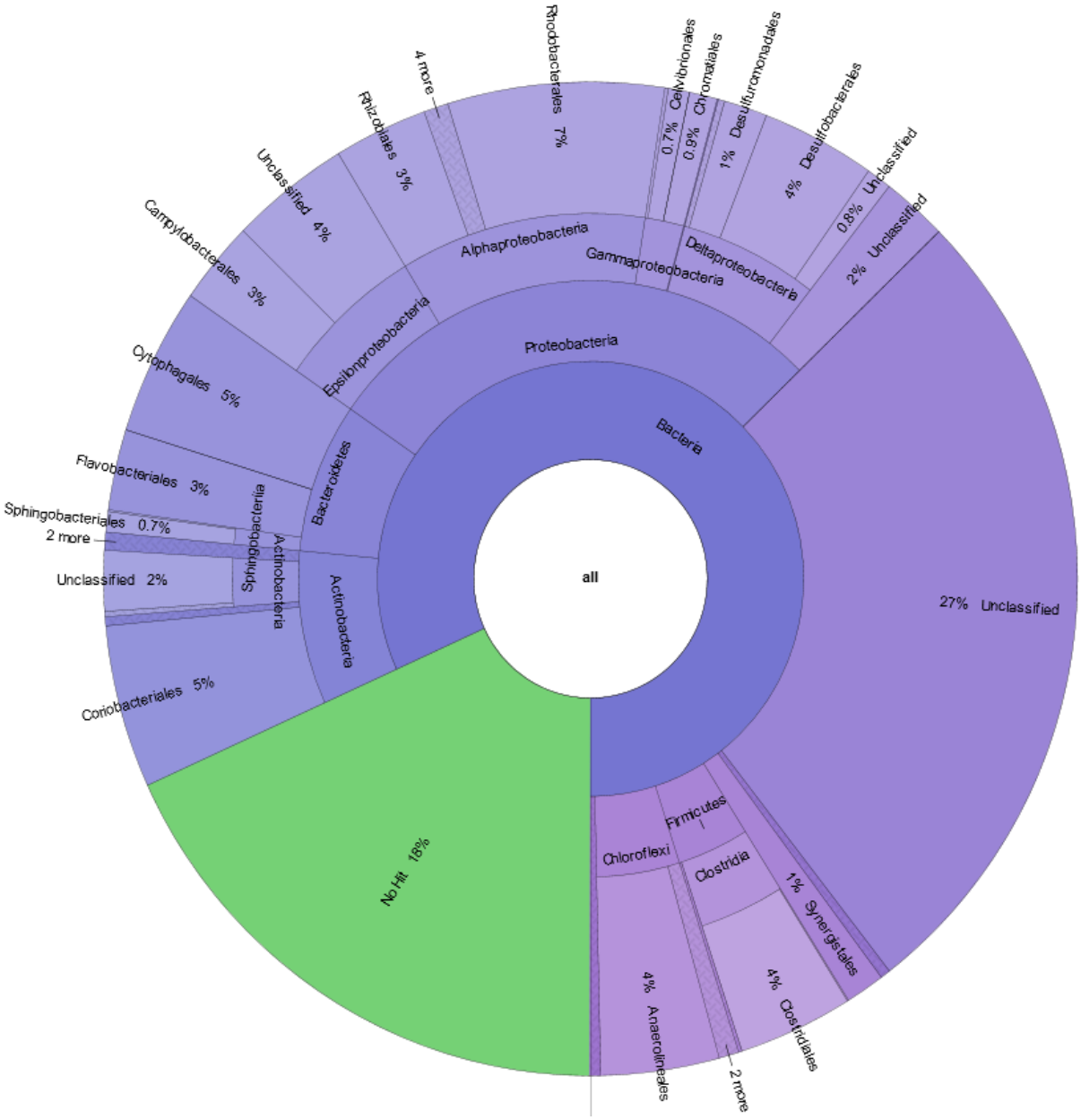

Figure 41. Bacteria hits in upper-most sediment sample from Glass + sand capped column.

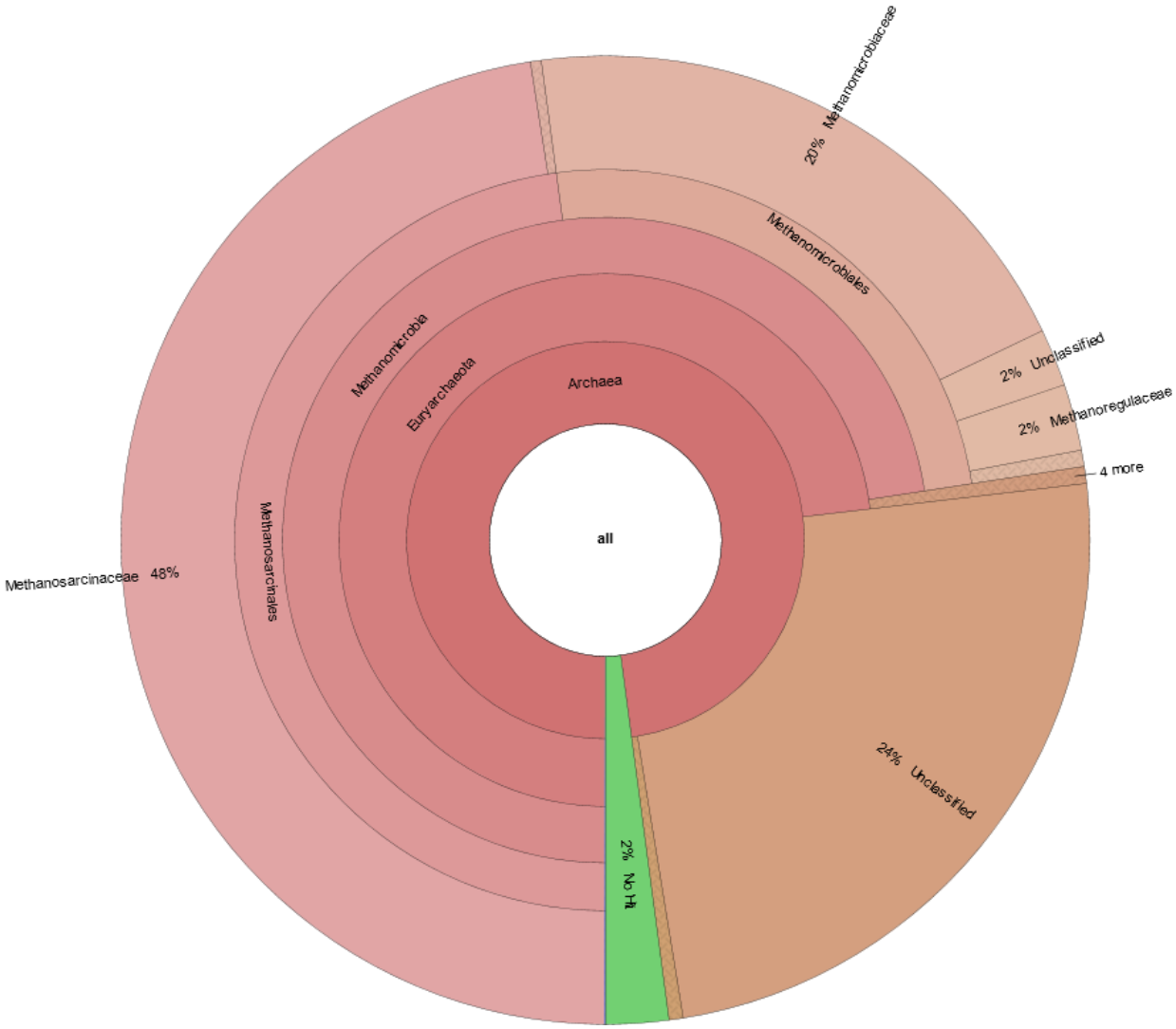

Figure 42. Archea hits in bottom-most sediment sample from Glass + sand capped column.

Figure 43. Bacteria hits in bottom-most sediment sample from Glass + sand capped column.

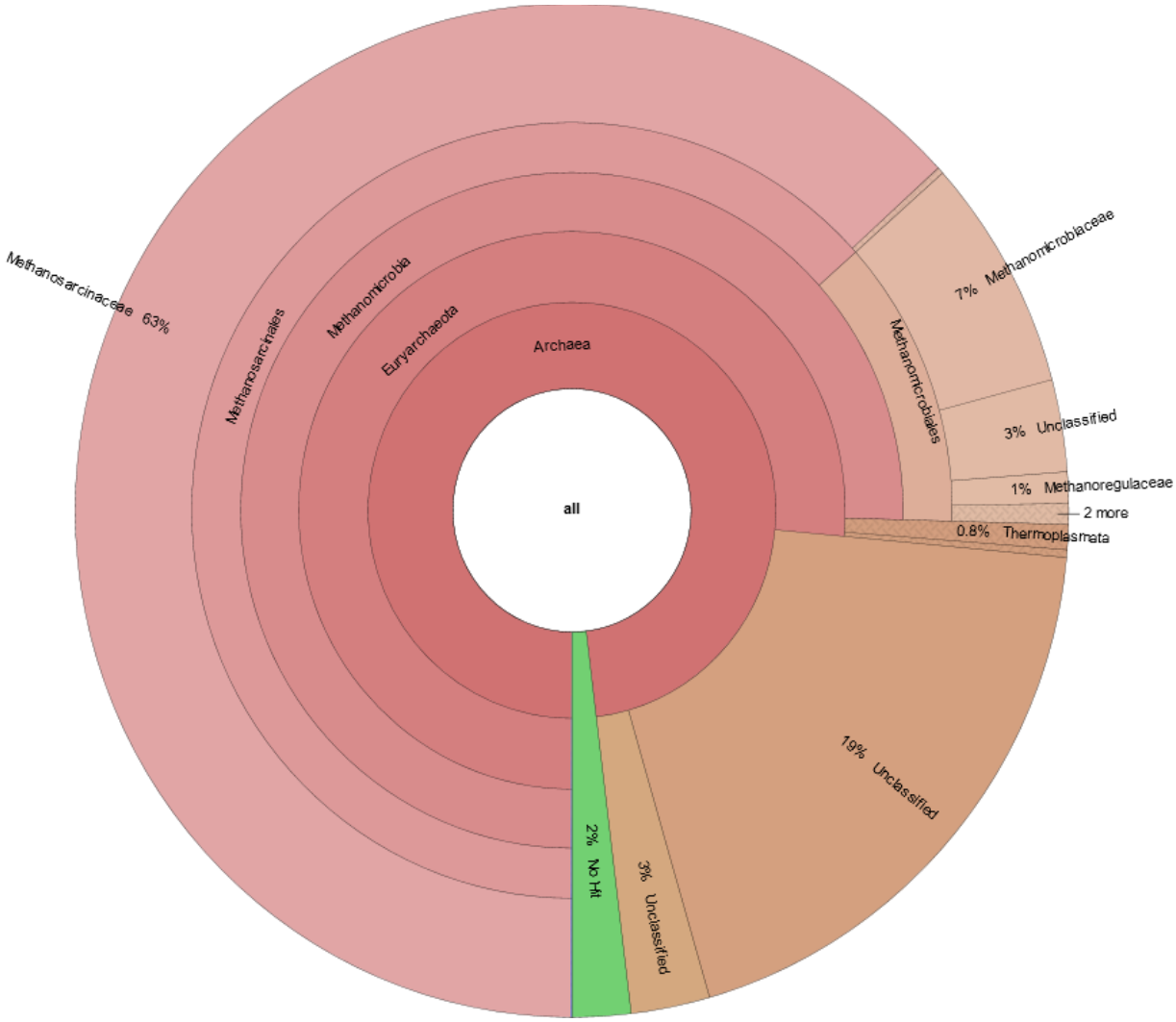

Figure 44. Archea hits in upper-most sediment sample from Uncapped column.

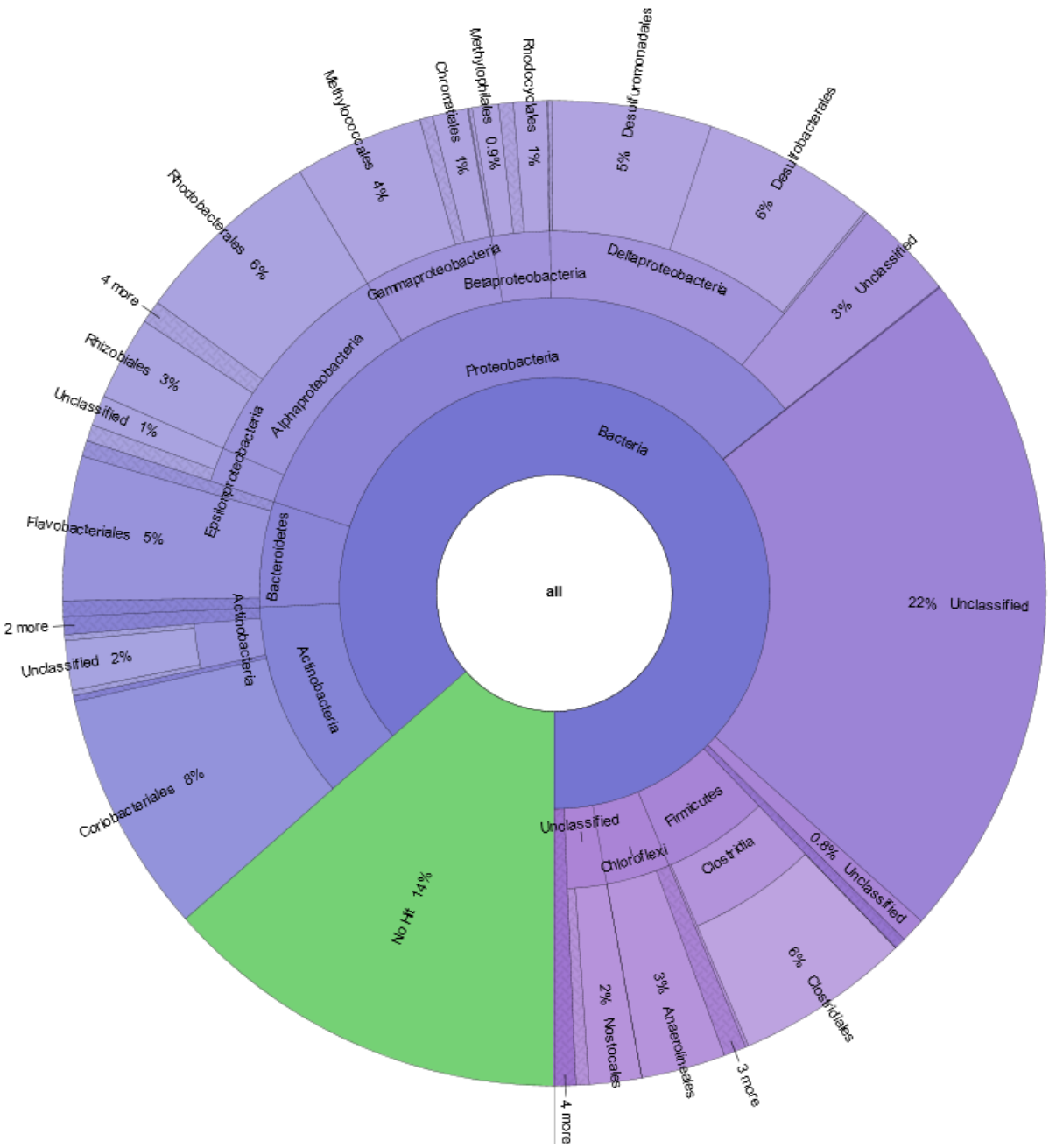

Figure 45. Bacteria hits in upper-most sediment sample from Uncapped column.

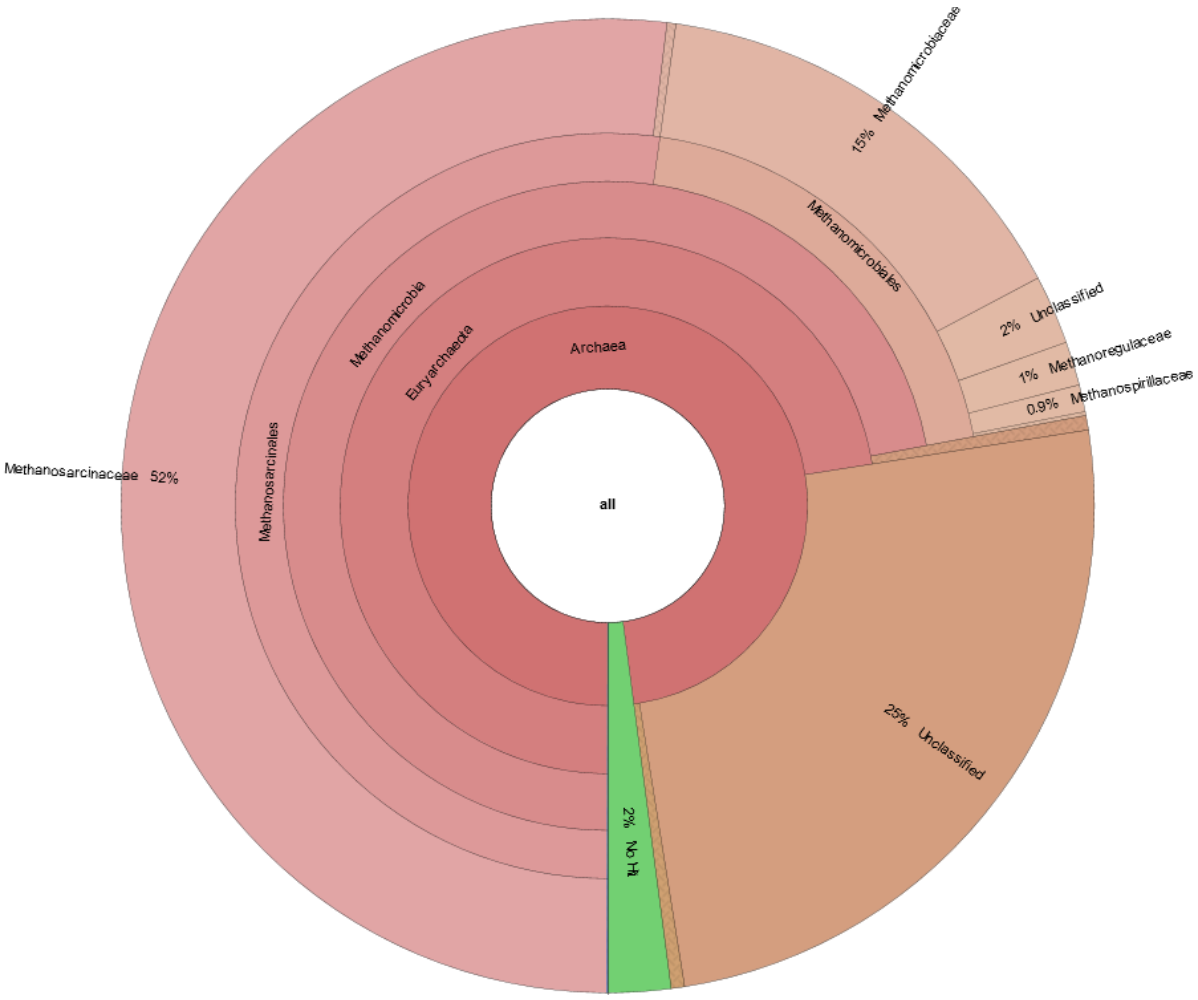

Figure 46. Archea hits in bottom-most sediment sample from Uncapped column.

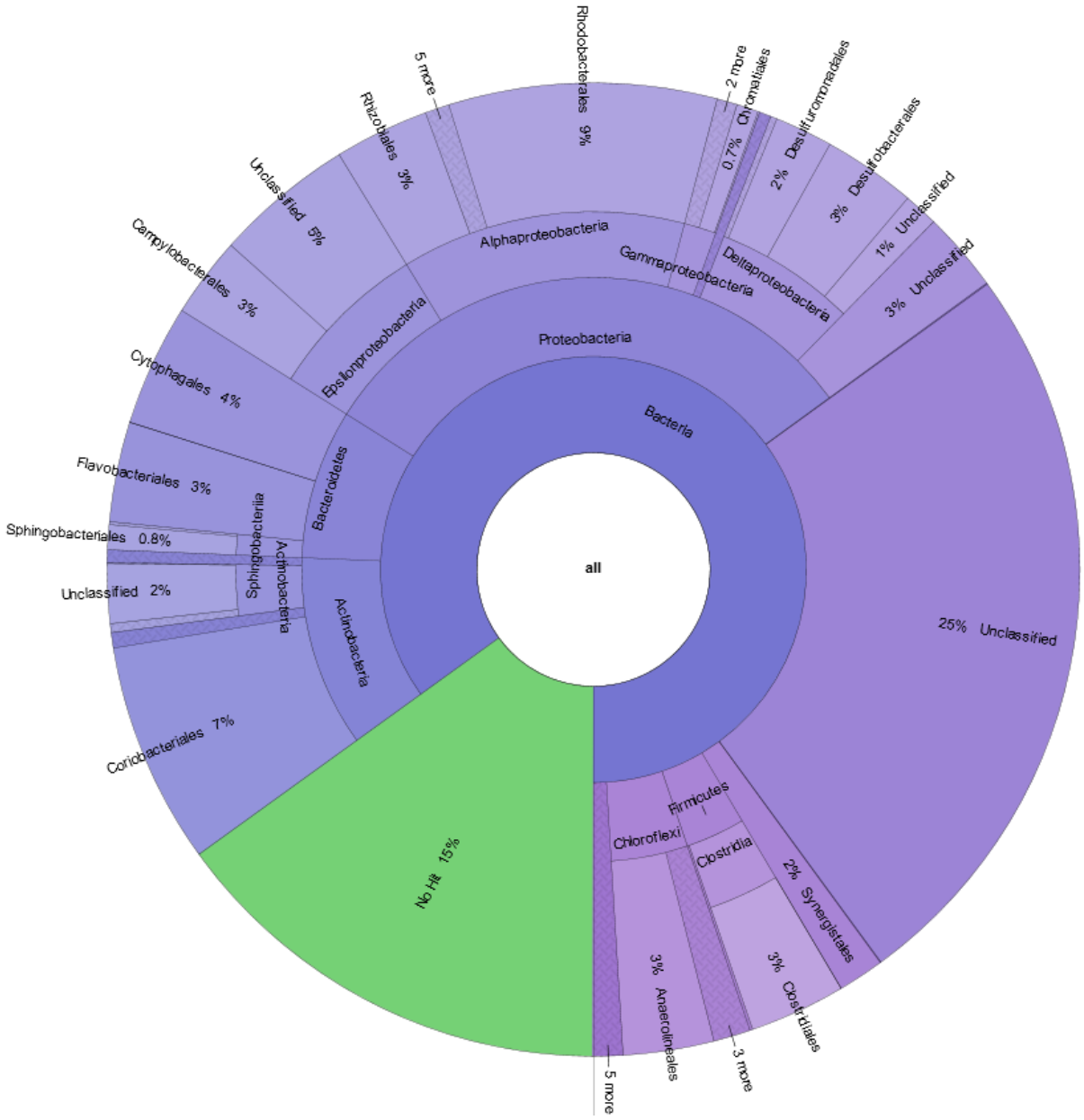

Figure 47. Bacteria hits in bottom-most sediment sample from Uncapped column.

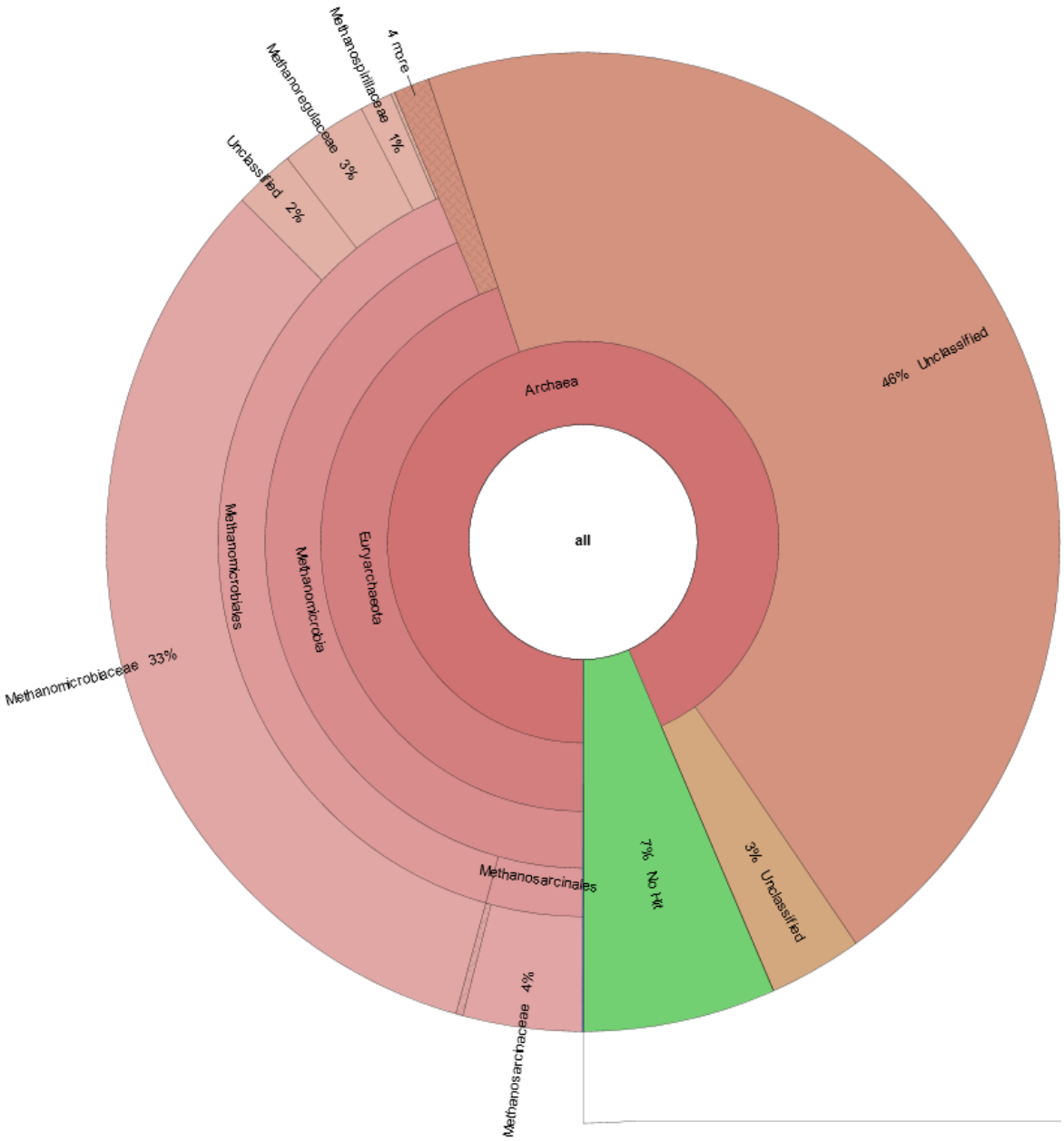

Figure 48. Archea hits in initial sediment sample.

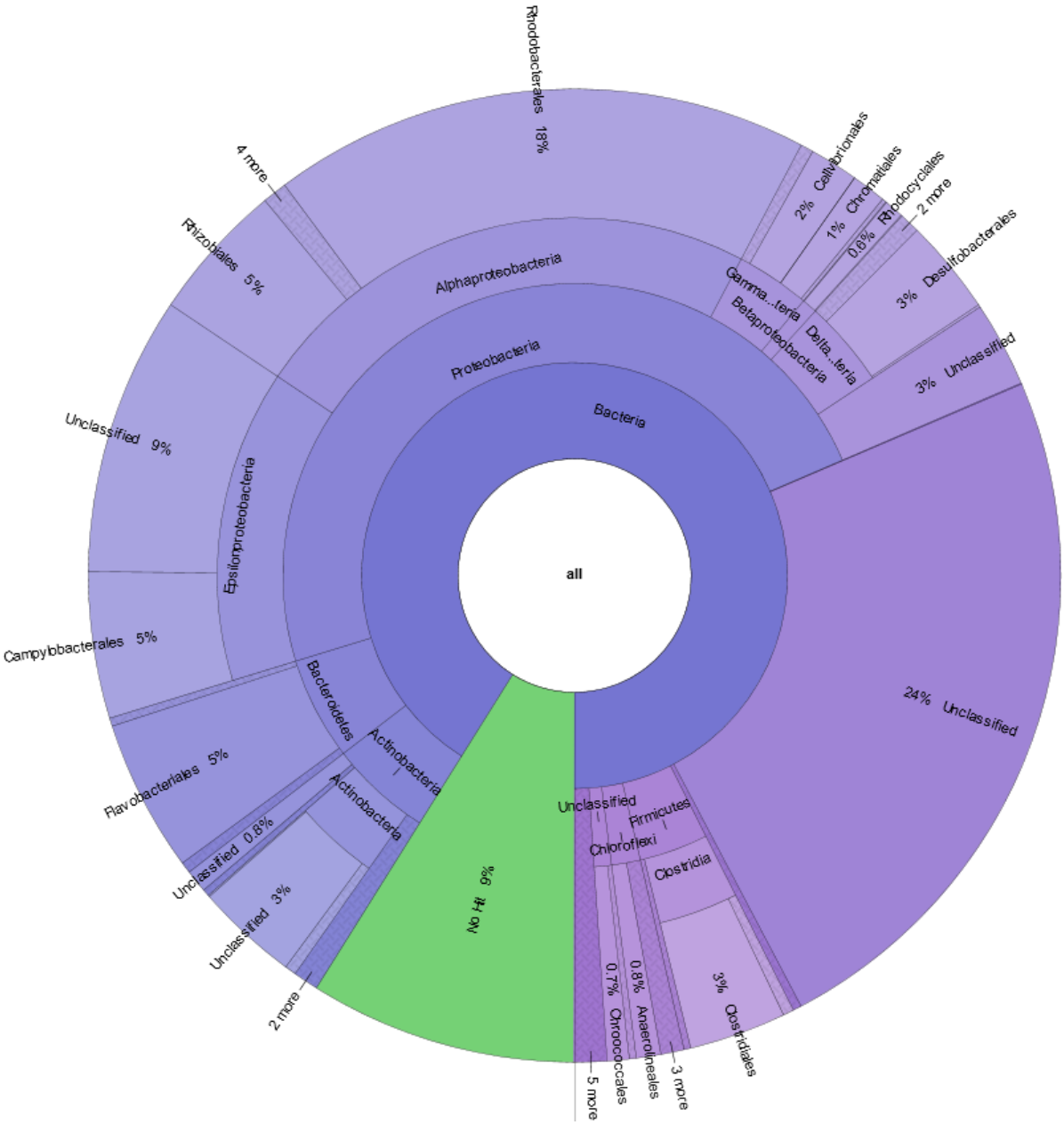

Figure 49. Bacteria hits in initial sediment sample.

14. APPENDIX H

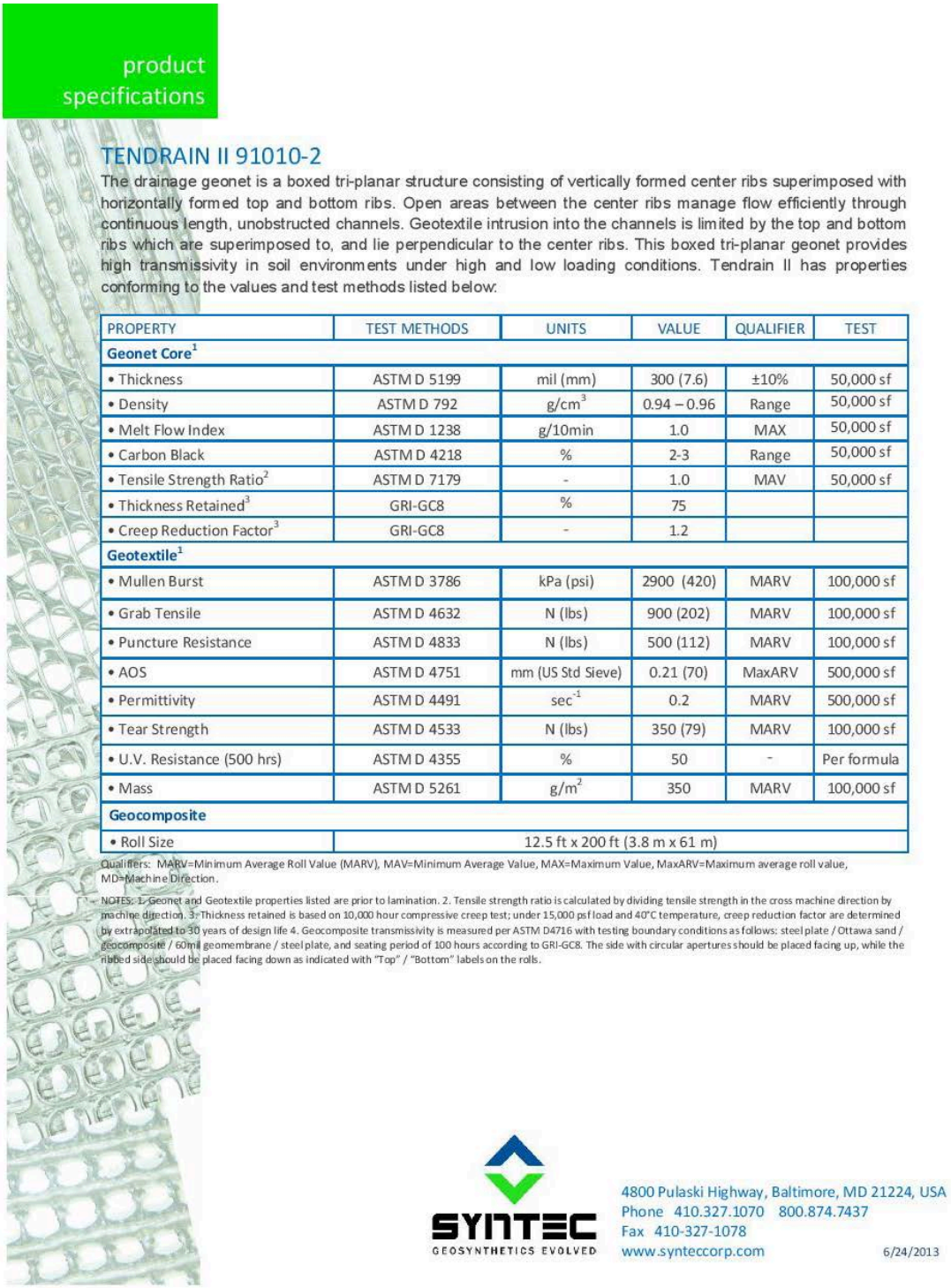

product specifications

TENDRAIN II 91010-2

The drainage geonet is a boxed tri-planar structure consisting of vertically formed center ribs superimposed with horizontally formed top and bottom ribs. Open areas between the center ribs manage flow efficiently through continuous length, unobstructed channels. Geotextile intrusion into the channels is limited by the top and bottom ribs which are superimposed to, and lie perpendicular to the center ribs. This boxed tri-planar geonet provides high transmissivity in soil environments under high and low loading conditions. Tendrain II has properties conforming to the values and test methods listed below:

PROPERTY	TEST METHODS	UNITS	VALUE	QUALIFIER	TEST
Geonet Core[1]					
• Thickness	ASTM D 5199	mil (mm)	300 (7.6)	±10%	50,000 sf
• Density	ASTM D 792	g/cm^3	0.94 – 0.96	Range	50,000 sf
• Melt Flow Index	ASTM D 1238	g/10min	1.0	MAX	50,000 sf
• Carbon Black	ASTM D 4218	%	2-3	Range	50,000 sf
• Tensile Strength Ratio[2]	ASTM D 7179	-	1.0	MAV	50,000 sf
• Thickness Retained[3]	GRI-GC8	%	75		
• Creep Reduction Factor[3]	GRI-GC8	-	1.2		
Geotextile[1]					
• Mullen Burst	ASTM D 3786	kPa (psi)	2900 (420)	MARV	100,000 sf
• Grab Tensile	ASTM D 4632	N (lbs)	900 (202)	MARV	100,000 sf
• Puncture Resistance	ASTM D 4833	N (lbs)	500 (112)	MARV	100,000 sf
• AOS	ASTM D 4751	mm (US Std Sieve)	0.21 (70)	MaxARV	500,000 sf
• Permittivity	ASTM D 4491	sec^{-1}	0.2	MARV	500,000 sf
• Tear Strength	ASTM D 4533	N (lbs)	350 (79)	MARV	100,000 sf
• U.V. Resistance (500 hrs)	ASTM D 4355	%	50	-	Per formula
• Mass	ASTM D 5261	g/m^2	350	MARV	100,000 sf
Geocomposite					
• Roll Size	12.5 ft x 200 ft (3.8 m x 61 m)				

Qualifiers: MARV=Minimum Average Roll Value (MARV), MAV=Minimum Average Value, MAX=Maximum Value, MaxARV=Maximum average roll value, MD=Machine Direction.

NOTES: 1. Geonet and Geotextile properties listed are prior to lamination. 2. Tensile strength ratio is calculated by dividing tensile strength in the cross machine direction by machine direction. 3. Thickness retained is based on 10,000 hour compressive creep test; under 15,000 psf load and 40°C temperature, creep reduction factor are determined by extrapolated to 30 years of design life 4. Geocomposite transmissivity is measured per ASTM D4716 with testing boundary conditions as follows: steel plate / Ottawa sand / geocomposite / 60mil geomembrane / steel plate, and seating period of 100 hours according to GRI-GC8. The side with circular apertures should be placed facing up, while the ribbed side should be placed facing down as indicated with "Top" / "Bottom" labels on the rolls.

SYNTEC GEOSYNTHETICS EVOLVED

4800 Pulaski Highway, Baltimore, MD 21224, USA
Phone 410.327.1070 800.874.7437
Fax 410-327-1078
www.synteccorp.com 6/24/2013

Figure 50. Geocomposite Product Sheet.

TECHNICAL REFERENCE

PHYSICAL PROPERTIES OF CETCO ORGANOCLAY® PM-100 PERTINENT TO USE IN PERMEABLE REACTIVE BARRIERS

CETCO PM-100 is a blend of 30% Organoclay adsorptive media and 70% Anthracite coal. Anthracite is chosen because its specific gravity is close to that of organoclay permitting homogenous mixing. The Anthracite provides spacing for the adsorptive media to prevent blinding off as the media adsorbs organics. The TOC for anthracite is approximately 63%, based on residual in TGA testing. CETCO can provide a mix ratio to meet your needs. Mixtures with Granular Activated Carbon can also be provided.

Particle Size Distribution

The (particle) size distribution (PSD) for PM-100 is 80% between .4 and 1mm with 20 percent passing the .4mm sieve. This distribution is dependant on the organoclay to anthracite mix ratio. The PSD for the anthracite and the pure organoclay (PM-199) is listed in the chart below. PSD can be varied to meet the project needs. CETCO can provide organoclay with maximum grain (particle) size of 3mm.

	Sieve (US standard)	mm	% Retained
Anthracite	10 mesh	2.00	0.0
	16 mesh	1.18	3.3
	18 mesh	1.00	12.6
	20 mesh	0.85	43.5
	25 mesh	0.71	27.5
	40 mesh	0.43	8.5
	Pan		4.6
PM-199	18 mesh	1.00	1% Max
	40 mesh	0.43	70% Min
	50 mesh	0.30	25% Max
	100 mesh	0.15	3% Max
	Pan		1% Max
PM-100	10 mesh	2.00	0.5% Max
	18 mesh	1.00	13% Max
	40 mesh	0.43	70% Min
	50 mesh	0.30	15% max
	Pan		2% Max

Hydraulic Conductivity

Hydraulic conductivity testing on PM-100 has shown an initial hydraulic conductivity of 1 x 10^{P-2P} cm per sec when tested at 25 psi confining stress. This result is for virgin media in fresh water. A decrease in permeability should be expected dependant as the media adsorbs contaminates. This is dependent on the contaminant of concern as well as the time and flow rates. It is recommended that project specific testing be conducted to ensure that the PRB will maintain adequate permeability over time.

Porosity

The porosity of PM-100 is approximately.55. This is based on a specific gravity of 1.8 for the PM-100 material and a bulk density of .78g/ml. The specific gravity for the PM-100 is 2.0 and for the anthracite is 1.66.

TR-802 revised 1/06

847.851.1800 | 800.527.9948

TR_802_AM_EN_201401_v1

CETCO® An AMCOL Company

www.CETCO.com

Figure 51. Bulk Organoclay Product Sheet.

REACTIVE CORE MAT™
WITH ORGANOCLAY®

DESCRIPTION
ORGANOCLAY® REACTIVE CORE MAT™ is a permeable composite of geotextiles and granular ORGANOCLAY that reliably adsorbs NAPL and low solubility organics from water. Batch isotherm testing by a university determined the following partition coefficients:

- Naphthalene, Kd = 3280 L/kg
- Phenanthrene, Kd = 117,000 L/kg
- Pyrene, Kd - 286,000 L/kg

REACTIVE CORE MAT™ is designed to provide a simple method of placing active materials into subaqueous sediment caps.

APPLICATION
ORGANOCLAY® REACTIVE CORE MAT™ is designed for use in the following applications:
- In situ subaqueous cap for contaminated sediments or post-dredge residual sediments
- Embankment seepage control
- Groundwater remediation

BENEFITS
- ORGANOCLAY® REACTIVE CORE MAT™ provides a reactive material that treats contaminants carried by advective/diffusive flow
- Reactive cap allows for thinner cap thickness than a traditional sand cap
- Geotextiles provide stability and physical isolation of contaminants

PACKAGING
15' by 100' rolls, packaged on 4" PVC core tubes wrapped with polyethylene plastic packaging.

AVAILABILITY
ORGANOCLAY® REACTIVE CORE MAT™ is available from the following CETCO plant locations:
- 92 Highway 37, Lovell, WY

TESTING DATA

PHYSICAL PROPERTIES		
PROPERTY	**TEST METHOD**	**RESULT**
ORGANOCLAY[1]		
Bulk Density Range	ASTM D 7481	44 – 58 lbs/ft³
Oil Adsorption Capacity	CETCO Test Method	0.5 lb of oil per lb of ORGANOCLAY, min
Quaternary Amine Content	ASTM D 7828	25 – 33% quaternary amine loading
FINISHED RCM PRODUCT		
ORGANOCLAY Mass per Area	CETCO Test Method	0.8 lb/ft²
Mat Grab Strength[2]	ASTM D4632	90 lbs. MARV
Hydraulic Conductivity[3]	ASTM D4491	1 x 10^{-2} cm/sec minimum

NOTES:
[1] ORGANOCLAY properties performed periodically on material prior to incorporation into the RCM
[2] All tensile testing is performed in the machine direction
[3] Permittivity at constant head of 2 inches and converted to hydraulic conductivity using Darcy's Law and RCM thickness per ASTM D5199 for geotextiles

North America: 847.851.1800 | 800.527.9948 | www.CETCO.com

UPDATED: NOVEMBER 2013 TDS_RCM-ORGANOCLAY_AM_EN_201311_v1

CETCO
OUR STANDARDS. YOUR PEACE OF MIND.
A Minerals Technologies Company

Figure 52. OrganoClay Reactive Core Mat Product Sheet.

Wastewater

Granular Activated Carbon - GAC 8x30

Filtration Media

CETCO's GAC 8x30 is a granular reactivated carbon made from select grades of bituminous coal. The activation process develops pores of molecular dimensions within the carbon particle giving the GAC extremely high internal porosity and surface area.

Application

Liquid phase applications where high surface area is needed for maximum adsorption

Features & Benefits

- Porous material manufactured from carbonaceous raw materials
- Meets ANSI/AWWA B-604 standards
- Suitable for hydraulic transfers and multiple thermal reactivation cycles
- Surface areas are in the range of 500 – 2,000 m^2/g

Technical Specifications

Properties	Value	Testing Method
Abrasion Number (min)	75	ASTM D3802
Moisture as Packed (max)	5%	ASTM D2867
Apparent Density (lbs./ ft^3)	31	ASTM D2854
Backwashed Apparent Density (lbs./ ft^3)	27	ASTM D2854
Mesh Size greater than 8 mesh (max) less than 30 mesh (max)	8 x 30 5% 5%	U.S. Sieve
Typical Surface Area (m^2/g)	1,050	BET N2
Ash Content (max)	12%	ASTM D2866
Iodine Number (mg/g)	900	AWWA B604

Figure 53. Bulk Activated Carbon Product Sheet.

REACTIVE CORE MAT™

WITH GRANULAR ACTIVATED CARBON CORE (GAC)

DESCRIPTION

REACTIVE CORE MAT™ GAC is an aqueous permeable composite of geotextiles and activated carbon that reliably adsorbs organics from water.

REACTIVE CORE MAT™ GAC is designed to provide a simple method of placing active materials into subaqueous sediment caps.

APPLICATION

REACTIVE CORE MAT™ GAC is designed for use in the following applications:

- In situ subaqueous cap for contaminated sediments or post-dredge residual sediments
- Embankment seepage control
- Groundwater remediation

BENEFITS

- REACTIVE CORE MAT™ GAC provides a reactive material that treats contaminants which are carried by advective or diffusive flow.
- Reactive cap allows for thinner cap thickness than a traditional sand cap.
- Geotextiles provide stability and physical isolation of contaminants.

TESTING DATA

PHYSICAL PROPERTIES		
PROPERTY	**TEST METHOD**	**RESULT**
ACTIVATED CARBON[1]		
Iodine Number	AWWA B604 or ASTM D4607	Min. 750 mg/g
FINISHED RCM PRODUCT		
Activated Carbon Mass per Area	Modified ASTM D5993	0.4 lb/ft²
Grab Strength[2]	ASTM D4632	80 lb. MARV
Permeability[3]	ASTM D 4491	1 x 10⁻³ cm/s min.

NOTES:

[1] Activated carbon properties performed prior to incorporation into the RCM

[2] All tensile testing in machine direction

[3] Permittivity at constant head of 2 inches and converted to hydraulic conductivity using Darcy's Law and RCM thickness per ASTM D5199 for geotextiles

PACKAGING

REACTIVE CORE MAT™ GAC is available in the following packaging option:

- 15' by 100' rolls, packaged on 4" PVC core tubes wrapped in polyethylene plastic

North America: 847.851.1800 | 800.527.9948 | www.CETCO.com

UPDATED: NOVEMBER 2013

TDS_RCM-GAC_AM_EN_201311_v1

CETCO

OUR STANDARDS. YOUR PEACE OF MIND.

A Minerals Technologies Company

Figure 54. Activated Carbon Reactive Core Mat Product Sheet.

15. APPENDIX I

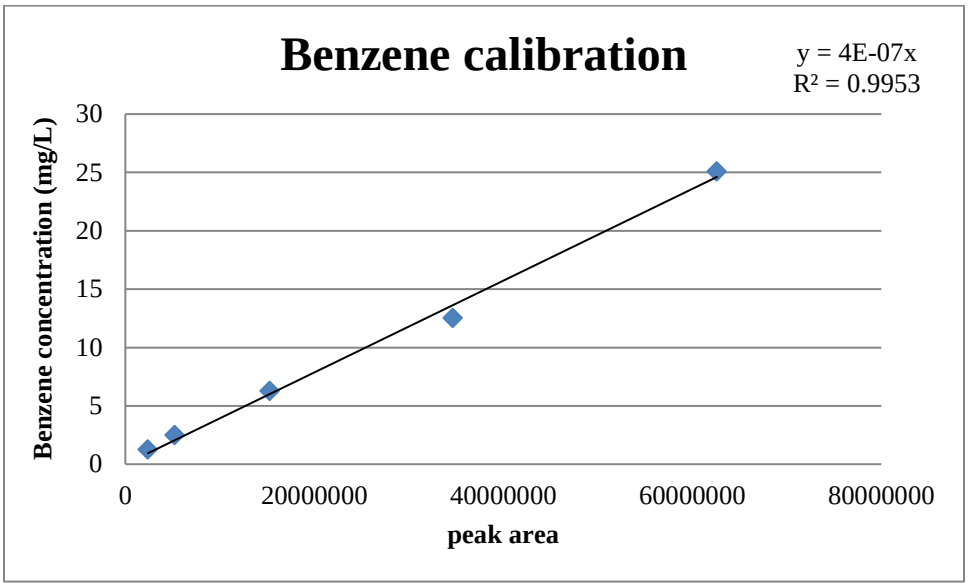

Figure 55. Example calibration curve for headspace analyses of porewater samples.

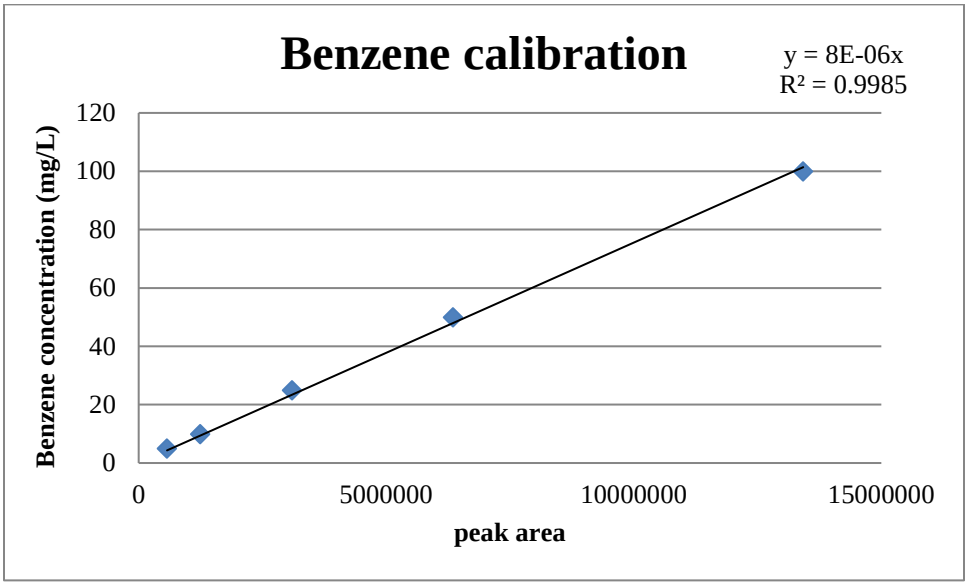

Figure 56. Example calibration curve for hexane extraction analyses of porewater samples.

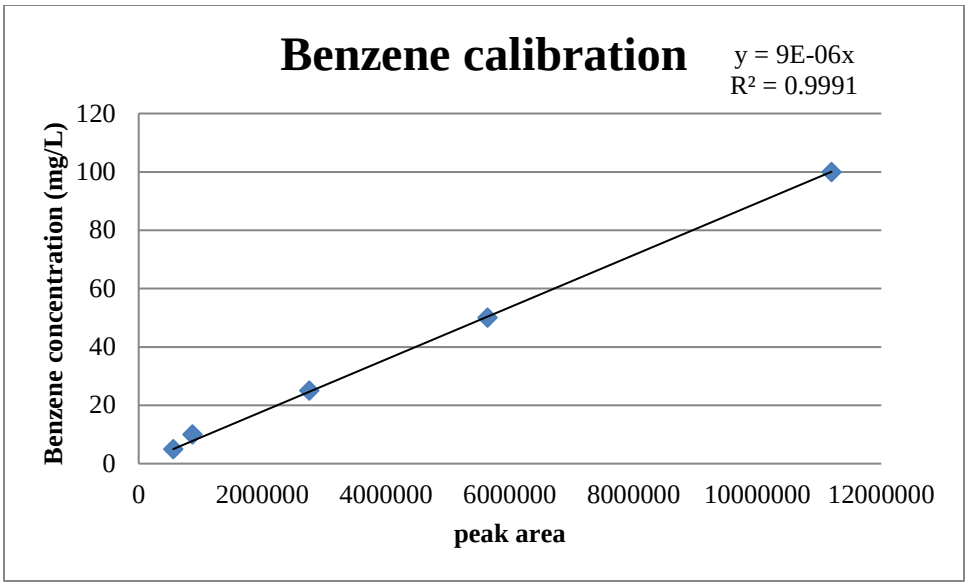

Figure 57. Example calibration curve for methanol extraction analyses of frozen sediment samples.

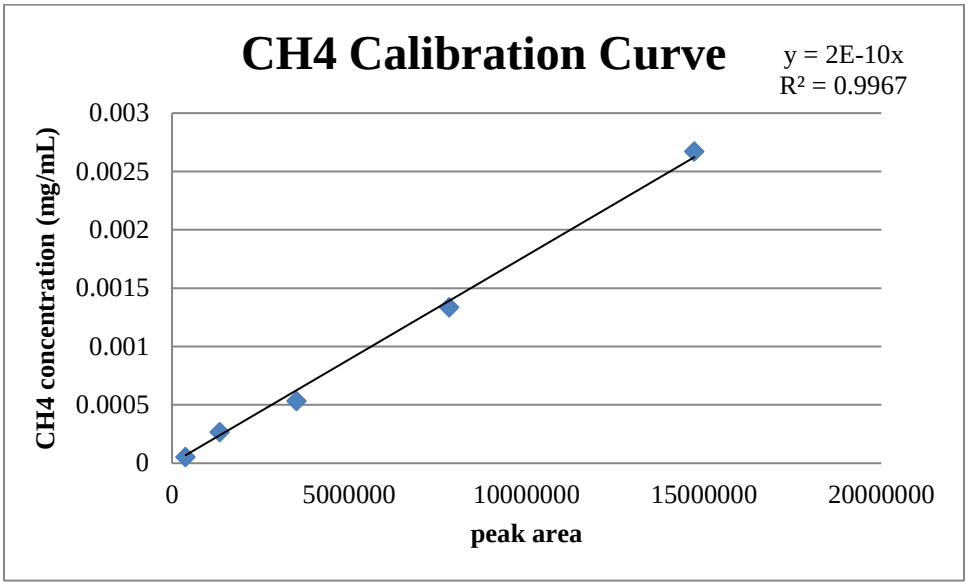

Figure 58. Example calibration curve for methane concentration analyses of frozen sediment samples.